Stony Brook University

Phospho-Sulindac Inhibits Pancreatic Cancer Growth: The Role of NFATc1

A Dissertation Presented

by

Onika T. Murray

to

The Graduate School

in Partial Fulfillment of the

Requirements

for the Degree of

Doctor of Philosophy

in

Molecular and Cellular Pharmacology

Stony Brook University

August 2012

Stony Brook University

The Graduate School

Onika T. Murray

We, the dissertation committee for the above candidate for the

Doctor of Philosophy degree, hereby recommend

acceptance of this dissertation.

Basil Rigas, M.D., DSc – Dissertation Advisor
Professor
Division of Cancer Prevention & Department of Molecular and Cellular Pharmacology

Todd Miller, Ph.D. - Chairperson of Defense
Professor
Department of Physiology and Biophysics

Roger Keresztes, M.D.
Professor
Department of Internal Medicine

Howard Crawford, Ph.D.
Associate Professor
Department of Cancer Biology
Mayo Clinic

This dissertation is accepted by the Graduate School

Charles Taber
Interim Dean of the Graduate School

Abstract of the Dissertation

Phospho-Sulindac Inhibits Pancreatic Cancer Growth: The Role of NFATc1

by

Onika T. Murray

Doctor of Philosophy

in

Molecular and Cellular Pharmacology

Stony Brook University

2012

While significant progress has been made in the battle against pancreatic cancer, it ranks 4th in cancer-related deaths in the U.S. Lending to the lethality of the disease is its ability to grow virtually undetected. Once pancreatic cancer is diagnosed, chances are that it has advanced beyond the point of surgical resection, as well as having become quite resistant to chemotherapy. While some chemotherapeutic agents have been able to improve patients' short-term quality of life, the impact on long-term survival has been minimal. Here I analyzed the effect of the novel agent phospho-sulindac (P-S) on pancreatic cancer growth *in vitro* and *in vivo*. From pharmacokinetic and metabolism studies to pancreatic cancer xenograft studies, the enhanced efficacy and safety of P-S in comparison to that of the parent, sulindac, was demonstrated.

In preliminary studies with P-S, NFATc1 gene expression and protein levels were elevated in response to treatment. Briefly, **N**uclear **F**actor of **A**ctivated **T**-cells (NFAT) family is a calcineurin-responsive group of transcription factors initially identified as regulators of T-

lymphocyte activation, though they are ubiquitously expressed in cells throughout the body. In particular, NFATc1 has been shown to be overexpressed in pancreatic cancer, likely adding to the aggressive nature of the disease. This finding prompted us to study the effects of P-S both in the absence and the abundance of NFATc1. My research focuses specifically on the effects that altered expression of NFATc1 (by genetically and pharmacologically silencing or by overexpressing it) has on pancreatic cancer growth *in vitro* and *in vivo*. We found that when the expression of NFATc1 was abrogated either by RNAi or pharmacological inhibition, pancreatic cancer cells were more responsive to treatment with P-S. In the same way, overexpressing the NFATc1 gene made the pancreatic cancer cells less responsive to treatment with P-S. NFATc1 localization is indicative of its activity, with nuclear localization being the active form. Treatment of pancreatic cancer cells with P-S facilitated the cytosolic localization of NFATc1, or the inactive form of the protein. NFATc1 knock-down and overexpression animal models were generated and the effect of P-S on tumor growth was analyzed. We observed the greatest reduction in tumor growth in our NFATc1 knock-down model. We conclude that P-S is a potentially important agent for the treatment of pancreatic cancer and that NFATc1 localization and activation in response to our compound may play a role in its pharmacological action.

Table of Contents

List of Abbreviations

5-FU	5-fluorouracil
CE	Carboxyesterases
CsA	Cyclosporine A
COX-2	Cyclooxygenase 2
CYP450	Cytochrome P450
DCFDA	2',7'-dichlorodihydrofluorecein diacetate
DMSO	Dimethyl sulfoxide
EGFR	Epidermal Growth Factor Receptor
FBS	Fetal Bovine Serum
HLM	Human liver microsomes
HPLC	High-performance liquid chromatography
IC_{50}	Half maximal inhibitory concentration
IF	Immunofluorescence
Kd	Knock-down
MAPK	Mitogen-activated protein kinases
MTT	3-(4,5-Dimethylthiazol-2-yl)-2,5-diphenyltetrazolium bromide
NFAT	Nuclear factor of activated T-cells
OCT	Optimal cutting temperature
Ov.	Overexpression
PBS	Phosphate buffered saline
PG	Prostaglandins

PK	Pharmacokinetics
Ras	Rat sarcoma
RLC	Rat liver cytosol
RLM	Rat liver microsomes
ROS	Reactive oxygen species
SSide	Sulindac sulfide
SSone	Sulindac sulfone
UGT	UDP-glucuronosyltransferases

List of Figures

Acknowledgements

I dedicate this to my God, my Family, and my Friends. Thank you for your support and your generosity. I love you all dearly.

I would like to say a special thank you to my thesis advisor, Dr. Basil Rigas, for seeing a sparkle in me and taking the time to mold me into a successful scientist. He has provided a great example for me to emulate, and I will take these life lessons with me into every step of my career.

I would also like to thank all my lab members for taking the time to train and educate me on all the techniques I have acquired during my doctoral training. Also, a special thanks to the Molecular & Cellular Pharmacology Class of 2007: Cindy Leiton, Oladapo Yeku, James McCann, Elizabeth Louie and Victoria Fischer.

I would like to thank the members of my committee for the time and effort they have put into this thesis project. I truly valued all their comments and advice. I'd also like to thank the Department of Pharmacology faculty and staff, especially to Lynda Perdomo-Ayala, Beverly Campbell and Dr. Styliani Tsirka.

Finally, a special thank you to my graduate fellowship 3MT IGERT NSF, and AGEP as well as the CIE for all their help throughout the years.

INTRODUCTION

1. PANCREATIC CANCER: A MAJOR HEALTH PROBLEM

Clinical Presentation & Prognosis

Pancreatic ductal adenocarcinoma (PDA or PDAC), more loosely referred to as pancreatic cancer, accounts for over 95% of all exocrine pancreatic malignancies (Hingorani, et al. 2003). Other types of pancreatic malignancies include neuroendocrine tumors, acinar cell carcinomas, lymphomas, sarcomas, serous cystadenocarcinoma, and pancreatoblastomas (Hruban, et al. 2006). Pancreatic cancer is the fourth leading cause of cancer mortality in the United States. According the American Cancer Society, about 44,030 new cases were anticipated in the year 2011, and 37,660 patients expected to die from the disease. This malignancy is very aggressive, and patients are often diagnosed at later stages due to the vague symptoms associated with pancreatic cancer. Surgical resection, when possible, provides the only opportunity for cure. Even with resection, pancreatic cancer still carries an overall dismal prognosis, with the 5-year survival rate for patients being <5% (Almhanna and Kim 2008). The poor prognosis of the disease is attributed to a high incidence of local recurrence, lymph node metastasis, peritoneal dissemination, and high levels of neural invasion (Nakajima, et al. 2004). For patients who cannot undergo surgery, chemotherapy is part of the standard treatment. Even if tumors respond to chemotherapy initially, almost all rapidly become resistant to the prescribed drugs. Together,

these reasons explain why most patients diagnosed with pancreatic cancer die within the first year—and why pancreatic cancer has such a dismal reputation (Bardeesy and DePinho 2002). These statistics underscore the urgent need to develop new agents against pancreatic cancer.

Pancreatic intraepithelial neoplasm (PanIN), mucinous cystic neoplasm (MCN), and intraductal papillary mucinous neoplasm (IPMN) are 3 precursor lesions that are implicated in the onset of pancreatic cancer. Of the three, PanIN lesions appear to be the most frequent, occurring in as many as 30% of reported cases (Hezel, Kimmelman, Stanger, Bardeesy and Depinho 2006). Histologically, PanINs show a spectrum of divergent morphological alterations relative to normal ducts that seem to represent graded stages (I-III, respectively) of increasingly dysplastic growth (Hruban, et al. 2001). Key events that occur during the early stages of PanIN growth are K-Ras mutations and loss of function of p16. Key events that arise later in PanIN progression include p53, SMAD4 as well as BRAC2 loss of function (Hezel, et al. 2006). Taken together, these occurrences contribute significantly in the onset of pancreatic cancer as well as its progression.

Current Therapies for Pancreatic Cancer

Surgery

Pancreaticoduodenectomy, or the Whipple procedure, is the most common curative surgical procedure for pancreatic cancer. Briefly, the pancreatic head and duodenum are removed and the billiary tree, gastric outlet, and pancreatic duct are reconnected to the jejunum (Gudjonsson 1987, Nitecki, Sarr, Colby and van Heerden 1995). Advances in surgical techniques have helped reduce the mortality rates associate with the procedure from approximately 20% to

less than 5%. Complete pancreatectomy is generally not recommended due to the complete loss of insulin and glucagon (both produced by the pancreas) resulting in difficult glucose homeostasis and eventually diabetes (Sarr, Behrns and van Heerden 1993). Less than 20% of patients diagnosed with pancreatic cancer are offered the procedure, as it can only be performed in the absence of metastasis, i.e. in localized pancreatic cancer. Thus for patients whose cancer has metastasized to distant organs, chemotherapy is the most recommended route for treatment.

Neoadjuvant Therapy

Pancreatic cancer patients with locally nonresectable tumors are typically placed on neoadjuvant therapy. This therapy is typically delivered as systemic chemotherapy combined with external beam radiation (EBRT) to the pancreatic mass and associated lymph nodes (Breslin, et al. 2001). This approach is beneficial as it provides immediate systemic therapy for a disease that is systemic at diagnosis in almost all patients. Further, there is the potential of downstaging locally advanced pancreatic cancer and selecting patients for pancreatic resection.

The results from neoadjuvant therapies in pancreatic cancer have been rather discouraging. Particularly, there have been Phase I and II clinical trials where various chemotherapy agents in combination with varying radiation doses have been evaluated. These studies have shown that 20-40% of patients treated with a neoadjuvant chemoradiation approach failed to go on to planned surgery as a consequence of disease progression or evolution of clinically significant medical comorbidities (Evans, et al. 1992). In brief, there is no concrete evidence of benefit from this approach and thus is not considered a standard therapy; further clinical evaluation is needed.

Adjuvant Therapy

Because the failure rate of the Whipple procedure is considerably high, leading to disease reoccurrence among patients, most adjuvant protocols have combined EBRT with systemic chemotherapy. Early studies conducted by the Gastrointestinal Tumor Study Group (GITSG) demonstrated a significant survival advantage when chemotherapy in combination with radiation was utilized in comparison to resection alone (20 vs 11 months) (Kalser, Barkin and MacIntyre 1985). Following these findings, a phase III study by the European Organization for Research and Treatment of Cancer (EORTC) also demonstrated a survival benefit of 17.1 months for patients who received adjuvant chemoradiation in comparison to a survival benefit of 12.6 months for those patients treated with surgery alone. (Klinkenbijl, et al. 1999). Finally, the most recent and largest randomized trial evaluating the role of adjuvant therapy for pancreatic cancer was performed by the European Study Group for Pancreatic Cancer (ESPAC-1) (Neoptolemos, et al. 2001). ESPAC-1 did not demonstrate a survival benefit with combined chemoradiotherapy; in fact, it was found to be detrimental compared to observation alone. In contrast, systemic chemotherapy provided a survival advantage. There were some concerns with this trial, including low compliance with prescribed therapy (suggesting inadequate central monitoring), absence of radiation quality control, and lack of standardized pathologic evaluation of surgical specimens (Raut, Evans, Crane, Pisters and Wolff 2004). The current standard of care after resection is systemic chemotherapy alone; concurrent chemotherapy and radiation are only used in select cases.

Systemic Therapy for Advanced Disease

Systemic therapy for metastatic disease has recently shown more promise. The use of single agent chemotherapy (gemcitabine) demonstrated clinical benefit in palliation, in addition to a statistically significant improvement in median survival (5.7 vs. 4.5 months) in comparison to previously used single agent chemotherapy (Rothenberg, et al. 1996). This study defined clinical benefit as improvements in pain intensity and analgesic intake. A second study confirmed the clinical benefit of gemcitabine after patients progressed on previous standard chemotherapy (Rothenberg, et al. 1996). Therefore, treatment with gemicitabine alone has become standard therapy for advanced pancreatic cancer. This drug is generally well tolerated by older patients and patients with poor performance. Although these benefits are significant, they are marginal overall. Thus, more clinical studies evaluating more effective chemotherapeutic agents are essential.

Novel Targeted Therapies

To date, Tarceva (erlotinib hydrochloride) in combination gemcitabine is the leading FDA approved treatment for pancreatic cancer. However, studies in non-small-cell lung cancer carcinoma have shown that Tarceva is ineffective in patients harboring a mutation in K-Ras (which exists in the majority of clinical presentations) or in those patients whose cancer demonstrates an epithelial to mesenchymal transition (EMT) (Pao, et al. 2004, Pao, et al. 2005). Tarceva is a small molecule anti-EGFR inhibitor of tyrosine kinase activity, acting on the intracellular domain of EGFR and blocking further downstream activity, including K-Ras signaling (Buck, et al. 2006a). The combination of Tarceva and gemcitabine is prescribed to patients with locally advanced, unresectable or metastatic pancreatic cancer. Initial studies

examining K-Ras mutation as a biomarker for resistance to EGFR-directed therapy hypothesized that mutations in K-Ras would lead to cancer growth, regardless of modulation of the EGFR signal. It has been demonstrated in clinical studies that patients with lung, colon and pancreatic cancer harboring mutations in K-Ras have 0% responsiveness to Tarceva (Riely and Ladanyi 2008). In fact, an *in vitro* study conducted by OSI Pharmaceuticals demonstrated that pancreatic cancer cell lines harboring a mutation in K-Ras showed insensitivity to varying concentrations of Erlotinib treatment when compared to those with wild type K-Ras activity (Buck, et al. 2006b). Another limitation of Erlotinib's efficacy is the presence of EMT. EMT has been associated with poor prognosis in pancreatic cancer as well as several cancers, including: prostate, breast, non-small-cell lung, and colorectal cancer (Javle, et al. 2007). There are several other targeted agents in the pipeline for development, and future clinical trials will be pursued to optimize therapy in pancreatic cancer.

The Need for New Agents for Pancreatic Cancer

Currently, there is a phase II study of anti-cytotoxic T-lymphocyte-associated antigen-4 monoclonal antibody (MDX-010) in patients with unresectable stage IV (locally or distantly metastatic) pancreatic adenocarcinoma (National Cancer Institute, 2008. 31 Mar. 2012 <http://www.cancer.gov/clinicaltrials/featured/trials/nci-05-c-0141>). MDX-010 is being evaluated for its efficacy in patients with advanced pancreatic cancer. MDX-010 binds to and blocks the activity of CTLA-4 (cytotoxic T-lymphocyte-associated antigen-4), a molecule produced by activated T. CTLA-4 transmits an inhibitory signal to T cells and this inhibition prevents the destruction of both non-malignant and malignant cells. Researchers hope that

blocking CTLA-4's inhibitory signal will lead to a more robust immune response against pancreatic cancer progression.

In another study, bevacizumab, the first U.S. Food and Drug Administration (FDA) approved therapy designed to inhibit angiogenesis, was used to treat patients with advanced pancreatic cancer (Kindler, et al. 2010). Currently, bevacizumab is approved in combination with intravenous 5-fluorouracil-based (5-FU) chemotherapy, for the first- or second-line treatment of patients with metastatic carcinoma of the colon or rectum; in combination with carboplatin and paclitaxel for the first-line treatment of patients with unresectable, locally advanced, recurrent or metastatic non-squamous non-small cell lung cancer (NSCLC); and for the treatment of metastatic renal cell carcinoma in combination with interferon alpha. The Cancer and Leukemia Group B (CALGB) conducted a randomized phase III trial of gemcitabine in combination with bevacizumab versus gemcitabine plus placebo in patients with advanced pancreatic cancer. The study showed that there were no significant differences in overall survival in patients treated with the agent versus the placebo group.

2. *PHOSPO-SULINDAC AND THE PHOSPHO-NSAID FAMILY OF COMPOUNDS*

Pharmacological Features

Nonsteroidal anti-inflammatory drugs (NSAIDs) have demonstrated antineoplastic properties in various types of cancer; however, they do not fully meet safety and efficacy criteria for use as anticancer agents. In response to this, several groups, including our lab, have modified the structure of NSAIDs to enhance their efficacy and/or decrease their side effects. Such modifications have centered on covalently modifying NSAIDs at their –COOH moiety, which is a structural feature of nearly all of them (Piazza, et al. 2009).

Structure

The general structure of phospho-NSAIDs studied by our lab is shown in Figure 1. The key structural features of these molecules are conventional NSAIDs bound to diethylphosphate via a butane linker molecule.

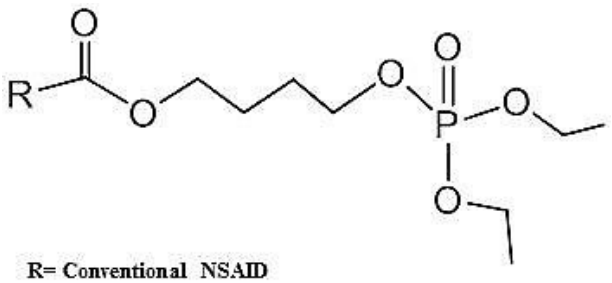

R= Conventional NSAID

Figure 1. General Phospo-NSAID Structure

The specific compound that is the subject of my work is phospho-sulindac, a modified derivative of sulindac, is shown below (Figure 2).

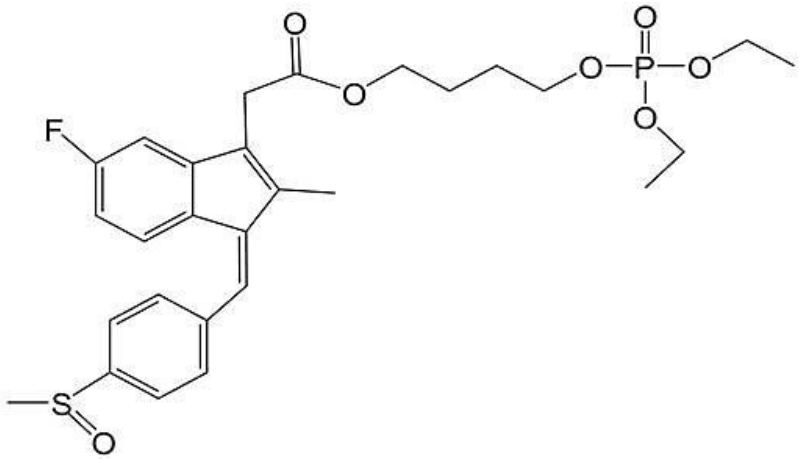

(*Z*)-4-(diethoxyphosphoryloxy)butyl 2-(5-fluoro-2-methyl-1-(4-(methylsulfinyl)benzylidene)-1*H*-inden-3-yl)acetate
Chemical Formula: $C_{28}H_{34}FO_7PS$
Molecular Weight: 564.60

Figure 2. Phospho-Sulindac Structure

Efficacy

Phospho-sulindac (P-S), compared to other modified NSAIDs, has demonstrated greater anticancer efficacy (Huang, et al. 2010). NSAIDs are primarily used to alleviate pain via cyclooxygenase (COX) enzyme inhibition and the consequent reduction of prostaglandin synthesis (Ulrich, Bigler and Potter 2006). Specifically, sulindac, an anti-inflammatory agent, has demonstrated the ability to reduce pancreatic cancer growth (Molina, Sitja-Arnau, Lemoine, Frazier and Sinicrope 1999). While sulindac demonstrates anticancer properties, the doses required to elicit these effects are quite high, causing undesired side effects in patients.

To study the efficacy of P-S, we tested its ability to inhibit the growth of human colon, pancreatic and breast cancer cell lines. We observed that P-S inhibited the growth of these cell

lines approximately 11- to 30-fold more potently than sulindac (Huang, et al. 2010). Compared to control, P-S inhibited cell proliferation by up to 67%, induced apoptosis 4.1 fold over control and blocked the G_1 to S cell cycle phase transition. P-S suppressed the levels of cell cycle regulating proteins including cyclins D_1 and D_3 and CDKs 4 and 6. It also suppressed the production of prostaglandin E_2 (PGE_2) and decreased cyclooxygenase-1 (COX-1) expression. Similar to sulindac, P-S enhanced spermidine/spermine N1-acetyltransferase activity, reduced the cellular polyamine content, and synergized with difluoromethylornithine (DFMO) to inhibit cancer cell proliferation and induce apoptosis. In summary, we have shown that P-S elicits its anticancer effects with greater efficacy than sulindac in various types of human cancer models.

In addition to P-S, our lab has studied the chemotherapeutic efficacy of four additional novel phospho-NSAIDs identified as phospho-desoxy-sulindac (PDS), phospho-flurbiprofen (P-F), phosphor-ibuprofen (P-I), and phosphor-aspirin (P-A). All compounds inhibited the growth of human breast, colon, and pancreatic cancer cell lines with greater potency than their conventional counterparts (Huang, et al. 2011). *In vivo* investigations confirmed the antitumor activity of P-A and P-S in inhibiting tumor growth in established human xenograft models, in which cell proliferation was suppressed and apoptosis enhanced in the absence of detectable animal toxicity. In culture cells, all of the phospho-NSAIDs tested induced reactive oxygen and nitrogen species (RONS), more loosely referred to as reactive oxygen species (ROS).In addition, our panel of modified phospho-NSAIDs also inhibited the thioredoxin system and the redox sensitive transcription factor NF-kB.

Additionally, P-S inhibited intestinal tumors alone and to a greater extent in combination with difluoromethylornithine (DFMO) in a colon cancer cells. Results from this analysis showed that P-S in comparison to sulindac was much more potent in inhibiting the growth of colon

cancer cells and more efficacious in preventing the growth of HT-29 xenografts in nude mice. P-S also prevented the growth of intestinal tumors in Apc/Min mice. When combined with DFMO, P-S reduced tumor growth in Apc/Min mice by 90% (Mackenzie, et al. 2010). P-S's enhanced safety in comparison to the parent compound was confirmed by both *in vitro* toxicological evaluation and animal toxicity studies.

Mechanistically, P-S increases the intracellular levels of ROS, which are key early mediators of its chemopreventive effect. Polyamine concentrations have been shown to be elevated in various types of cancer, including colon, and their inhibition has been shown to have positive effects on tumor regression/inhibition (Bachrach 2004). P-S induces spermidine/spermine N1-acetyltransferase enzymatic activity, and together with DFMO it reduced polyamine levels *in vitro* and *in vivo* (Mackenzie, et al. 2010).

Taken together, P-S as well as other modified phospo-NSAIDs exhibited greater effects on tumor regression than the parent compounds in a way that is both safe and efficacious.

Safety

A remarkable feature of P-S is its safety (Huang, et al. 2010, Mackenzie, et al. 2010). The genotoxicity of P-S was evaluated by measuring its ability to induce reverse mutations at selected loci of 2 strains of Salmonella typhimurium in the presence and absence of S9 activation. The results from this study revealed that P-S was non-genotoxic.

To assay for acute toxicity, six-week-old female C57BL/6J$^{+/+}$ mice were treated for 5 days by oral gavage with equimolar amounts of P-S, sulindac or vehicle. Both vehicle and P-S treated animals maintained their body weight, showed no evidence of gastrointestinal or other toxicity, were alive and healthy at the conclusion of the study and showed no abnormalities upon

inspection of the heart, lungs, spleen, kidneys, and liver. In contrast, sulindac-treated mice lost 20% of their weight, showed significant mortality, necropsies showed upper gastrointestinal toxicity with macroscopically evident gastric ulcers, gastric bleeding and perforation. Further, the stomachs of sulindac treated animals were larger than those of the two aforementioned groups and livers also appeared hyperemic.

To test for gastrointestinal toxicity, six-week-old Sprague-Dawley rats were treated for 4 days by oral gavage with equimolar amounts of P-S, sulindac, indomethacin, or vehicle. Indomethacin is known to produce gastric ulceration in rats, and as expected, treatment with it produced predominantly medium and large ulcerations in the small intestine. Animals treated with vehicle and P-S showed no gastrointestinal toxicity, with no signs of ulcerations or mucosal damage. Sulindac, on the other hand, mirrored the results observed in indomethacin treated rats, exhibiting medium and large ulcerations in the small intestine.

In brief, the anticancer effect of P-S was achieved without presentation of toxicity to the animals, thus fulfilling a necessary requirement of drug development—enhanced safety and efficacy.

Mechanism of Action

A Redox-mediated Effect

Cellular redox changes have emerged as a pivotal and proximal event in cancer. At low concentrations, ROS play protective roles in cellular homeostasis; at higher concentrations they can damage many biological molecules, such as DNA, proteins, and lipids, and may also prevent cancer by initiating the death of the transformed cell (Rigas and Sun 2008).

Our lab has shown that P-S and its phospho-NSAID counterparts induce ROS in various cancer models (Sun and Rigas 2008, Huang, et al. 2010, Mackenzie, et al. 2010, Huang, et al. 2011). Further, that the induction ROS leads to apoptosis, necrosis, and finally cancer cell death, while leaving noncancerous cells intact.

Particularly, ROS are broadly defined as oxygen-containing, reactive chemical species. There are two types of ROS, those of free radicals, which contain one or more unpaired electrons in their outer molecular orbitals, and non-radical ROS, which do not have unpaired electrons but are chemically reactive and can be converted to radical ROS. Examples of radical ROS that are commonly seen in biological systems are superoxide, nitric oxide and hydroxyl radicals (Trachootham, Alexandre and Huang 2009).

Compared with normal cells, malignant cells seem to function with higher levels of endogenous oxidative stress (Szatrowski and Nathan 1991, Kawanishi, Hiraku, Pinlaor and Ma 2006). Although the precise pathways leading to ROS stress in cancer cells remain unclear, several intrinsic and extrinsic mechanisms are thought to cause oxidative stress during cancer development and disease progression. Activation of oncogenes, aberrant metabolism, mitochondrial dysfunction and loss of functional p53 are intrinsic factors known to cause increased ROS production in cancer cells (Irani, et al. 1997, Horn and Vousden 2007, Rodrigues, Reddy and Sattler 2008). The expression of genes that are associated with tumor transformation, such as Ras, Bcr-Abl and c-Myc, were found to induce ROS production (Behrend, Henderson and Zwacka 2003, Kissil, et al. 2007).

Therapeutic selectivity is essential in cancer treatment. As cancer cells have elevated ROS generation and are under increased intrinsic oxidative stress, it is conceivable that these malignant cells would be more dependent on antioxidants for cell survival and, therefore, more

vulnerable to further oxidative insults induced by ROS-generating agents or by compounds that abrogate the key antioxidant systems in cells (Trachootham, et al. 2009).

In sum, a common thread among P-S and its broader class of phospho-NSAIDs is the induction of ROS. Increased generation of ROS and an altered redox status have long been observed in cancer cells, and recent studies, including those from our lab, suggest that this biochemical property of cancer cells can be exploited for therapeutic benefits. Cancer cells in advanced stage tumors frequently operate at high levels of oxidative stress, suggesting that it might be possible to preferentially eliminate these cells by pharmacological ROS interference (Trachootham, et al. 2009). However, the upregulation of antioxidant capacity in adaptation to intrinsic oxidative stress in cancer cells can confer drug resistance (such as thioredoxin reductase). Abrogation of such drug-resistant mechanisms by redox modulation could have significant therapeutic implications. It is quite conceivable that the modulation the unique redox regulatory mechanisms of cancer cells might be an effective strategy to eliminate them.

Phospho-NSAIDs and the Thioredoxin System

Thioredoxin (Trx) is an a oxidoreductase involved in redoxregulation and cell signaling (Kaimul, Nakamura, Masutani and Yodoi 2007). Trx is a member of the Trx system that also includes Trx reductase (TrxR) and NADPH. The expressed Trx system and glutathione (GSH) are the two main antioxidant systems that reduce thiol (-SH) groups. Three distinct forms of Trx have been identified which are Trx-1 (the 12-kDa cytosolic form), Trx-2 (the mitochondrial isoform), and SpTrx (highly expressed in spermatozoa). Trx-1 acts as an intracellular reductase using two vicinal cysteine residues (Cys32 and Cys35) at its conserved active site (-Cys-Gly-Pro-Cys-) (Arner and Holmgren 2006).

The redox-active center of reduced Trx-1 interacts with the oxidized protein that it is about to reduce, which has a disulfide bond (Kaimul, et al. 2007). Trx-1 reduces the target protein by converting its disulfide bond to two-SH groups, whereas, in the process, Trx-1 itself becomes oxidized, with its two -SH groups forming a disulfide. TrxR and NADPH reduce Trx-1 back to its original state. Trx-1 has three additional cysteines, Cys62, Cys69, and Cys73. Further oxidation of Trx-1 first leads to the formation of a disulfide bond between Cys62 and Cys69 and, next, to a disulfide bond between Cys73 of two different Trx-1 molecules, which ultimately leads to the formation of a dimer (Sun, et al. 2008).

Numerous proteins are redox-regulated by the Trx system (Berndt, Lillig and Holmgren 2007). Examples of such regulation include the reduction by Trx-1 of a cysteinyl residue of the p50 subunit of nuclear factor-κB (NF-κB), which is required for its DNA binding, and the activation through similar reduction reactions of many transcription factors. Trx is implicated in a number of diseases (Maulik and Das 2008), seem to play a vital role in cancer biology and in cancer response to chemotherapeutic agents. Trx, overexpressed in pancreas, colon, lung, and other cancers, suppresses apoptosis by activating the Akt pathway or through the apoptosis signal-regulating kinase-1 (Saitoh, et al. 1998).

In particular, the redox effect of two modified phospo-NSAIDs, P-A and P-S, was examined in SW480 and HT-29 colon cancer cells (Huang, et al. 2010, Sun, Huang, Mackenzie and Rigas 2011). All compounds inhibited the growth of both cell lines as well as induced ROS. NF-κB and mitogen-activated protein kinases were modulated by ROS. Trx-1was heavily oxidized in response to ROS and mediated the growth inhibitory effect of the anticancer agents. Knocking-down Trx-1expression by small interfering RNA abrogated cell death induced by P-A or P-S. These compounds also inhibited the activity of Trx reductase that reduces oxidized Trx-1.

These findings demonstrated that the Trx system mediates redox-induced cell death in response to anticancer agents. The exact mechanism by which oxidized Trx-1 participates in the induction of cell death by these compounds is not fully delineated. It isclear that NF-κB and MAPKs are modulated in our experimental system. Based on the known role of Trx-1 in the regulation of transcription factors, it is likely that the oxidation of Trx-1 is proximal to NF-κB and MAPKs. Indeed, in the case of MAPK activation, the release of ASK1 from its complex with Trx-1 represents a convincing mechanistic link between the two (Sun, et al. 2008).

Figure 3 summarized the effect of phospho-NSAIDs on the Trx system. These agents induce ROS, leading to a conversion of Trx-1 from its completely reduced form to its partially oxidized form ($Trx\text{-}1_{ox\text{-}I}$) and further to its fully oxidized form ($Trx\text{-}1_{ox\text{-}II}$). TrxR, which reverses the oxidation of Trx-1, was also inhibited by the compounds we studied. At low ROS concentrations, when Trx-1 is in its reduced form, cell death is minimal. As ROS concentrations increase, cell death is evident, becoming the most abundant at the highest ROS concentrations. Our findings indicate that to a large extent, the Trx system mediates redox-induced cell death in response to anticancer agents.

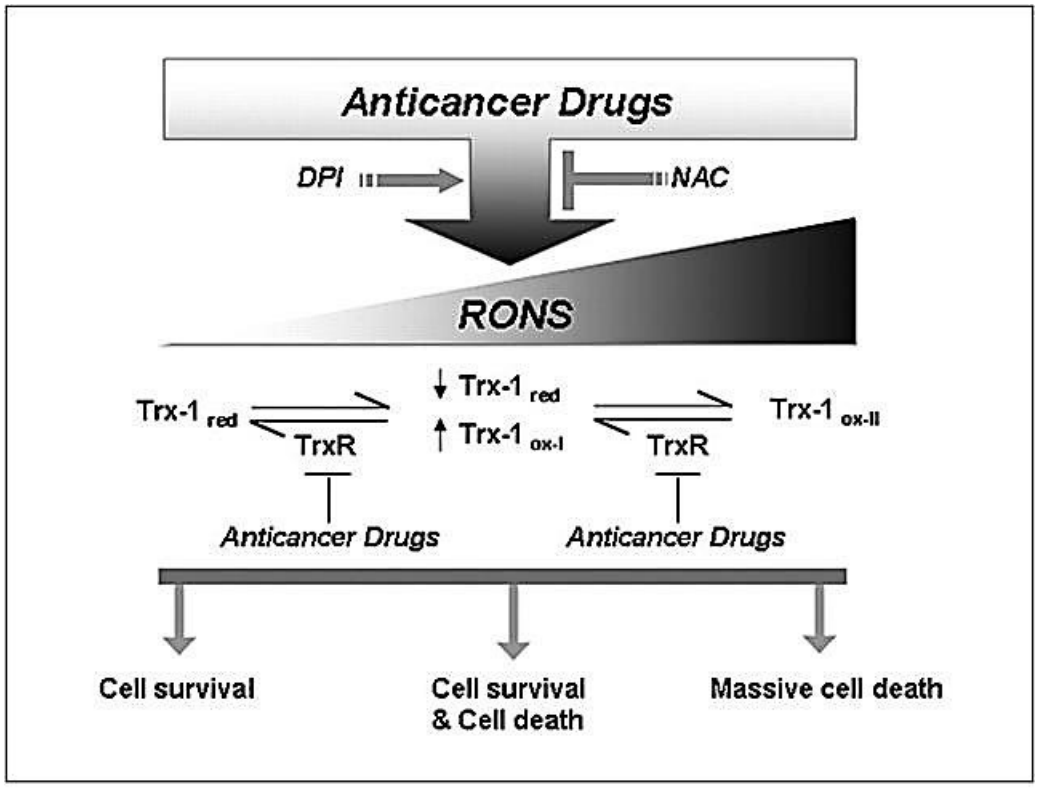

Figure 3. Trx-1 Modulates Cell Survival. (*Image adapted from Sun, Y., and Rigas, B. (2008), "The Thioredoxin System Mediates Redox-Induced Cell Death in Human Colon Cancer Cells: Implications for the Mechanism of Action of Anticancer Agents," Cancer Res, 68, 8269-8277.*)

3. NFATc1 AND ITS SIGNIFICANCE IN PANCREATIC CANCER

My interest in the role of NFATc1 in pancreatic cancer began via a microarray analysis of P-S treated MIAPaCa-2 human pancreatic cancer cell lines. Of over 47,000 genes analyzed, 2 genes had greater than 2-fold upregulation in response to treatment with our drug—among them, NFATc1. The Nuclear Factor of Activated T-cells (NFAT) family is a calcineurin-responsive group of transcription factors initially identified as regulators of T-lymphocyte activation, though they are ubiquitously expressed in cells throughout the body (Muller and Rao 2010). The NFAT family consists of five proteins: NFAT1 (also known as NFATc2 or NFATp), NFAT2 (also known as NFATc1 or NFATc), NFAT3 (also known as NFATc4), NFAT4 (also known as NFATc3 or NFATx) and NFAT5 (also known as tonicity enhancer binding protein (TonEBP) (Hogan, Chen, Nardone and Rao 2003, Crabtree and Schreiber 2009). Emerging evidence has shown the role of NFATc1 in carcinogenesis, and the way in which it regulates cancer progression.

Sustained activation of the Ca^{2+} /calcineurin/NFAT signaling pathway has emerged as a powerful regulatory principle governing cancer growth (Trachootham, et al. 2009). NFATc1, in its basal state, is localized to the cytoplasm in an inactive conformation. Dephosphorylation of NFATc1 by calcineurin exposes a nuclear localization sequence and masks a nuclear export sequence, therefore promoting nuclear import leading to transcriptional activation (Tinsley, et al. 2009). Nuclear export of NFATc1 terminates its transcriptional activity. Cytoplasmic accumulation of NFATc1 is achieved by several mechanisms, including the inhibition of calcineurin activity, which can retain cytoplasmic NFATc1 or promote nuclear export of NFATc1 (Sun, et al. 2011). Both the nuclear translocation of NFATc1 as well as the NFATc1

dependent activation of gene transcription are reversed by either a decrease in intracellular calcium concentrations or treatment of cells with the calcineurin inhibitor cyclosporin A (CsA) (Waypa, et al. 2006a). Conversely, ionomycin increases intracellular calcium concentrations, and in effect the active form of NFATc1.

Calcium signaling affects tumor cell proliferation and invasive migration. Calcium signaling also controls key aspects of cell death by apoptosis, necrosis or autophagy. Overload of calcium in mitochondria affects mitochondrial integrity, which in turn promotes apoptosis. By contrast, changes in calcium flux can also promote the survival of cancer cells, whereby phosphorylation of inositol-1,4,5-triphosphate receptors by the PI3K–Akt pathway results in reduced calcium release and in turn reduced sensitivity to pro-apoptotic signals (Pelicano, Carney and Huang 2004).

NFATc1 Regulates c-Myc and COX-2 Expression

c-Myc: Several studies have attributed the pro-proliferative effect of NFATc1 to the direct binding of activated NFATc1 to the promoter of the c-Myc oncogene, resulting in upregulation of c-myc transcription and accelerated G1/S phase transition. These results provide important insights into the mechanisms of oncogenic c-Myc activation in pancreatic cancer, especially in tumors that lack genomic amplifications of the c-Myc gene locus (Buchholz, et al. 2006, Guzy and Schumacker 2006, Schumacker 2006). c-Myc is a transcription factor that regulates cell growth, proliferation, differentiation and apoptosis.The c-Myc oncogene keeps G1/S phase cyclins on, encouraging pancreatic cancer cell growth and tumor progression (Waypa and Schumacker 2006b). It has been demonstrated that c-Myc transcription and

anchorage-dependent and -independent cell growth is significantly attenuated by inhibition of Ca^{2+}/calcineurin signaling or siRNA-mediated knock-down of NFATc1 expression (Buchholz, et al. 2006). These results showed that ectopic activation of NFATc1 and the Ca^{2+}/calcineurin signaling pathway is an important mechanism of oncogenic c-Myc activation in pancreatic cancer.

COX-2: It has been demonstrated that NFAT recognition sequences are present in the human cyclooxygenase 2 (COX-2) proximal promoter. Deletion analysis has shown that recognition sequences are important in COX-2 transcriptional activation in T lymphocytes (Iniguez, Martinez-Martinez, Punzon, Redondo and Fresno 2000). NFAT has also been shown to be active in human breast and colon carcinoma cells. Gene expression profiling by cDNA microarray of cells induced to express NFAT revealed up-regulation of COX-2. Increased NFAT expression and activity induced COX-2 expression as well as prostaglandin E_2 synthesis (Yiu and Toker 2006). These findings demonstrated that NFAT promotes breast cancer cell invasion through the induction of COX-2 and the synthesis of prostaglandins. COX-2 is one of the pro-inflammatory mediators whose expression may be induced at the very early steps of carcinogenesis (Surh and Kundu 2005). COX-2 is constitutively expressed in a number of cancers (Cao and Prescott 2002). Studies have shown that when COX-2 is expressed, a poor prognosis is frequently associated (Sobolewski, Cerella, Dicato, Ghibelli and Diederich 2010). Evidence has been collected from models of adherent cancers, including colon (Brown and DuBois 2005, Ogino, et al. 2008), prostate (Sonpavde, et al. 2007, Cai, et al. 2008) and breast (Sucic, et al. 2003, Zhao, et al. 2008), where the expression of COX-2 is paralleled by a higher incidence of chemotherapy failure. Moreover, COX-2-deficient mice are more resistant to different forms of cancers (Langenbach, Loftin, Lee and Tiano 1999), as shown in models of colon (Oshima, et al. 1996,

Chulada, et al. 2000) and skin carcinogenesis (Tiano, et al. 2002, Akunda, et al. 2007). This implies a multi-step role for COX-2 in tumorigenesis, in early tumor promotion and in the late development of chemoresistance and metastatic formation (Sarkar, Adsule, Li and Padhye 2007). Different mechanisms regulating COX-2 expression appear to be involved in this instance, with a transcriptional activation implicated in early phases, and with post-transcriptional modulation crucially contributing at late tumorigenic steps.

CHAPTER I

THE PHARMACOKINETICS AND METABOLISM OF P-S

INTRODUCTION

Countless studies have revealed that chronic inflammation predisposes to different forms of cancer and that usage of non-steroidal anti-inflammatory drugs (NSAIDs) provides some degree of protection against various tumors (Mantovani, Marchesi, Porta, Sica and Allavena 2007). NSAIDs are primarily used to alleviate pain via cyclooxygenase (COX) enzyme inhibition and the reduction of prostaglandin synthesis, though their chemopreventive properties have been extensively documented (Ulrich, Bigler et al. 2006).

An early clinical observation that NSAIDs may inhibit cancer progression derives from studies of patients with familial adenomatous polyposis (FAP) and Gardner's syndrome (Waddell and Loughry 1983, Waddell, Ganser, Cerise and Loughry 1989). FAP patients develop numerous intestinal polyps during early adulthood because of an inherited mutation in the APC (adenomatous polyposis coli) gene, a major modulator of Wnt signaling. In this patient population, chronic ingestion of sulindac for one year decreased polyp multiplicity and induced regression of polyps (Waddell, et al. 1989). These studies were consistent with findings in a carcinogen-induced animal model, which showed regression of intestinal polyps following NSAID treatment (Pollard, Luckert and Schmidt 1983). In 1991, a large, population-based, observational study demonstrated that low-dose NSAID use reduced the relative risk of fatal colon cancer (Thun, Namboodiri and Heath 1991), and subsequent studies revealed that chronic

ingestion of NSAIDs significantly reduces colon polyp formation and recurrence, resulting in a 40%–50% reduction in the relative risk of colorectal cancer (Gupta and Dubois 2001).

Sulindac, for more than a decade, has been of interest as a chemopreventive treatment for adenomatous colorectal polyps and colon cancer (Boolbol, et al. 1996, Taketo 1998), especially in patients with familial adenomatous polyposis (Guldenschuh, et al. 2001). Sulindac has also been reported as a chemopreventive agent for mouse urinary bladder cancer (Rao, et al. 1996). Of utmost significance to this project, sulindac has also demonstrated the ability to reduce pancreatic cancer growth (Molina, Sitja-Arnau et al. 1999). The anti-tumorigenic activity of sulindac against colon cancer may involve both COX inhibition (Boolbol, et al. 1996) and activities that are independent of COX inhibition (Shiff and Rigas 1999, Grosch, Tegeder, Niederberger, Brautigam and Geisslinger 2001, Tegeder, Pfeilschifter and Geisslinger 2001).

The drawback is that ingesting sulindac, like most NSAIDs, is not risk-free. Some of the NSAIDs notorious side effects (includingdyspepsia, gastritis, peptic ulcer, gastrointestinal bleeding, hemorrhagic stroke, and perforation of gastroduodenal ulcers (Wolfe, Lichtenstein and Singh 1999) are thought to involve defects in the maintenance of intestinal mucosal integrity. NSAIDs also inhibit wound healing, including ulcer healing.

Initially, several groups attempted to modify NSAIDs to enhance their efficacy and/or safety and evaluated nitric oxide-donating NSAIDs and anamide derivative of sulindac (Rigas and Williams 2008, Piazza, et al. 2009). While highly efficacious, NO-donating agents showed evidence of genotoxicity. For our synthesis of P-S, we used a linker molecule to bridge the conventional NSAID sulindac to adiethylphosphate moiety. We observed that P-S is more efficacious compared to conventional sulindac when used in both colon cancer prevention and treatment. In particular, in Min mice, a model of colon cancer in which mice develop numerous

polyps in the small and large bowel, P-S combined with DFMO prevented 91% of tumors (Mackenzie, et al. 2010). The safety of P-S has been documented in several preclinical models, including nude mice, Min mice and rats. When compared directly to conventional sulindac, P-S demonstrated both safety and efficacy.

In this chapter, I report on P-S's metabolism, PK and biodistribution in mice. Our results establish the metabolic pathways of P-S *in vivo* and *in vitro,* as well as its PK and biodistribution.

MATERIALS AND METHODS

Reagents

P-S was kindly provided by Medicon Pharmaceuticals, Inc, Stony Brook, NY. Sulindac, sulindac sulfide (SSide), sulindac sulfone (SSone), bis(4-nitro phenyl)-phosphate, and CH3CN of HPLC grade were obtained from Sigma-Aldrich (St. Louis, MO). Sulindac glucuronide, SSide glucuronide and SSone glucuronide were obtained from CacheSyn Inc, (Mississauga, Canada). Mouse, rat and human liver microsomes, human intestinal microsomes, rat and human liver cytosol and NADPH regenerating solution were obtained from BD Biosciences (San Jose, CA).

Cell Lines

SW480 and HT-29 colon cancer cells were obtained from ATTC (Manassas, VA). Cell viability was determined using an MTT assay as per the manufacturer's protocol (Roche Diagnostics).

Cells were grown at 37 °C in 5% CO_2 in the specific medium suggested by ATCC and supplemented with 10% fetal calf serum (Mediatech, Herndon, VA), penicillin (50 U/ml) and streptomycin (50 µg/ml; Life Technologies, Grand Island, NY).

HPLC Analysis

The HPLC system consisted of a Waters Alliance 2695 Separations Module equipped with a Waters 2998 photodiode array detector (328 nm) and a Thermo Hypersil BDS C18 column (150 x 4.6 mm, particle size 3 µm) as previously described (Xie, et al. 2011a). Briefly, the mobile phase consisted of a gradient between buffer A (formic acid, CH_3CN, H2O (0.1:4.9:95 v/v/v)) and buffer B (CH_3CN) at a flow rate of 1 ml/min at 30^{o}C. An application of

gradient elution from 70% buffer A to 100% buffer B from 0-6 min, and it was maintained at 100% buffer B until 8 min.

LC-MS/MS Analysis

The LC-MS/MS system consisted of a Thermo TSQ Quantum Access (Thermo-Fisher) triple quadrupole mass spectrometer interfaced by an electrospray ionization probe with an Ultimate 3000 HPLC system (Dionex Corporation, Sunnyvale, CA). Analysis was carried out as previously described (Xie, et al. 2011a). In brief, chromatographic separations were achieved on a Luna C18 column (150 x 2 mm), and the mobile phase consisted of a gradient from 10% to 95% CH_3CN.

P-S Metabolism by Liver Microsomes

P-S was preincubated at 37°C for 5 min with NADPH-regenerating solution (1.3 mM NADP, 3.3 mM D-glucose 6-phosphate, 3.3 mM MgCl2, and 0.4 U/ml glucose-6-phosphate dehydrogenase) in 0.1 M potassium phosphate buffer (pH 7.4) as previously described (Xie, et al. 2011a). In short, the reaction was initiated by the addition of liver microsomes (protein concentration 0.5 mg/ml) or intestinal microsomes (protein concentration 0.25 mg/ml) and samples were maintained at 37°C for various time points. Next, 0.3 ml aliquots were mixed with 0.6 ml of CH_3CN, vortexed, and then as previously described (Gao et al., 2005). The supernatants were subjected to HPLC analyses.

P-S Metabolism by Rat and Human Liver Cytosol

P-S (100 μM) was preincubated at 37°C for 5 min with 10 mM dithiothreitol in 0.1 M Tris buffer (pH 7.4). The reaction was initiated by the addition of liver cytosol (protein

concentration 2 mg/ml) and samples were maintained at 37°C for various time points as previously described (Xie, et al. 2011a). Next, 0.3-ml aliquots were mixed with 0.6 ml of CH_3CN, vortexed, and then centrifuged. Supernatants were subjected to HPLC analyses.

P-S Metabolism by Cultured Human Colon Cancer Cells

To study the metabolism of P-S, SW480 human colon cancer cells were seeded overnight in 60 mm plates at a density of $2.5x10^5$ cells/mL. As previously described (Xie, et al. 2011a), P-S was added to the medium (final concentration 100 μM) and incubated with the cells for up to 6h. Cells were washed with PBS and lysed. CH_3CN was added to extract P-S and its metabolites from the cells, and the extracts were analyzed by HPLC analysis.

PK Studies in Mice

As previously described (Xie, et al. 2011a) female BALB/C mice were treated with P-S or sulindac by gastric gavage. Animals were euthanized at various time points after drug administration. Blood samples were collected and immediately centrifuged. The resulting plasma was deproteinized by a predetermined volume of CH_3CN. P-S and its metabolites were analyzed by HPLC.

PK parameters in plasma were determined by noncompartmental PK data analysis using PK Solutions 2.0 software (Summit Research Services, Montrose, CO). The PK parameters determined include maximal plasma concentration (C_{max}), time to reach maximal plasma concentration (T_{max}), elimination half-life ($t_{1/2}$), and the area under the concentration–time curve (AUC).

Tissue Distribution Study

Following P-S administration, the heart, liver and kidney of sacrificed animals were collected, homogenized and sonicated in PBS. P-S and its metabolites were extracted as previously described (Xie, et al. 2011a). After centrifugation, the supernatants were subjected to HPLC analysis.

As previously described (Xie, et al. 2011a), levels of P-S and its metabolites were detected in the lining of the stomach and duodenum, we harvested these two organs in toto after washing away their contents with PBS 3x, followed by a 10% DMSO in PBS 2x to remove gastric contents as well as P-S that may have been absorbed on the gastroduodenal mucosa. Control experiments revealed that 10% of DMSO preserved intact the mucosa and removed quantitatively adhering P-S residues following its oral administration.

Statistical Analysis

Results from at least 3 independent experiments and expressed as mean $\pm$ SD were analyzed by the student's t-test. *$p<0.05$ was considered significant.

RESULTS

P-S Metabolism by Liver and Intestinal Microsomes

Initially, our approach in the analysis of metabolism of P-S was to determine its transformations by liver microsomes. These microsomes represent an enriched source of the major metabolic enzymes that, in general, render xenobiotic drugs more polar andeasier to eliminate from the body (Bajrami, Zhao, Schenkman and Rusling 2009). Of note, oxidative drug metabolism is the principle means of drug clearance.

Dr. Gang Xie determined metabolism of P-S by rat liver microsomes (RLM) generated three metabolites, P-S sulfone, sulindac and sulindac sulfone (SSone). Sulindac and SSone were identified by comparing their chromatographic retention time and UV spectra to those of authentic compounds (Figure 1-1). P-S sulfone was identified by LC-MS/MS analysis. The mass spectrum of P-S sulfone showed a [M+Na]+ ion at m/z 602.8, which was further fragmented at its carboxyester and phosphotriester bonds to generate m/z 355 and 427, respectively (Figure 1-1B, C). Of note, this fragmentation pattern has also been observed for other phospho-NSAIDs such as phospho-ibuprofen (Xie, et al. 2011b), indicating that the fragmentation at ester bonds is common for phospho-compounds. The identification of P-S sulfone was also supported by its UV absorption spectrum that is identical to that of SSone. Apparently, the linker-phosphate moiety of P-S does not contribute to its UV absorption.

These findings, indicating oxidative and hydrolytic transformations of P-S, suggest two metabolic pathways (Figure 1-1D). First, P-S is oxidized to form P-S sulfone, which is then hydrolyzed to SSone. Second, P-S can be hydrolyzed to produce sulindac, which can be then

oxidized to produce SSone. In summation, P-S sulfone and sulindac are intermediate products in the metabolic transformations of P-S by RLM, with SSone being the final product.

The metabolism of P-S by RLM was rather quick (Figure 1-2A). Approximately 75% of P-S was consumed within 10 min after the initiation of the reaction, and its conversion to metabolites was almost complete 40 min later, when only ~2% of P-S remained in the reaction mixture. Consistent with this result, levels of SSone, the final product, steadily increased reaching a plateau at ~40 min. The two intermediate products, sulindac and P-S sulfone, shared a similar kinetic behavior because both of these metabolites were produced from P-S and both can be converted to SSone. The levels of sulindac and P-S sulfone increased rapidly during the first 10 min of the reaction, indicating that initially the production of sulindac and P-S sulfone from P-S was dominant due to the high concentration of P-S. With the P-S level decreasing rapidly, the formation rate of sulindac and P-S sulfone from P-S decreased, leading to the steady decrease of the level of sulindac and P-S sulfone during the later phase of the reaction.

The differences between species in the isoform composition of drug-metabolizing enzymes, expression, and catalytic activity (Liu et al., 2010) led us to study the metabolism of P-S by human liver microsomes (HLM). HLM also converted P-S to sulindac, P-S sulfone and SSone (Figure 1-2B). The level of P-S in the reaction mixture decreased continuously, while that of SSone showed a steady increase. On the other hand, the levels of sulindac and P-S sulfone increased rapidly within the first 5 min, then plateaued (Figure 1-2B).

The metabolism of P-S by HLM was qualitatively similar to that of RLM but differed from it in terms of the reaction rates (Figure 1-2). Compared to RLM, P-S is more stable in HLM, the elimination $t_{1/2}$ of P-S in HLM is >3 times longer (38.8 min vs. 12.1 min) and the

production of SSone is much slower in HLM (the final concentration of SSone is ~5 times lower). Thus, P-S was more rapidly and more extensively metabolized by RLM than by HLM.

P-S Metabolism by Liver Cytosol

Previous studies have shown that sulindac is reduced to SSide by rat liver cytosol (RLC) (Ratnayake, Hanna, Anders and Duggan 1981), we examined the metabolism of P-S by RLC. Three metabolites of P-S (sulindac, P-S sulfide and SSide) were readily detected in the reaction mixture of P-S and RLC, indicating that P-S undergoes hydrolysis and reduction reactions in RLC. P-S can be hydrolyzed and reduced to form sulindac and P-S sulfide, respectively, both of which can further be transformed to SSide (Figure 1-3A). RLC P-S levels decreased continuously, while SSide continually increased (Figure 1-3B). Sulindac and P-S sulfide displayed similar kinetic patterns: both reached their peak value at approximately 2h and subsequently became stable or slightly decreased until the end of the observation.

P-S Metabolism in Colon Cancer Cells

Having demonstrated the ability of P-S to inhibit cancer cell growth (Mackenzie et al., 2010), we studied its metabolism in SW480 colon cancer cells. P-S is immediately uptaken by the cells (Figure 1-4A). Its levels reached a plateau within 10 min and primarily remained intact in the cells while sulindac, the hydrolysis product of P-S, was undetectable. This finding is consistent with reports of low esterase activity in cells (Lamboursain et al., 2002).

Approximately 10% of unhydrolyzed P-S is reduced and oxidized to form P-S sulfide and P-S sulfone, the two processes displaying somewhat different kinetics (Figure 1-4A). P-S sulfone reached its peak level within 10 min and then remained stable, whereas P-S sulfide reached its peak level at about the same time but dropped afterwards (the reduction reaction of P-S is

reversible while the oxidation of P-S is irreversible). As the cells lacked significant amounts of sulindac and have low esterase activity, we did not detect reduction/oxidation products of sulindac.

Metabolism and PK of P-S in a Mouse Model

In this part of the study I conducted an analysis of the PK properties of P-S in mice. Animals were treated with a single dose of P-S (158 mg/kg in corn oil) by gastric gavage. Three major metabolites, sulindac, SSide and SSone, were detected by HPLC in plasma (Figure 1-5). Sulindac was the main metabolite of P-S; its plasma C_{max} was 234 μM, the T_{max} was 2 hr and the $t_{1/2}$ was 3.5h. Underscoring the rapid metabolic disposition of P-S, plasma levels of sulindac dropped substantially by 4 hr, becoming negligible at 8 hr. SSone followed a similar pattern, but with much smaller C_{max} and markedly prolonged $t_{1/2}$ (19.9 hr). SSide appeared at even lower levels and with a broad peak.

Intact P-S in murine plasma was not detectable by the UV detector, suggesting high carboxyesterase activity in blood. To test this idea, we evaluated the effect of bis(4-nitro phenyl)-phosphate (BNPP), a specific inhibitor for carboxyesterase (Morishita et al., 2005), on the hydrolysis of P-S by plasma *in vitro*. We then evaluated the effect of BNPP on the hydrolysis of P-S *in vivo*. P-S (158 mg/kg in corn oil) generated 2.9 μM intact P-S in mouse blood 1hr following its co-administration with BNPP (200 mg/kg), whereas intact P-S was not detected in the blood of mice not receiving BNPP. These results indicate that BNPP effectively inhibits the hydrolysis of P-S *in vitro* and *in vivo*.

For purposes of comparison, I performed parallel PK studies of conventional sulindac administered to mice orally at a dose equimolar to P-S (100 mg/kg in corn oil). In addition to

intact sulindac, we detected its two main metabolites in plasma, SSide and SSone. Their $AUC_{0\text{-}24hr}$ were SSide >> sulindac >> SSone. As shown in Table 1-1, there are four main PK differences between P-S and conventional sulindac. First, in terms of $AUC_{0\text{-}24h}$ the three main metabolites of P-S have similar $AUC_{0\text{-}24hr}$ values (632-707 μM*hr), whereas those of conventional sulindac vary widely (357-2,697 μM*hr). Second, the PK parameters of SSone derived from P-S differ from those of SSone derived from conventional sulindac: T_{max}: 2 vs. 24 hr; t½: 19.9 vs. 3.2 hr; $AUC_{0\text{-}24hr}$: 673 vs. 357 μM*hr. And, third, even though the doses of the P-S and sulindac were equimolar, the sum of the plasma $AUC_{0\text{-}24hr}$ of the three compounds (sulindac, SSone and SSide) derived from P-S is 44% of the $AUC_{0\text{-}24hr}$ of the same three compounds derived from conventional sulindac.

We also determined the PK parameters of P-S administered at the same dose either orally dissolved in carboxymethyl cellulose or intraperitoneally dissolved in PBS (Figure 1-6, Table 1-1). Compared to the values of P-S administered orally in corn oil, in both cases, the C_{max} of each compound was significantly lower; the $t_{1/2}$ was similar with the exception of SSone that was reduced by about 75%; and the total $AUC_{0\text{-}24hr}$ (sulindac, SSone, SSide) was reduced by 80-90%).

Tissue Distribution of P-S in Mice

To evaluate the biodistribution of P-S in mice, Dr. Ting Nie determined the levels of P-S and its metabolites in heart, liver and kidney. In addition to the three major metabolites that we detected in plasma, we also detected intact P-S and P-S sulfone in these tissues (Table 1-2). It is evident that, despite its rapid hydrolysis in blood, P-S survives in appreciable amounts in other tissues, with the liver showing the highest level of P-S.

The simplest explanation of our findings was that at the dose of 150 mg/kg, P-S plasma levels are below our detection limit. Consequently, a dose of P-S three times higher (450 mg/kg) was administered to mice. Three glucuronidation metabolites of P-S (sulindac glucuronide, SSone glucuronide and SSide glucuronide) were detected in liver; whereas their levels in plasma and other tissues are quite low (Table 1-2). SSone glucuronide and SSide glucuronide were identified by LC-MS/MS analysis. The mass spectrum of SSone glucuronide showed a [M-H]- ion at m/z 547, which was fragmented at its acyl-glucuronide bond to generate m/z 326.8 and 192.7 (Figure 1-6A). This fragmentation pattern was also observed for other glucuronides such as indomethacine glucuronide, indicating that the fragmentation at their glucuronide bonds is common for acyl glucuronides. The identification of SSone glucuronide and SSide glucuronide were also confirmed using authentic compounds. SSide glucuronide was detected in abundance (704 μM) in bile obtained from the gallbladder of mice 4 hr after the oral administration of P-S 500 mg/kg.

Given the superior gastrointestinal safety of P-S over conventional sulindac (Mackenzie et al., 2010; Huang et al., 2011), we determined the $AUC_{0\text{-}24hr}$ of drug levels in the gastroduodenal wall of mice following oral administration of equimolar amounts of P-S or sulindac. As expected, the equimolar doses of P-S and sulindac generated similar total drug levels (Table 1-3). Unlike other organs (Table 1-2), however, 71% of P-S was intact, sulindac was its major metabolite, and SSide and SSone were present at very low levels. Conventional sulindac remained largely intact (66%) and SSide was its main metabolite (29% of the total mass), whereas SSone represented only 5% of the total. Compared to mice treated with an equimolar amount of conventional sulindac, in mice treated with P-S the amount of sulindac was 3.0 times lower, the amount of SSide was 9.4 times lower, and SSone was 1.8 times lower. These

striking differences between the two compounds may account for their differences in gastroduodenal toxicity.

DISCUSSION

Our results establish the metabolic pathways of P-S *in vitro* and *in vivo* and determine its PK parameters and tissue distribution in mice. The metabolism of P-S established through a series of studies that included liver microsomes, cultured cells and mice, follows four metabolic pathways: (1) Oxidation/reduction reactions, (2) hydrolysis reactions, (3) transformations of sulindac, and (4) Glucuronidation reactions.

At least two enzymes appear to play important roles in these transformations of P-S: carboxyesterases and UDP-glucuronosyltransferases (UGTs). Carboxyesterases (CEs) participate in the hydrolysis of P-S, an ester drug. This idea was supported by our finding that bis(4-nitro phenyl)-phosphate, a specific inhibitor for CEs, completely inhibited the hydrolysis of P-S. CEs are abundant in mouse small intestine, plasma and liver microsomes (Taketani et al., 2007), likely accounting for the significant hydrolysis of P-S in mice. Based on their substrate specificities, CEs are primarily classified into CEs1, which hydrolyze esters with a large acyl moiety, and CEs2, which hydrolyze those with a small acyl group (Hosokawa, 2008) (Taketani et al., 2007). P-S has a much larger acyl group than the substrates for CEs1 such as cocaine, meperidine, methylphenidate and oseltamivir (Hosokawa, 2008), suggesting that P-S may be a substrate for CEs1.

Glucuronidation is one of the major pathways that eliminates and detoxifies lipophilic xenobiotics. UGTs glucuronidate the three metabolites of P-S (sulindac, SSone or SSide) at their -COOH group to form the corresponding acyl-glucuronides. Thus it was not surprising to find that their levels in bile approached mM concentrations, whereas in blood they were in the sub-μM range, indicating that the bile is a major excretion route for P-S. Acyl glucuronides are known to be susceptible to intramolecular acyl migration and to show high electrophilicity in

reactions with sulfanyl and hydroxyl groups of proteins (Kirschning et al., 1997). These two properties of the acyl glucuronides may explain, in part, their low blood levels.

Mouse, rat and human liver microsomes generated the same metabolites of P-S, suggesting the same metabolic pathway of P-S in these species. This finding, reflecting the highly conserved drug-metabolizing enzymes among different species, helps to predict the efficacy of P-S in humans, since its metabolites appear important for its anticancer effect. On the other hand, P-S was metabolized more extensively and rapidly by the liver microsomes of mouse and rat than of human. These *in vitro* kinetic data, correlated with our PK data in mice, could help predict its PK in humans (Liu et al., 2010).

PK and biodistribution studies demonstrated that following its administration to mice, P-S is rapidly absorbed, metabolized and distributed to blood and other tissues. Our PK findings provide important information concerning several aspects of the pharmacology of P-S, including its administration, efficacy and safety, as discussed below.

It is clear from our data that corn oil is far superior to carboxymethyl cellulose and PBS for the administration of P-S, overcoming its poor aqueous solubility, which hinders efficiency and bioavailability (Gupta and Moulik, 2008). Corn oil is known to form microemulsions, which enhance the bioavailability of hydrophobic drugs by increasing their solubility and residence time in the intestine through bioadhesion (Acosta et al., 2004).

The PK study shows that P-S undergoes rapid hydrolysis in mice, which nonetheless is not complete, allowing its transport to other tissues where it is present at variable but always low levels (except for the gastroduodenal wall). Given that P-S inhibits cancer cell growth ≥13-fold more potently than sulindac (Mackenzie et al., 2010), its presence in tissues may be critical to its anticancer efficacy. In addition to intact P-S, four of its metabolites, which are present at

substantial concentrations, are known to have anticancer potency. Sulindac and SSide inhibit cancer cell growth through a multitude of mechanisms, both COX-dependent and COX-independent (Shiff et al., 1995; Shiff and Rigas, 1999; Hanif et al., 1996). P-S sulfide inhibits the growth of human colon cancer cells more potently than P-S by reducing the intracellular polyamine pool that is essential for cancer cell growth (Huang et al., 2010). Finally, SSone inhibits cancer growth by stimulating polyamine acetylation and export from the cell (Babbar et al., 2003).

These PK data indicate that P-S behaves both as a primary anticancer agent and as a pro-drug. Lowering exposure of P-S to CEs may enhance its anticancer efficacy. Of great interest, human plasma has ~10-fold lower CE activity compared to mice (Nagy et al., 2000). Thus, it is reasonable to predict that in humans the plasma and tissue levels of intact P-S will be higher, leading to greater anticancer efficacy. The role of esterases in the efficacy of P-S is underscored by our finding that cultured human cancer cells and a normal colon cell line lack detectable esterase activity. Thus, P-S is not hydrolyzed by these cells, a finding consistent with its higher potency compared to its hydrolysis products (Mackenzie et al., 2010).

The PK comparison between P-S and conventional sulindac yielded results that likely explain the greater safety of P-S, particularly concerning gastroduodenal toxicity, the most cited side effect of sulindac. A striking feature of the PK of P-S vs. sulindac was that equimolar concentrations of these two compounds generated very different amounts of blood metabolites: the $AUC_{0\text{-}24h}$ of the total metabolites (sulindac, SSide and SSone) in plasma following P-S administration is approximately 2.3-fold lower than that obtained with sulindac administered at an equimolar dose. Furthermore, in terms of individual metabolites, P-S generated roughly half the amount of sulindac, ¼ the amount of SSide, and twice the amount of SSone in plasma based

on $AUC_{0\text{-}24hr}$ values. These are very favorable differences in terms of safety. SSone has a better safety profile than SSide, in particular regarding gastrointestinal toxicity (Glavin and Sitar, 1986). The underlying mechanisms have been investigated extensively; for example, SSide inhibits COX-1 and COX-2 >48-fold more potently than SSone, depleting the physiologically important prostaglandins (PGs) and contributing to the higher toxicity of SSide (Piazza et al., 2009). Likewise, SSide, but not SSone, inhibits 5-lipoxygenase, suppressing production of leukotrienes, important immune mediators similar to PGs (Steinbrink et al., 2010). Moreover, SSide, but not SSone, causes mitochondria uncoupling that induces hepatic toxicity (Leite et al., 2006).

In this chapter, I have shown that P-S undergoes extensive transformations *in vivo* and *in vitro* yielding at least eight metabolites. These metabolites, together with intact P-S, may play important roles in cancer control. The PK and biodistribution features of P-S provide a likely explanation of its superior safety, especially regarding its ability to spare the gastroduodenal mucosa.

FIGURES

Table 1-1. PK parameters of P-S and sulindac in mice.

Drug administered	Delivery vehicle	Delivery route	Measurement	C_{max} (μM)	T_{max} (h)	Elimination $t_{1/2}$ (h)	AUC (μM*h)	Sum of AUC (μM*h)
Phospho-sulindac	Corn oil	Oral	sulindac	234	2.0	3.5	707	2,012
			sulindac sulfone	69	2.0	19.9	673	
			sulindac sulfide	45	8.0	2.9	632	
	Carboxy methyl cellulose	Oral	sulindac	15	4.0	3.1	117	462
			sulindac sulfone	21	4.0	4.9	269	
			sulindac sulfide	6	4.0	3.0	76	
	PBS	IP	sulindac	11	0.8	5.2	41	168
			sulindac sulfone	8	4.0	4.1	97	
			sulindac sulfide	4	4.0	4.2	30	
Sulindac	Corn oil	Oral	sulindac	261	1.0	5.4	1,476	4,530
			sulindac sulfone	20	24.0	3.2	357	
			sulindac sulfide	190	8.0	4.3	2,697	

Experiments were done at least twice; values were generally within 10%

Mice were administered 158 mg/kg phosphosulindac or 100 mg/kg sulindac

Table 1-2. Drug levels in mouse tissue with oral administration of P-S.

	Intact PS	PS sulfone	Sulindac	Sulindac sulfide	Sulindac sulfone	Sulindac glucuronide	SSone glucuronide	SSide glucuronide
	pmol/mg protein (mean ± SEM)							
Dose = 150 mg/kg								
Liver	39±17	18±8	204±49	19±2	79±42	15±4	13±3	25±12
Heart	5±1	1±1	152±34	12±3	39±7	2±0	3±0	1±0
Kidney	4±1	3±1	499±105	25±7	94±18	2±1	3±1	2±0
***Plasma**	ND	ND	64±10	5±1	14±2	1±0	1±0	1±0
Dose = 450 mg/kg								
Liver	52±8	17±6	372±40	21±6	84±40	66±11	14±2	17±4
Heart	31±6	8±1	538±63	19±4	99±27	22±6	15±4	4±2
Kidney	14±3	6±1	888±107	25±8	136±66	52±15	10±2	7±2
***Plasma**	5±1	1±0	157±2	6±2	26±8	8±2	4±1	1±0

**Plasma levels were expressed as μM.*

ND, Not Detectable

Table 1-3. Gastroduodenal drug levels in mice treated with P-S or sulindac

	Phospho-sulindac		Sulindac	
	$AUC_{0\text{-}24\ h}$ in stomach-duodenum			
	pmol/mg protein*h	% of total	pmol/mg protein*h	% of total
PS	16,698	71	0	0
PS sulfone	94	0	0	0
Sulindac	5,551	23	16,465	66
Sulindac sulfide	774	3	7,298	29
Sulindac sulfone	567	2	1,037	4
Total	23,684	100	24,800	100

PS 150 mg/kg or sulindac 100 mg/kg (equimolar) in corn oil were given orally once.

Samples were obtained at 0, 1, 2, 4, 8, 12 and 24 h post-dosing.

Values are the average of two mice; results from each pair were within 15%

Figure 1-1. P-S metabolism by rat and human liver microsomes. (A) HPLC profile of P-S and its metabolites generated by RLM 10 min after P-S was incubated with RLM. P-S and its metabolites were extracted and fractionated by HPLC as described in Methods. (B) Mass spectrometry spectrum of P-S sulfone fraction collected from HPLC. (C) MS/MS spectrum of the major fragment ions of the P-S sulfone ion. (D) Metabolic transformations of P-S by liver microsomes**.** *(Experiment performed by Dr. Gang Xie)*

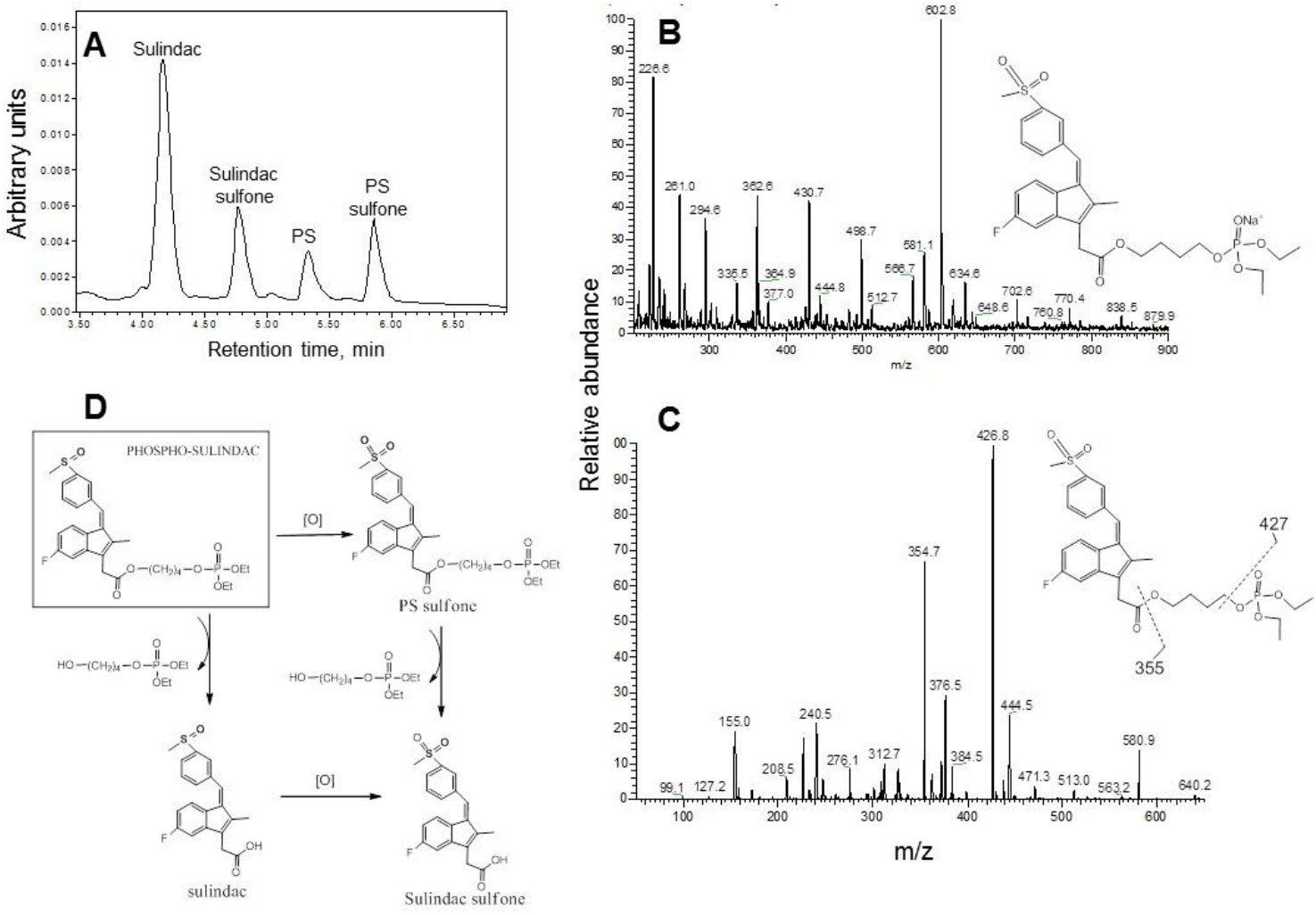

Figure 1-2. **Kinetics of P-S and its metabolites by rat and human liver microsomes.** P-S (35 μM) was incubated with RLM (A) or HLM (B) at 37°C for up to 90 min. P-S and its metabolites were extracted at the designated time points and assayed.

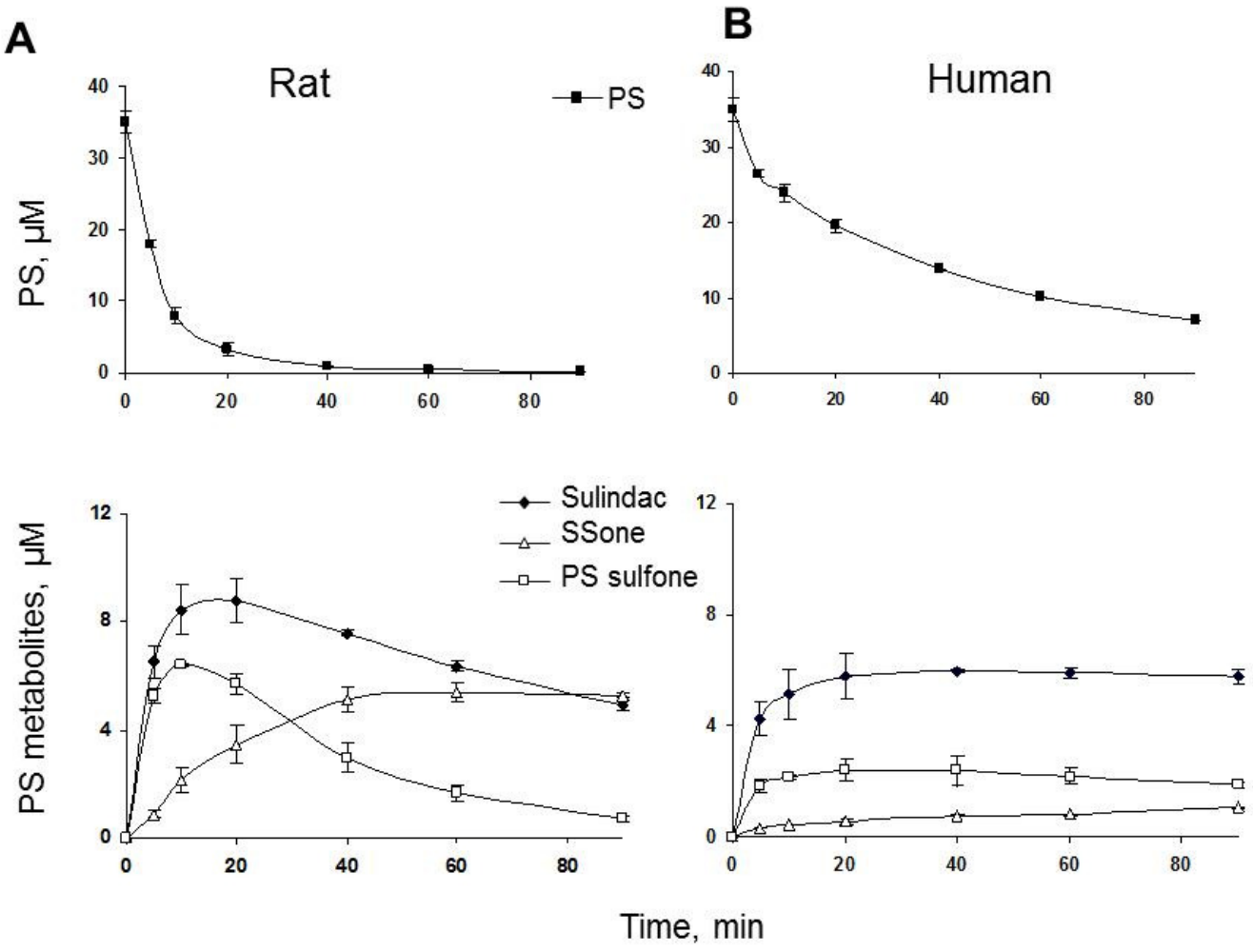

Figure 1-3. Metabolism of P-S by rat liver cytosol. Kinetics of P-S and its metabolites by rat liver cytosol. P-S (100 μM) was incubated with rat liver cytosol at 37°C for up to 7 hr. P-S and its metabolites were extracted at the designated time points and assayed.

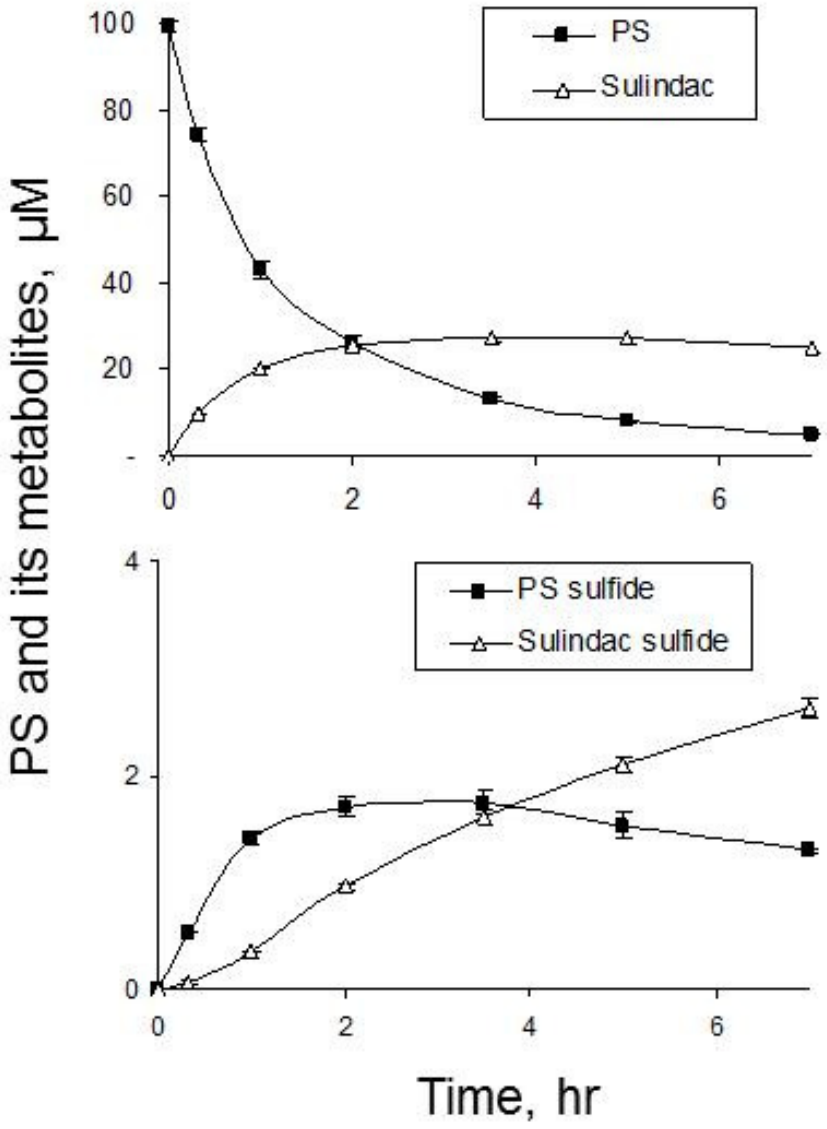

Figure 1-4. Kinetics of P-S and its metabolites in SW480 colon cancer cells. P-S (100 μM) was incubated with SW480 cells at 37°C for up to 6 hr. P-S and its metabolites were extracted at the designated time points and assayed.

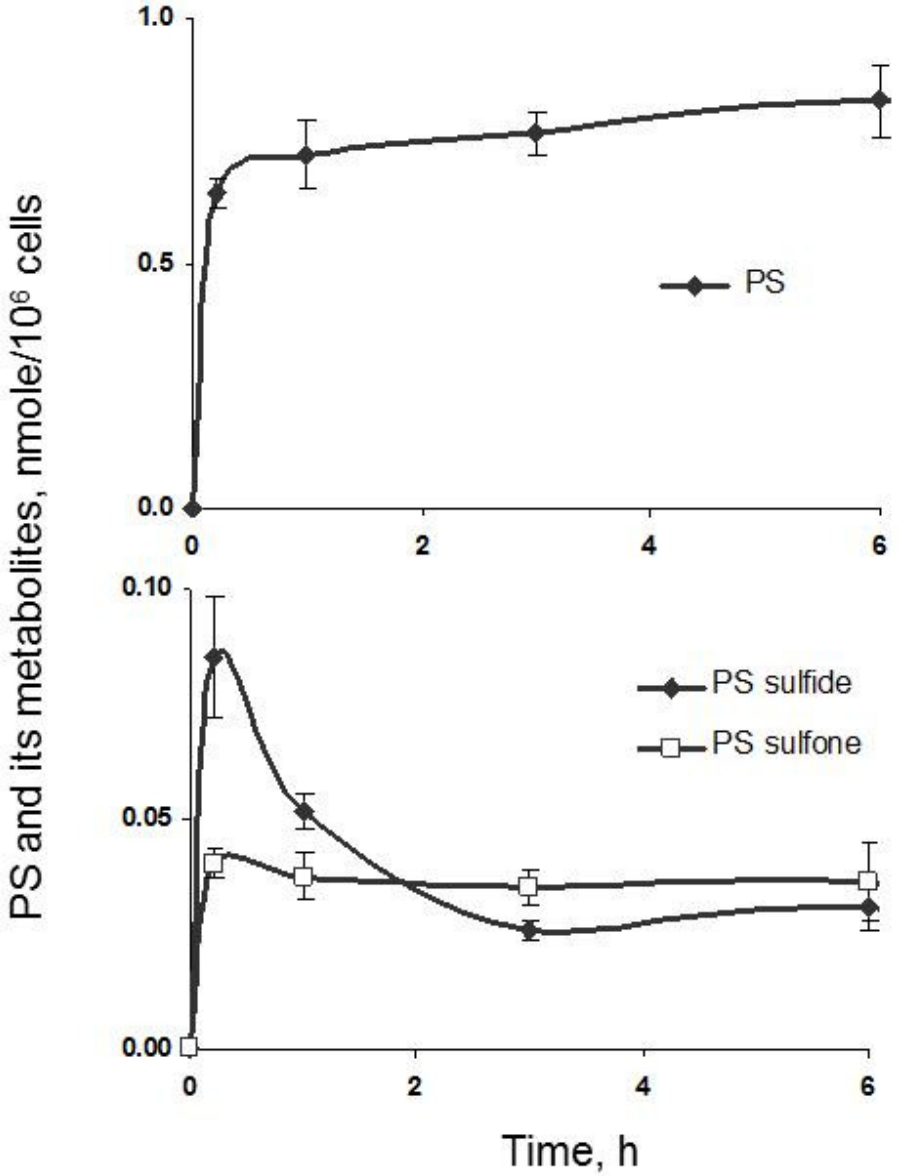

Figure 1-5. P-S and sulindac PK comparison in mice. Equimolar doses of sulindac (100 mg/kg) and P-S (158 mg/kg) in corn oil were administered to mice as a single dose by gastric gavage. Plasma levels of P-S metabolites were determined as described in Methods.

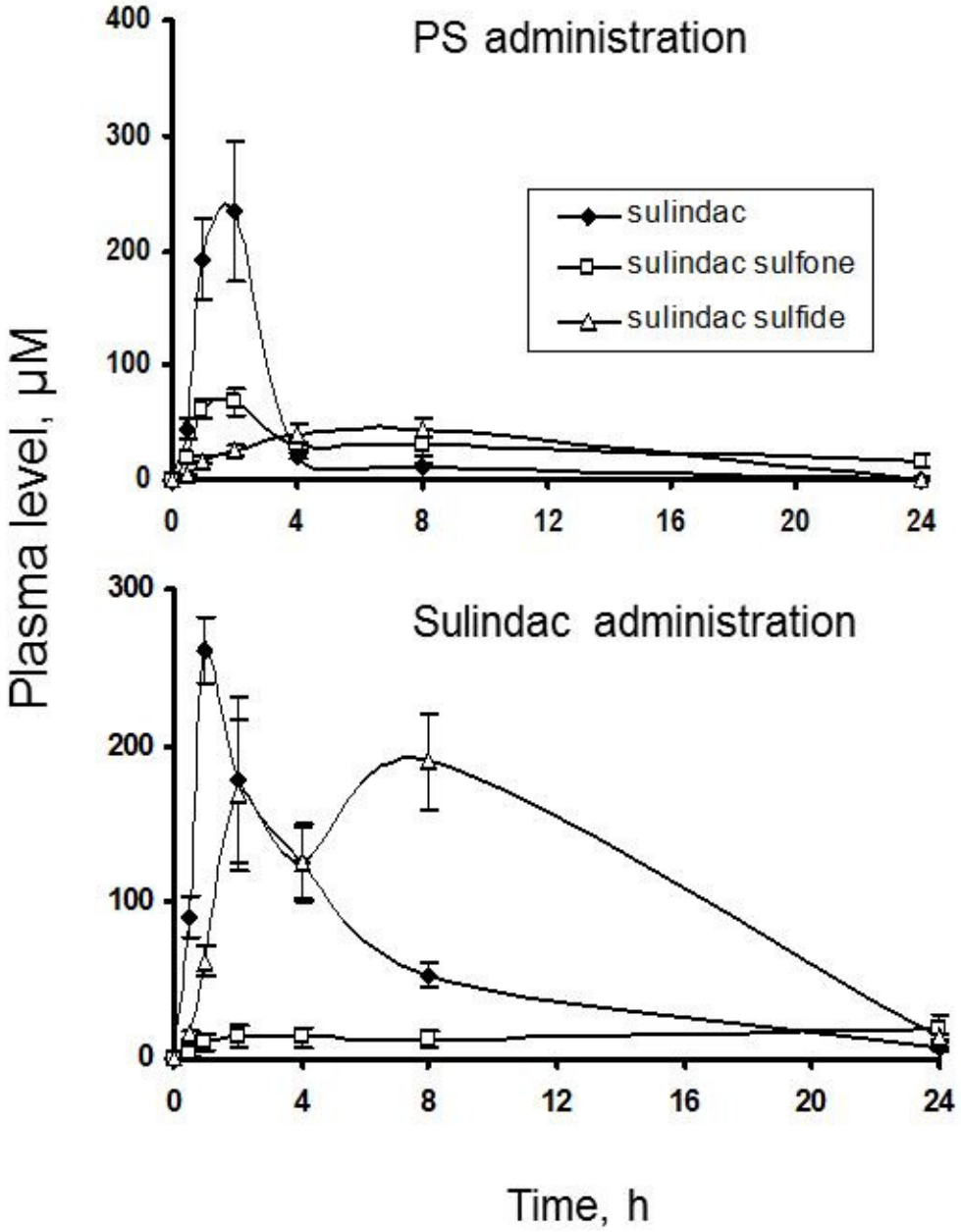

Figure 1-6. PK of P-S administered in carboxymethyl cellulose or PBS in mice. P-S (150 mg/kg) was administered to mice as a single dose orally in carboxymethyl cellulose (top) or intraperitoneal in PBS (bottom). Plasma levels of P-S metabolites were determined. *(Experiment performed by Dr. Gang Xie).*

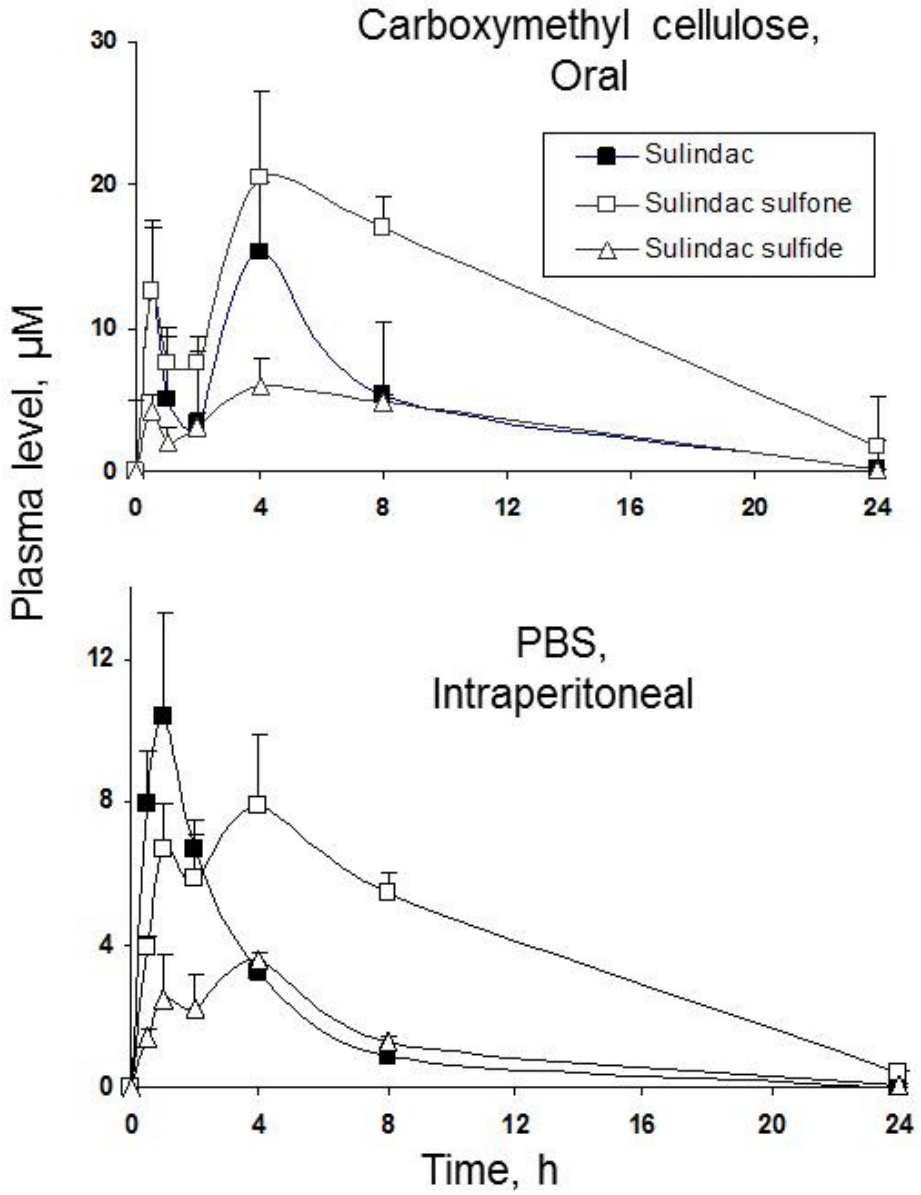

Figure 1-7. Overall metabolic pathways of P-S *in vitro* and *in vivo*. P-S is subjected to a series of reduction/oxidation reactions of its sulfoxide group and/or hydrolytic cleavages of its carboxy ester bond. The end result is eight metabolic products through three distinct and ultimately converging pathways.

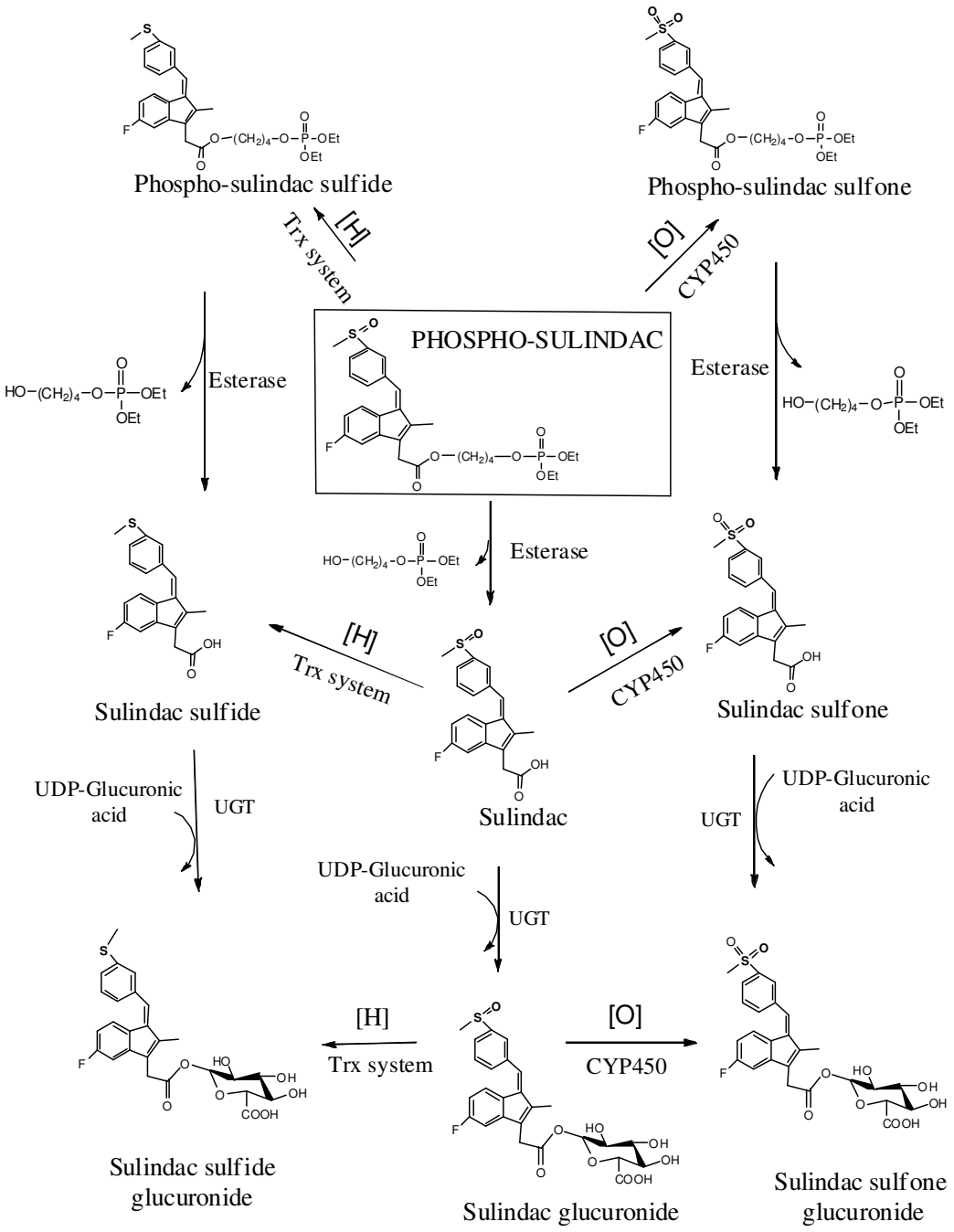

CHAPTER II

P-S AND PANCREATIC CANCER: EFFICACY

INTRODUCTION

The very limited progress in the treatment of pancreatic cancer in recent years combined with the dismal performance of currently available modalities creates an urgent need for the development of new therapeutic agents for this lethal cancer.

Nonsteroidal anti-inflammatory drugs (NSAIDs), such as sulindac, have shown chemopreventive activity against pancreatic cancer in preclinical trials. Although their chemotherapeutic properties have been demonstrated in numerous studies, their appeal is stunted for two major reasons: their limited efficacy and the undesired side effects associated with prolonged treatment periods (Sun, et al. 2011).

The chemotherapeutic potential of sulindac alone or in combination with other agents against pancreatic cancer has been explored in preclinical models. For example, Yip-Schneider *et al* have demonstrated inhibition of the growth of pancreatic cancer xenografts by sulindac alone or in combination with a derivative of the NF-κB inhibitor parthenolide (Yip-Schneider, et al. 2007). Although the efficacy of this combination was modest, these findings indicate the antitumor potential of sulindac against pancreatic cancer. Exisulind (sulindac sulfone) has also shown preclinical efficacy in pancreatic cancer (Haanen 2001).

Niitsu's group has reported the first human study in pancreatic cancer prevention using an NSAID. In their study they used sulindac for the prevention of pancreatic cancer in patients with branch duct-intraductal papillary mucinous neoplasms (BD-IPMNs). Sulindac 150 mg twice daily (combined with omeprazole to diminish its gastrointestinal toxicity), administered for 18 months significantly reduced branch duct diameter and mural nodule height of BD-IPMN (Hayashi, et al. 2009). Collectively, these studies suggest that NSAIDs, particularly sulindac, have some intrinsic efficacy against pancreatic cancer. Prompted by these findings, we studied P-S as an agent for the control of pancreatic cancer.

P-S consists of conventional sulindac bound to diethylphosphate via butane linker molecule (Figure 1). P-S displayed two pharmacologically important properties, compared to conventional sulindac: P-S: inhibited the growth of several cancer cell lines more potently both *in vivo* and *in vitro*, and was much safer. Of note, P-S, has shown significant chemopreventive activity against colon cancer (Mackenzie, et al. 2010).

In light of these findings, we explored the efficiency of P-S towards the treatment of pancreatic cancer. In addition to delivering this compound in conventional formulations, I explored nanoscience-based drug formulations, since the method of delivery can affect the pharmacological effect of a given drug (Papahadjopoulos, et al. 1991). I also analyzed the effect of liposome-encapsulated P-S (Lipo P-S) in pancreatic cancer models. For example, doxorubicin in liposomes is more efficacious than free doxorubicin (Batist, Harris, Azarnia, Lee and Daza-Ramirez 2006). Such enhanced efficacy is explained by the enhanced permeability and retention effect, which represents the preferential uptake of liposomes by tumor cells due to the leakiness of the vessels traversing a tumor (Maruyama 2011).

In this chapter, I describe my work on both the *in vitro* and *in vivo* efficacy of free P-S and P-S incorporated in liposomes in a pancreatic cancer animal model.

MATERIALS AND METHODS

Reagents

Phospho-sulindac (P-S) was synthesized as reported (Yiu, et al. 2006). Sulindac was purchased from Sigma (St Louis, MO). Annexin V was purchased from Invitrogen (Grand Island, NY). Propidium iodide (PI) and 5-bromo-2'-deoxyuridine (BrdU) were obtained from BD Bioscience (San Jose, CA). All general solvents and reagents were of HPLC grade or the highest grade commercially available.

Liposome-encapsulated P-S

Liposome-encapsulated P-S (Lipo P-S) was generated following standard procedures by Encapsula NanoSciences LLC (Nashville, TN, USA). The formulation is L-a-phosphatidylcholine (80 mg/ml), PEG-2000-DSPE (14.8 mg/ml) and P-S (100 mg/ml). The particle size is 200 nm. The concentration of Lipo P-S was determined by HPLC prior to use (Xie, et al. 2012).

Cell Lines

Human pancreatic cancer cell lines BxPC-3, MIA PaCa-2, Panc-1 and HPAF II were obtained from ATTC (Manassas, VA). Cells were grown at 37 °C in 5% CO_2 in the specific medium suggested by ATCC and supplemented with 10% fetal calf serum (Mediatech, Herndon, VA), penicillin (50 U/ml) and streptomycin (50 µg/ml; Life Technologies, Grand Island, NY).

Cell Viability Assay

Cell viability was measured by the 3-(4,5-dimethylthiazol-2-yl)-2,5-diphenyltetrazoliumbromide assay following the protocol of the manufacturer (Roche

Diagnostics). Cells ($1x10^5$/mL) were seeded overnight in 96-well plates. On the following day, cells were treated with either P-S or sulindac for 24, 48 or 72 hr. Following incubation with P-S, cells were treated with MTT reagents and cell determined.

Flow Cytometry

***Proliferation assay*.** Cells were seeded ($1.5x10^5$ cells/mL) in 6-well plates and treated with P-S or sulindac as indicated. Cells were trypsinized and treated with 5-bromo-2'-deoxyuridine and their fluorescence intensity was analyzed by FACSCaliber (BD Bioscience, San Jose, CA).

***Apoptosis assay*.** Cells were seeded ($1.5x10^5$ cells/mL) in 6-well plates and treated with P-S or sulindac as indicated. Cells were trypsinized and stained with Annexin V-FITC and PI for 15 min. Annexin V-FITC and PI fluorescence intensity was analyzed by FACSCaliber (BD Bioscience, San Jose, CA).

Pancreatic Cancer Xenograft

Six-week-old female BALB/c nude mice (Charles River, Wilmington, MA) were subcutaneously injected with $3.0x10^6$ MIA PaCa-2 cells ($1.5x10^6$ in the right and left flank, respectively).

Study #1: P-S vs Sulindac. Animals were separated into 3 cohorts, vehicle, P-S and sulindac. In each cohort there were 6 mice. Animals were treated by oral gavage with vehicle (corn oil), P-S (100 mg/kg/d), and sulindac (33mg/kg/d) for 4 weeks.

***Study #2: Lipo P-S*:** Animals were separated into 4 cohorts: vehicle, P-S, Lipo P-S and empty liposome. In each cohort there were n=6 mice. Animals were treated by oral gavage 1x/day with

vehicle (corn oil), or P-S (100 mg/kg/d), Lipo P-S (100mg/kg/d) by intraperitoneal injection (IP), or emply lipo (IP) for 4 weeks.

Tumor size was determined with a digital microcalipter. Upon completion of the study, animals were euthanized and tumors collected, measured and embedded in paraffin sections.

Immunohistochemistry

MIA PaCa-2 xenograft tissue was fixed in 10% phosphate buffered formalin for 16 hours, as previously described (Ouyang, et al. 2006). The formalin-embedded tissue was cut into approximately 2 cm intervals and after dehydration each piece was embedded individually into paraffin blocks.

Proliferation (Ki-67): Paraffin-embedded sections were de-paraffinized, rehydrated, and microwave heated for 10 min in 0.01 M citrate buffer (pH 6.0) for antigen retrieval. Then, 3% hydrogen peroxide was applied to block endogenous peroxidase activity. After blocking, Ki-67 (proliferation marker) or control IgG were incubated overnight at 4^{o}C. Slides were washed for 5m each, 3x's with PBS. The biotinylated secondary antibody and the streptavidin-biotin complex (Vector Laboratories, Burlingame, CA) were applied, each for 30 min at room temperature. After rinsing with PBS, the slides were immersed for 5 min in the coloring substrate 3,3V-diaminobenzidine (DAB, Sigma) 0.4 mg/mL with 0.003% hydrogen peroxide, then rinsed with distilled water, counterstained with hematoxylin, dehydrated, and mounted.

Apoptosis (TUNEL): Terminal deoxyribonucleotide transferase–mediated nick-end labeling (TUNEL) staining was done using the In situ Cell Death Detection kit from Roche Applied Science (Indianapolis, IN) as previously described (Ouyang, et al. 2006). Briefly, paraffin-embedded tissues were deparaffinized and rehydrated. Endogenous peroxidase activity

was quenched by hydrogen peroxide and tissue protein was hydrolyzed with proteinase K. Sections were incubated with TUNEL reaction mixture (fluorescein-labeled nucleotides) or negative control (without terminal deoxynucleotidyl transferase enzyme) at 37^{o}C for 1 hr. Slides were then incubated with converter-POD solution (antifluorescein antibody conjugated with POD) for 30 min at 37^{o}C, treated with DAB, and counterstained with hematoxylin, dehydrated, and mounted.

A trained pathothologist unaware of sample identity identified positively stained cancer cells (cells with a brown nucleus were considered labeled and those with a blue nucleus unlabeled). Cells were counted and imaged using Adobe Photoshop and Image J (NIH).

Statistical Analysis

Results from at least 3 independent experiments and expressed as mean $\pm$ SD were analyzed by the student's t-test. *$p<0.05$ was considered significant.

RESULTS

P-S is More Efficacious than Sulindac in inhibiting the growth of Pancreatic Cancer Cells

Table 2-1 summarizes the 24, 28, and 72h IC_{50} of P-S as well as that of sulindac in a panel of 4 pancreatic cancer cell lines, namely BxPC-3, MIA PaCa-2, Panc-1 and HAPF-II. There was a marked difference in IC_{50} between P-S and sulindac in all 4 cell lines. The IC_{50} of sulindac was consistently >2,000 μM, and in fact, its true value could not be determined due to its limited solubility that would require high concentrations of its respective solvent DMSO in the culture medium. Of note, P-S showed enhanced potency when compared to sulindac. This potency enhancement was time dependent, becoming higher the longer the incubation period with P-S. At 24 hr, P-S showed an average potency enhancement of 22.5 over sulindac; at 48 hr, 36.0; and at 72 hr, 60.8.

In Vitro Cytokinetic Effect of P-S

A critical property of chemotherapeutic agents is their ability to modify the kinetics of the target cell. Ideally, efficacious chemotherapeutic agents inhibit cell renewal (proliferation) and enhance cell death, primarily by the induction of apoptosis. The cumulative net effect translates into inhibition of cancer growth, the sought-after outcome of chemotherapy. The same applies to chemoprevention, a case in which the test agent often attacks cells of lower complexity compared to fully-blown cancer cells. Thus, I determined the effect of P-S on both cell proliferation and apoptosis using cell staining by BrdU and Annexin-V/PI, respectively, as described in Methods.

Bromodeoxyuridine (BrdU) is a synthetic thymidine analog that gets incorporated into a cell's DNA when the cell is dividing (during the S-phase of the cell cycle). Antibodies against

BrdU that are conjugated to fluorescent markers (like FITC) can be used to label these cells, thereby providing visual evidence of cell proliferation. P-S had a significant effect on cellular proliferation, reducing BrdU-FITC (+) cells by 87.0% at 0.5xIC_{50}, and 93.3% at 1.0xIC_{50} (Figure 2-1A). Sulindac 1.0xIC_{50} reduced BrdU (+) cells by 70.3% (Figure 2-1A), 20% less in comparison to P-S 1.0xIC_{50}. These results show that while both P-S and sulindac are able to reduce pancreatic cancer cell proliferation significantly, P-S was more potent than its parent compound.

Annexin V staining is a simple and effective method to detect one of the earliest events in apoptosis—the externalization of phosphatidylserine—in living cells. This assay takes advantage of the fact that phosphatidylserine (PS) is translocated from the inner (cytoplasmic) leaflet of the plasma membrane to the outer (cell surface) leaflet soon after the induction of apoptosis, and that the Annexin V protein has a strong, specific affinity for PS (Xu, et al. 2008). PS on the outer leaflet is available to bind labeled Annexin V, providing the basis for a simple staining assay (Martin, et al. 1995). The effect of P-S on apoptosis was analyzed in BxPC-3 cells (Figure 2-1B). There was no significant induction in apoptosis at P-S 1.0xIC_{50} or sulindac 1.0xIC_{50}. However, when the concentration of P-S was increased to 2.0xIC_{50}, there was a dramatic increase in Annexin V-FITC (+) cells (Figure 1-1B), with the apoptotic cells comprising 60% of the total. These results show that P-S induces cell death in BxPC-3 cells in a concentration-dependent manner.

P-S inhibits the Growth of Human Pancreatic Xenografts

We evaluated the safety and efficacy of P-S in nude mice bearing human pancreatic cancer cell xenografts. In all P-S treated groups (as described in Methods) there were no signs of

toxicity; they were similar to the control groups. In the sulindac-treated group, however, 2 animals died within the first few days of treatment (50 mg/kg/d). As a result, the dose was adjusted to (33mg/kg/d). Even with the reduced dosage of sulindac, animals in this group exhibited a 10.3% reduction in body weight in comparison to vehicle (Figure 2-2B), an indicator of drug toxicity; while animals treated with P-S did not show a reduction in body weight. As demonstrated in Figure 2-2A, tumor volume was decreased by 45.3% in P-S treated group in comparison to vehicle ($p=0.047$) and only 36.5% in the sulindac treated cohort, an effect that was not statistically significant. While tumor volume was reduced by both P-S and sulindac, animals treated with the latter compound were sickly, and upon analyses of the stomach, liver and other major organs, evidence of toxicity was noted (data not shown). This emphasizes that sulindac, while chemopreventive, has rather detrimental side effects associated with its administration, as previous reports have indicated (Sun, et al. 2011).

In Vivo Cytokinetic Effect of P-S

The cytokinetic effect of P-S on proliferation and apoptosis was analyzed *in vivo* utilizing Ki-67 and TUNEL assays (Figure 2-3A). Briefly, Ki-67, commonly used as a proliferation marker, is a nuclear protein that is expressed in dividing, but not in quiescent cells. As shown in Figure 2-3B, P-S-treated versus vehicle-treated tissue, a significant reduction in Ki-67 (+) cells was observed, specifically a 44.9% reduction ($p=0.006$). While a 38.4% reduction was observed in sulindac treated mice ($p=0.013$). These findings highlight the ability of P-S to reduce pancreatic cancer proliferation *in vivo* more efficaciously than sulindac.

The TUNEL method is used for detection and quantification of apoptosis at single cell level, based on labeling of DNA strand breaks. Cleavage of genomic DNA during apoptosis may

yield double stranded as well as single strand breaks, which can be identified by labeling free 3'-OH terminal with modified nucleotides in an enzymatic reaction (Gavrieli, Sherman and Ben-Sasson 1992). As shown in Figure 2-3C, TUNEL (+) cells were increased by 31.9% in P-S treated group in comparison to vehicle. There was no increase in TUNEL (+) cells in sulindac treated group, highlighting P-S's increased ability to affect apoptosis in a pancreatic cancer xenograft model. Much like its ability to reduce proliferation, P-S was also able to significantly induce apoptosis in pancreatic cancer xenografts.

Liposomal Encapsulation

To evaluate the affect of drug delivery mode on the efficacy of P-S, we encapuslated the compound in liposomes. Among several promising new drug-delivery systems, liposomes represent an advanced technology to deliver active molecules to the site of action. Mice were subcutaneously injected with MIA PaCa-2 cells as described in Methods. As demonstrated in Figure 2-4A, tumor volume was decreased by 40.3% ($p=0.054$) in comparison to vehicle. In animals treated with Lipo P-S, tumor volume was reduced by 54.7% ($p=0.029$) compared to empty liposome. Animals treated with Lipo P-S had a tumor volume that was 30.1% less than those treated with free P-S, this reduction, however, was not statistically significant. There were no significant changes in body weight in either P-S or Lip P-S groups in comparison to vehicle (Figure 2-4B).

DISCUSSION

Pre-requisites for ideal drug candidates are their ability to inhibit tumor growth with minimal presentation of toxicity to the patient. In this chapter, I have shown that P-S is more potent than sulindac in pancreatic cancer cells. Notably, in a panel of 4 pancreatic cancer cell lines (BxPC-3, MIA PaCa-2, Panc-1 and HPAF-II), P-S was consistently more potent than sulindac in inhibiting pancreatic cancer growth, with potency increasing with increased incubation with our compound.

Cytokinetic data on cellular proliferation and apoptosis showed that P-S had a significant effect on cellular proliferation *in vitro*, reducing BrdU-FITC (+) cells significantly in a concentration-dependent fashion. Specifically, P-S significantly reduced proliferation by 87.0% and 9.3.3% at 0.5x and 1.0xIC_{50}. Sulindac also reduced proliferation by 70.3% at 1.0xIC_{50}, but not as effectively as P-S. Apoptosis was also increased in a concentration-dependent fashion, demonstrating a staggering 89.8% increase in Annexin V-FITC (+) cells at 2.0xIC_{50}. Again, ideal chemotherapy candidates are those that both block cellular proliferation and induce apoptosis. Here I have shown that P-S is able to fulfill both requirements, with greater efficiency than sulindac.

To corroborate our *in vitro* findings, I also analyzed the efficacy and safety of P-S in a pancreatic cancer xenograft model. MIA PaCa-2, human pancreatic cancer cells were subcutaneously injected into female BALB/c nude mice and tumor growth analyzed. In particular, tumor volume was significantly reduced by 45.3% in P-S treated group in comparison to vehicle. Animals treated with sulindac had a 36.5% reduction in tumor volume, though not significant. P-S was able to reduce tumor more efficaciously than sulindac, and most

importantly, without presentation of toxicity to animals. Mice treated with sulindac either died, or had a marked reduction in body weight. The dose of sulindac had to be reduced in response to the diminished health of the animals in this group. Generally, a bench mark for toxicity is the percentage of weight loss in patients undergoing chemotherapy in comparison to those treated with placebo. In fact, a reduction in body weight of >10% is attributed to toxicity affiliated with drug administration. In this study, mice treated with sulindac showed a 10.3% reduction in body weight when compared to vehicle, highlighting the toxicity of conventional sulindac. On the contrary, animals treated with P-S had no reduction in body weight.

Evidence into the toxicity of sulindac was evaluated in a previous gastrointestinal study conducted in rats (Mackenzie, et al. 2010). The animals were treated for 4 days by oral gavage with equimolar amounts of P-S (317 mg/kg/d) or sulindac (200 mg/kg/d), indomethacin (4.75 mg/kg/d), or vehicle. As expected, treatment with indomethacin (a known inducer of gastric ulcerations) produced predominantly medium and large ulcerations (>4 mm) in the small intestine. Vehicle and P-S–treated rats showed no gastrointestinal toxicity, with no signs of ulcerations or mucosal damage. Sulindac, on the other hand, produced medium and large ulcerations in the small intestine, much like the positive control indomethacin (Mackenzie, et al. 2010).

Based on *in vivo* cytokinetic data, animals P-S treated animals showed a 44.9% reduction in Ki-67 (+) cells, while a 38.4% reduction was observed in animals treated with sulindac. These findings highlight the ability of P-S to reduce pancreatic cancer proliferation *in vivo* more efficaciously than sulindac. TUNEL (+) cells were increased by 31.9% in P-S treated group in comparison to vehicle, while there was no increase in TUNEL (+) cells in sulindac treated group. As aforementioned, an ideal drug candidate will inhibit tumor proliferation as well as induce

apoptosis. P-S was able to satisfy both requirements *in vitro* and *in vivo*. Sulindac, on the other hand was able to block proliferation, though it had no effect on the induction of apoptosis—hence, disqualifying the agent as an ideal chemotherapy candidate.

As a liposome based delivery system can concomitantly improve the pharmacokinetics, reduce the side effects, and potentially increase selective tumor uptake, the optimal role of current liposomal formulations in the treatment of pancreatic cancer remains to be defined (Yang, et al. 2012). In this study, we evaluated the effect of both free P-S and Lipo P-S on tumor growth. While animals in Lipo P-S exhibited tumor volume at 30.1% less than free P-S, it was not statistically significant. Both P-S and Lip P-S were well tolerated by the mice, as evidenced by the similar body weights across treatment groups. These result show that liposomal formulations of P-S is a viable approach, though a drug combination may be required to further enhance the anticancer effects of P-S.

FIGURES

Table 2-1. P-S Reduces cell viability more potently than sulindac in pancreatic cancer cells. BxPC-3, MIA PaCa-2, Panc-1 and HPAF-II cells were incubated with either P-S or sulindac for 24, 48 or 72 hr utilizing an MTT cell viability assay to determine the effect of treatment on IC_{50}. Across all 4 panels of pancreatic cancer cells lines, P-S showed enhanced potency, reducing cell viability more efficiently than sulindac.

	24h		48h		72h	
	P-S (μM)	Potency Enhancement (Sulindac/ P-S)	P-S (μM)	Potency Enhancement (Sulindac/ P-S)	P-S (μM)	Potency Enhancement (Sulindac/ P-S)
BxPC-3	106 ± 4.0	>19	42 ± 2.0	>48	15 ± 2.0	>133
MIAPaCa-2	79 ± 2.0	>25	60 ± 2.0	>33	55 ± 1.0	>36
Panc-1	99 ± 2.0	>20	83 ± 4.0	>32	51 ± 2.0	>39
HPAF-II	76 ± 2.0	>26	65 ± 2.0	>31	57 ± 1.0	>35

* Sulindac IC_{50} >2000 μM for all cell lines

Figure 2-1. Cytokinetic effect of P-S on proliferation and apoptosis in BxPC-3 cells. (A) BxPC-3 cells were treated with vehicle, P-S 0.5, 1.0, or 2.0 xIC_{50}, and sulindac 1.0xIC_{50} for 24 hr. Proliferation was inhibited in a concentration dependent manner in response to P-S, as indicated by a significant reduction in BrdU (+) cells. Cells were then harvested, followed by incubation with BrdU-FITC and PI, or (B) Annexin V-FITC and PI for 30 min. Samples were analyzed by flow cytometry. (* = $p<0.05$)

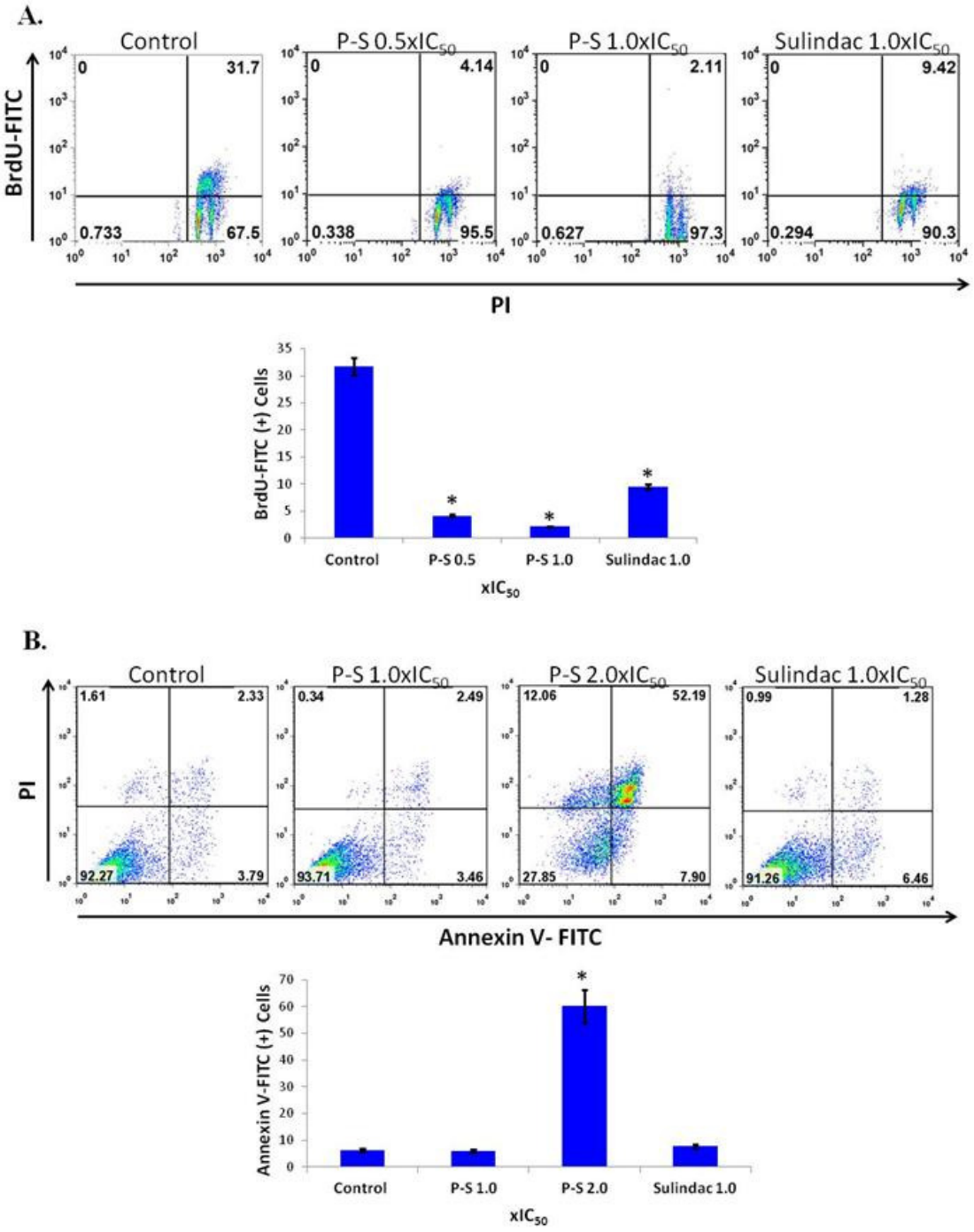

Figure 2-2. P-S inhibits tumor growth in Mia PaCa-2 xenograft. Female BALB/c mice were subcutaneously injected with MIA PaCa-2 cells. Animals were treated by gavage with vehicle (corn oil), P-S (100 mg/kg/d), or sulindac (33mg/kg/d) for 4 weeks. (A). Tumor volume was reduced by 45.3% in P-S treated animals (p=0.047). Although tumor volume was reduced by 36.5% in animals treated with sulindac, it was not significant. (B) Animals in vehicle and P-S treated groups had similar body weights, while those in sulindac were 10.3% than vehicle.

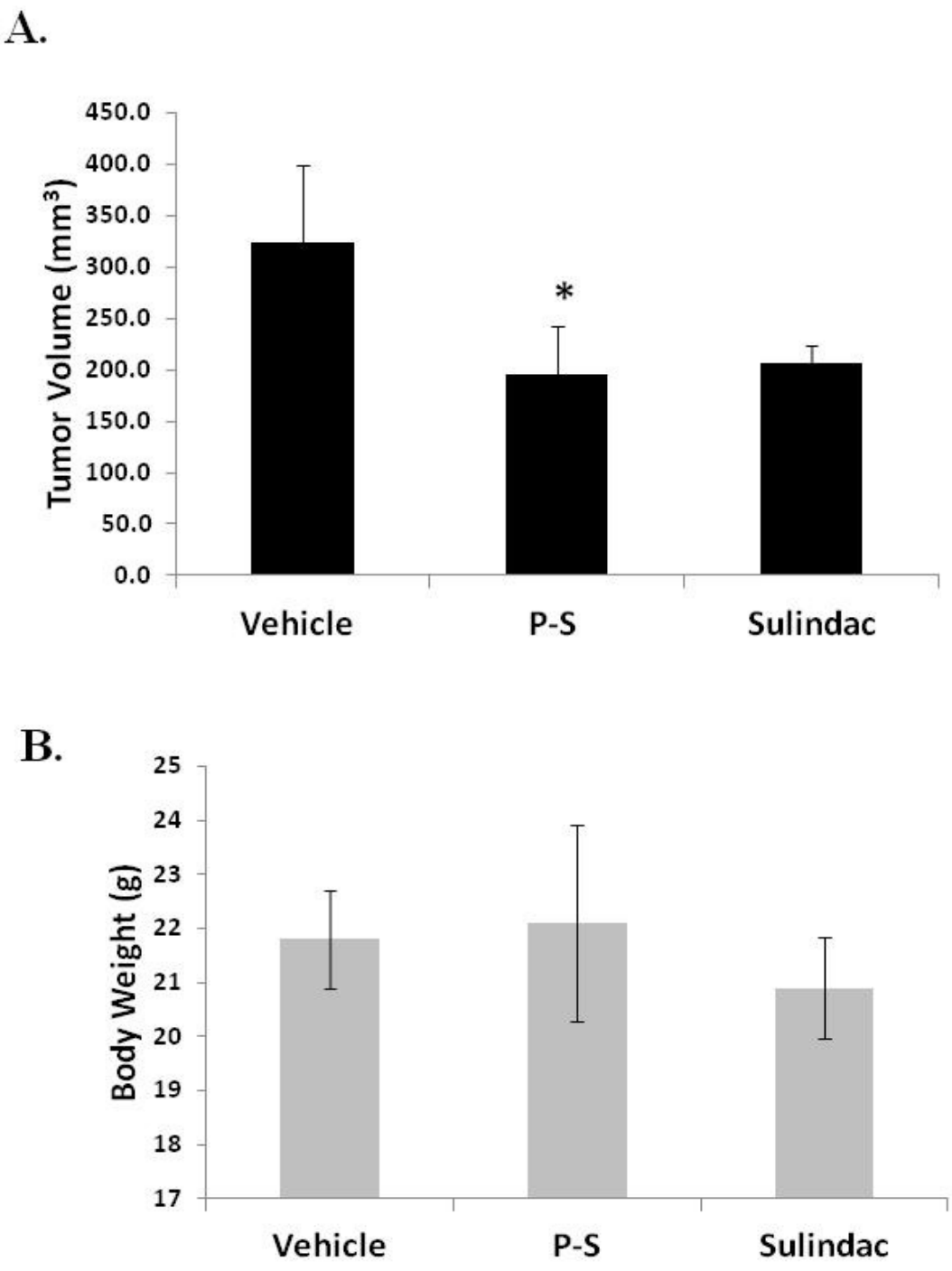

Figure 2-3. Cytokinetic effect of P-S in pancreatic cancer xenograft. (A) MIA PaC-2 pancreatic cancer xenograft tissue was analyzed by IHC. A significant decrease of 44.9% (p=0.006) in Ki-67 (+) cells was observed in animals treated with P-S; and a 38.4% reduction (p=0.0013) in animals treated with sulindac. (B) P-S increased TUNEL (+) cells by 31.9% in comparison to control, while no change was observed in animals treated with sulindac.

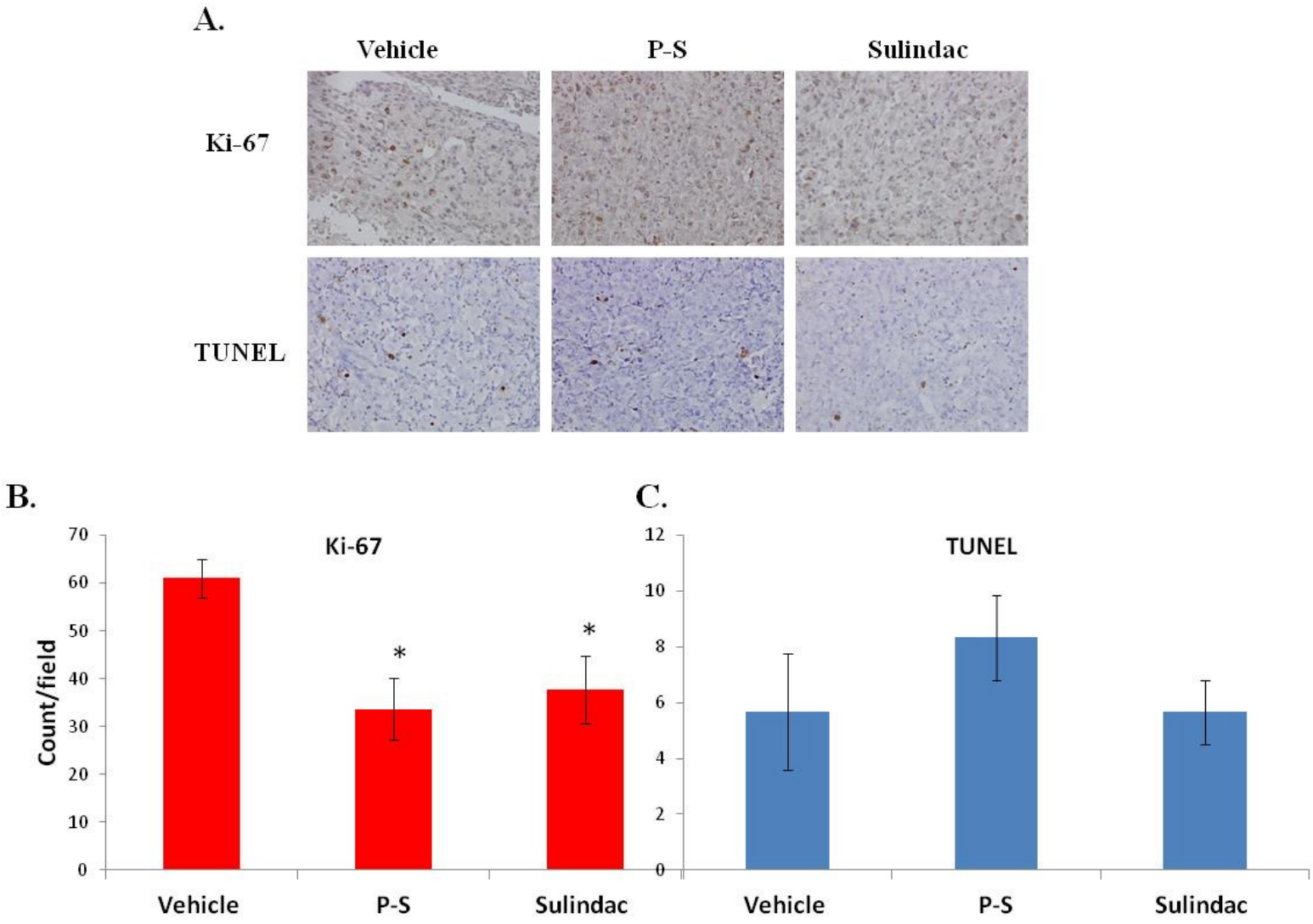

Figure 2-4. P-S and Lipo P-S inhibits tumor growth in Mia PaCa-2 xenograft. Female BALB/c mice were subcutaneously injected with MIA PaCa-2 cells. Animals were treated with vehicle, P-S (100 mg/kg/d), or via IP with either Lipo P-S (100mg/kg/d) or Empty Lipo for 4 weeks. (A) Tumor volume of mice treated with P-S was reduced by 40.3% (p=0.054) in comparison to vehicle. In animals treated with Lipo P-S, tumor volume was reduced by 54.7% (p=0.029) compared to empty liposome. (B) There were no significant changes in body weight in either P-S or Lipo P-S groups in comparison to vehicle.

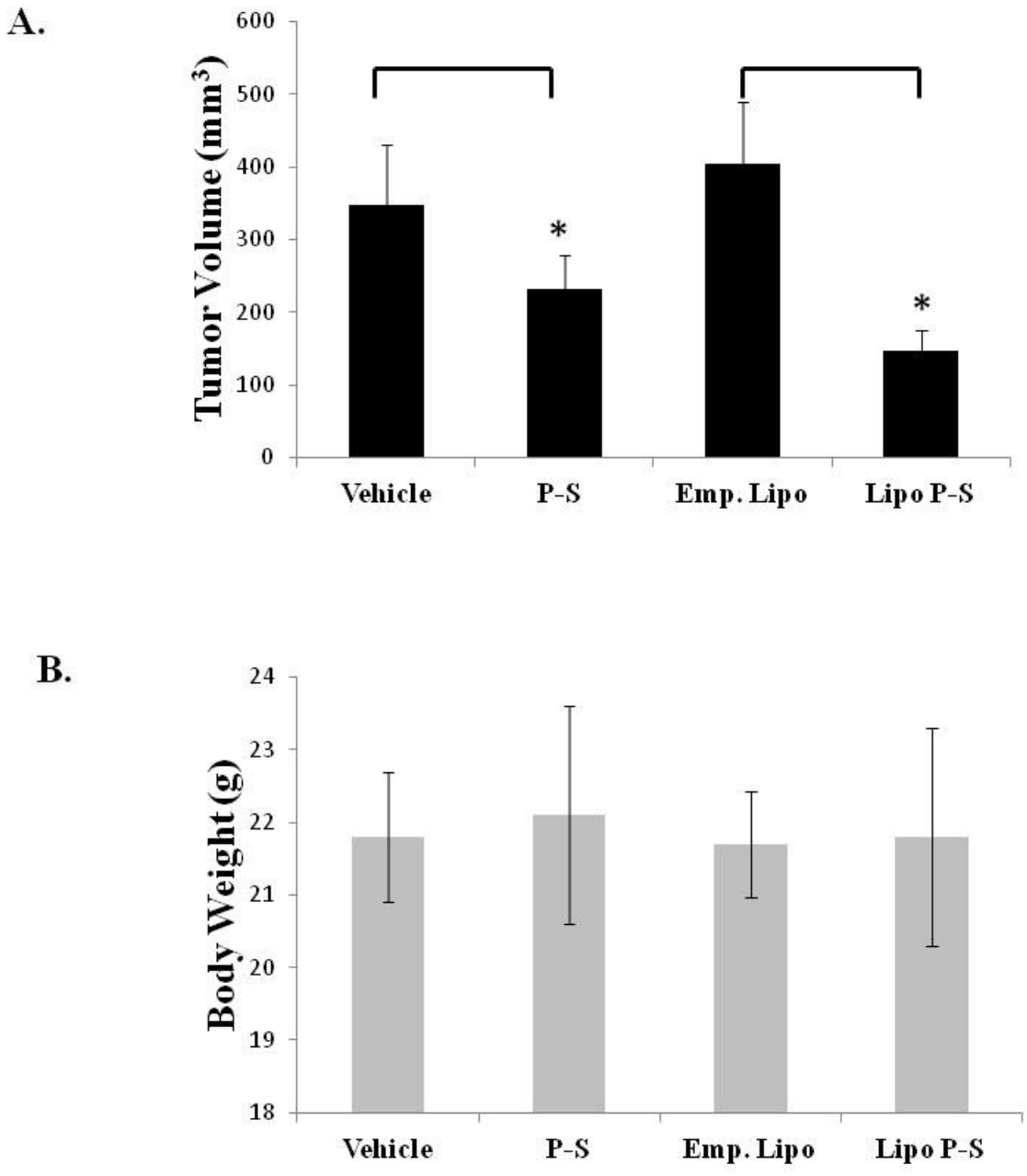

Chapter III

P-S AND PANCREATIC CANCER: MOLECULAR MECHANISM OF ACTION

INTRODUCTION

As outlined in the previous chapter, P-S has a significant anticancer effect mediated through a strong cytokinetic effect encompassing both proliferation and apoptosis. The next important question concerns the molecular mechanism underlying this cytokinetic effect that culminates in cancer growth inhibition. I approached this question initially by employing a high throughput gene expression analysis in the hope that it would provide an initial insight into the pathways influenced by P-S.

As detailed in Results, a prominent change concerned the expression of NFATc1, a gene that has a potentially significant role in pancreatic carcinogenesis. As a consequence, its upregulation by P-S could represent at least one of the molecular signaling pathways by which this novel agent exerts its pharmacological activity. To summarize the information previously presented on NFATc1: (1) it acts like an oncogene during cancer progression, (2) it induces the expression of protein such as c-Myc and COX-2, known to have significant proproliferative effects, (3) sustained activation of the Ca^{2+} /calcineurin/NFAT signaling pathway is a powerful regulatory principle governing pancreatic cancer growth (Trachootham, et al. 2009), (4) NFAT isoforms promote the migration and invasion of tumor cells, prerequisites for metastatic

dissemination, and (5) the active form of NFATc1 is localized in the nucleus (Muller, et al. 2010).

Based on these considerations, the effect of P-S on the expression and activity of NFATc1 assumed particular importance as a potential mediator of P-S's effect in pancreatic cancer. Therefore, I explored (1) an in vitro system (cultured pancreatic cancer cells), (2) the effect of P-S on NFATc1 expression and its effect on relevant downstream signaling, and (3) determined the relevance of NFATc1 and the effect of P-S by genetically silencing and overexpressing the NFATc1 gene.

MATERIALS AND METHODS

Cell Lines

Human pancreatic cancer cell lines BxPC-3 and MIA PaCa-2 were obtained from ATTC (Manassas, VA).

NFATc1 knockdown BxPC-3 and MIA PaCa-2 cell lines were generated using MISSION Lentiviral Packaging Mix (Sigma Aldrich). Cells were infected with the lentivirus and then subjected to 3 ug/ml of puromycin to generate stable cell lines. Decreased levels of NFATc1 were confirmed by western blot.

NFATc1 MIA PaCa-2 overexpression cell line was generated using NFATC1 Human cDNA Clone from OriGene (Rockville, MD). Cells were transfected using Lipofectamine 2000 (Invitrogen) and selected with 1mg/ml of G418.

Cells were grown at 37°C in 5% CO_2 in the specific medium suggested by ATCC and supplemented with 10% fetal calf serum (Mediatech, Herndon, VA), penicillin (50 U/ml) and streptomycin (50 µg/ml; Life Technologies, Grand Island, NY).

Gene Expression Microarray

MIA PaCa-2 Cells were treated with vehicle or 1.5xIC_{50} P-S for 30 min and 2 hr. Total RNA was isolated from cell lines using an RNA Extraction Kit (Qiagen Inc.,Valencia, CA). Samples were sent to Genome Explorations (Memphis, TN) and analyzed on Affymetrix Human Genome U133 gene chip (Cleveland, OH).

Cell Viability Assay

Cell viability was measured by the 3-(4,5-dimethylthiazol-2-yl)-2,5-diphenyltetrazolium bromide assay following the protocol of the manufacturer (Roche Diagnostics). Briefly, cells were seeded overnight in a 96-well plate. On the following day, P-S, sulindac, 5-FU, valproic acid, or irinotecan was added to cells. Cells were incubated with drugs for 24 hr and cell viability assessed.

Immunocytochemistry

Cells were seeded in an 8-well glass chamber slide (Lab-Tek, Rochester, NY). The following day, cells were treated with respective concentrations of vehicle (DMSO) or P-S for 24 hr. Cells were fixed in 4% paraformaldehyde (15 min). Block and NFATc1 antibody (Abcam, Cambridge, MA) incubations were in PBS, 2% BSA and 0.3% Triton. Cells were mounted with Vectashield mounting media with diamidinophenylindole (DAPI) (Vector Laboratories Inc., Burlingame, CA). Cells were imaged using Zeiss Axioplan inverted fluorescence microscope (Thornwood, NY, USA).

Western Blot

After treatment, cells were lysed on ice with 1% Triton lysis buffer with 2.5 mmol/L 4-nitrophenylphosphate, 1% SDS, and 0.25% sodium deoxycholate for 30 min. The cell lysate (25 µg) was loaded onto SDS-electrophoresis gel and transferred onto a PVDF membrane. The membrane was then immunoblotted with NFATc1 (Abcam), p-NFATc1 (Santa Cruz Biotechnology) p38, p-p38, ERK, p-ERK, JNK, p-JNK (Cell Signaling), and Cox-2 (Cayman Chemical) antibodies. Secondary antibodies conjugated with horseradish peroxidase (HRP) (Santa Cruz Biotechnology) were applied to membrane, followed by development on X-ray film.

qRT-PCR

Total RNA was isolated from cell lines using Triazol reagent as per the instructions of the manufacturer (Life Technologies, Grand Island, NY). Ten micrograms of RNA was used in reverse-transcription using random primers and the M-MLV Reverse Transcriptase Kit (Sigma, St Louis, MO). The following primer pairs were used for qRT–PCR mouse NFATc1: forward 5'CCAGTCATCGGCGGGAAGAAGA-3'; reverse 5'-TATACACCCCCAGACCGCATCAGC-3'.

Cancer Xenografts

Six-week-old female BALB/c nude mice (Charles River, Wilmington, MA) were subcutaneously injected with 3.0x 10^6 MIA PaCa-2 NFATc1 WT, Kd and Ov. cells (1.5x10^6 in right and left flank, respectively). Animals were separated into 6 cohorts. In each cohort there were n=6 in vehicle, and n=6 in treat. Following a prevention protocol, animals were first treated by gavage with P-S (100 mg/kg/d), or vehicle (corn oil) for one week prior to subcutaneous injection. Once inoculated with cancer cells, animals were treated for 4 weeks. Tumor size was determined with a digital microcalipter. Upon completion of the study, animals were euthanized and tumors collected, measured and embedded in OCT.

Immunofluorescence

OCT embedded xenograft tissues were sectioned (20 micron) onto glass slides. Slides were washed in 1X PBS for 5, 10, and 15 min. Block and NFATc1 antibody (Abcam, Cambridge, MA) incubations were in PBS, 3% BSA and 0.3% Triton. Cells were mounted with Vectashield mounting media with diamidinophenylindole (DAPI) (Vector Laboratories Inc., Burlingame, CA). Cells were imaged using an inverted confocal laser microscope (Zeiss LSM

510). Mean pixel intensity of NFATc1 was determined using Adobe Photoshop and Image J (NIH).

Statistical Analysis

Results from at least 3 independent experiments and expressed as mean $\pm$ SD were analyzed by the student's t-test. *$p<0.05$ was considered significant

RESULTS

Microarray Analysis of Gene Expression in MIA PaCa-2 Cells Treated with P-S

Utilizing an Affymetrix Human Genome U133 gene chip, I was able to achieve complete coverage of the Human Genome U133 Set plus 6,500 additional genes for analysis of over 47,000 transcripts. MIA PaCa-2 cells were treated with P-S or vehicle for 30 min and 2 hr. RNA was extracted and samples sent to Genome Explorations for analysis. Of the genes analyzed, NFATc1 and AP1, members of the B- and T-Cell Receptor pathways, were upregulated in response to treatment with P-S (shown in red). The data is summarized below in reports generated by Genome Explorations.

The KEGG Table organizes genes based on the KEGG biochemical pathways.
The KEGG Table shows KEGG pathways associated with the gene set (column 1), the number of genes in each pathway (column 2) and the Entrez Gene IDs for the genes (column3).
The 4th column gives the parameters for the enrichment of the KEGG pathway.
O is the observed gene number in the KEGG pathway
E is the expected gene number in the KEGG pathway (Expected number of genes in a specific KEGG pathway for an interesting gene set=Total number of genes in the KEGG pathway for the reference set * Total number of genes in the interesting set / Total numbe of genes in the reference set)
R is the ration of enrichment for the KEGG pathway (R=O/E)
P is the p value indicating the significance of enrichment calculated from Hypergeometric test. It is given for the KEGG pathways with R>1.
The 4th column is colored red for KEGG pathways with at least 2 genes and with p<0.05
Each pathway name in the KEGG Table is hyperlinked to the KEGG Map, in which genes in the gene set are highlighted in red.

KEGG pathway	Gene number	Entrez Gene IDs	Enrichment
B cell receptor signaling pathway	2	2353 4775	O=2;E=0.0732;R=27.3224;P=2.40e-3
T cell receptor signaling pathway	2	2353 4775	O=2;E=0.1112;R=17.9856;P=5.45e-3
Wnt signaling pathway	1	4775	O=1;E=0.1735;R=5.7637;P=1.60e-1
Axon guidance	1	4775	O=1;E=0.1505;R=6.6445;P=1.40e-1
Colorectal cancer	1	2353	O=1;E=0.1057;R=9.4607;P=1.01e-1
Toll-like receptor signaling pathway	1	2353	O=1;E=0.099;R=10.101;P=9.45e-2
Natural killer cell mediated cytotoxicity	1	4775	O=1;E=0.1315;R=7.6046;P=1.24e-1
Neuroactive ligand-receptor interaction	1	7252	O=1;E=0.3674;R=2.7218;P=3.10e-1
MAPK signaling pathway	1	2353	O=1;E=0.3308;R=3.023;P=2.84e-1
VEGF signaling pathway	1	4775	O=1;E=0.0854;R=11.7096;P=8.21e-2

Table 3-1. KEGG Table of Genomic Response to P-S in Human Pancreatic MIAPaCa-2 Cells.

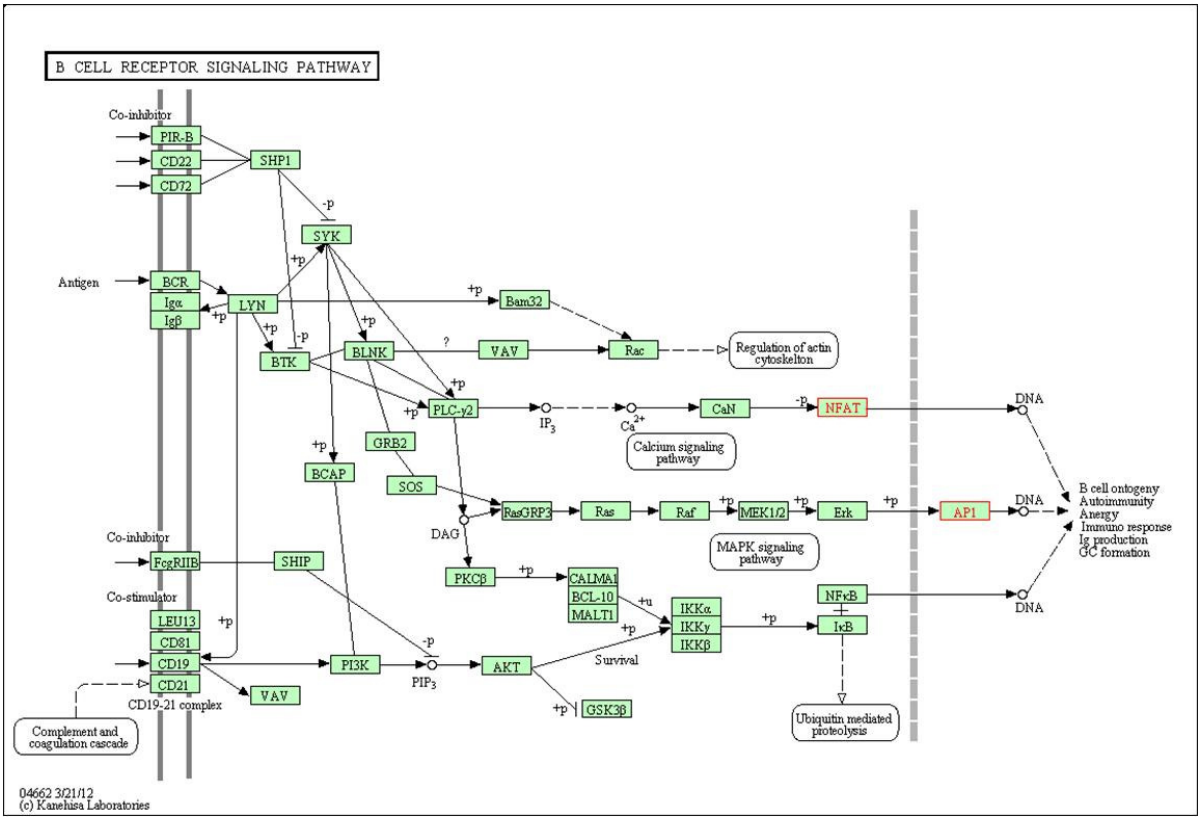
B CELL RECEPTOR SIGNALING PATHWAY
Co-inhibitor
PIR-B
CD22
CD72
SHP1
SYK
Antigen
BCR
Igα
Igβ
LYN
Bam32
BTK
BLNK
VAV
Rac
Regulation of actin cytoskelton
PLC-γ2
IP3
Ca2+
CaN
NFAT
DNA
Calcium signaling pathway
GRB2
BCAP
SOS
RasGRP3
Ras
Raf
MEK1/2
Erk
AP1
DNA
B cell ontogeny
Autoimmunity
Anergy
Immuno response
Ig production
GC formation
DAG
MAPK signaling pathway
Co-inhibitor
FcgRIIB
SHIP
PKCβ
CALMA1
BCL-10
MALT1
IKKα
IKKγ
IKKβ
NFκB
IκB
DNA
Co-stimulator
LEU13
CD81
CD19
CD21
CD19-21 complex
PI3K
PIP3
AKT
Survival
VAV
GSK3β
Ubiquitin mediated proteolysis
Complement and coagulation cascade
04662 3/21/12
(c) Kanehisa Laboratories

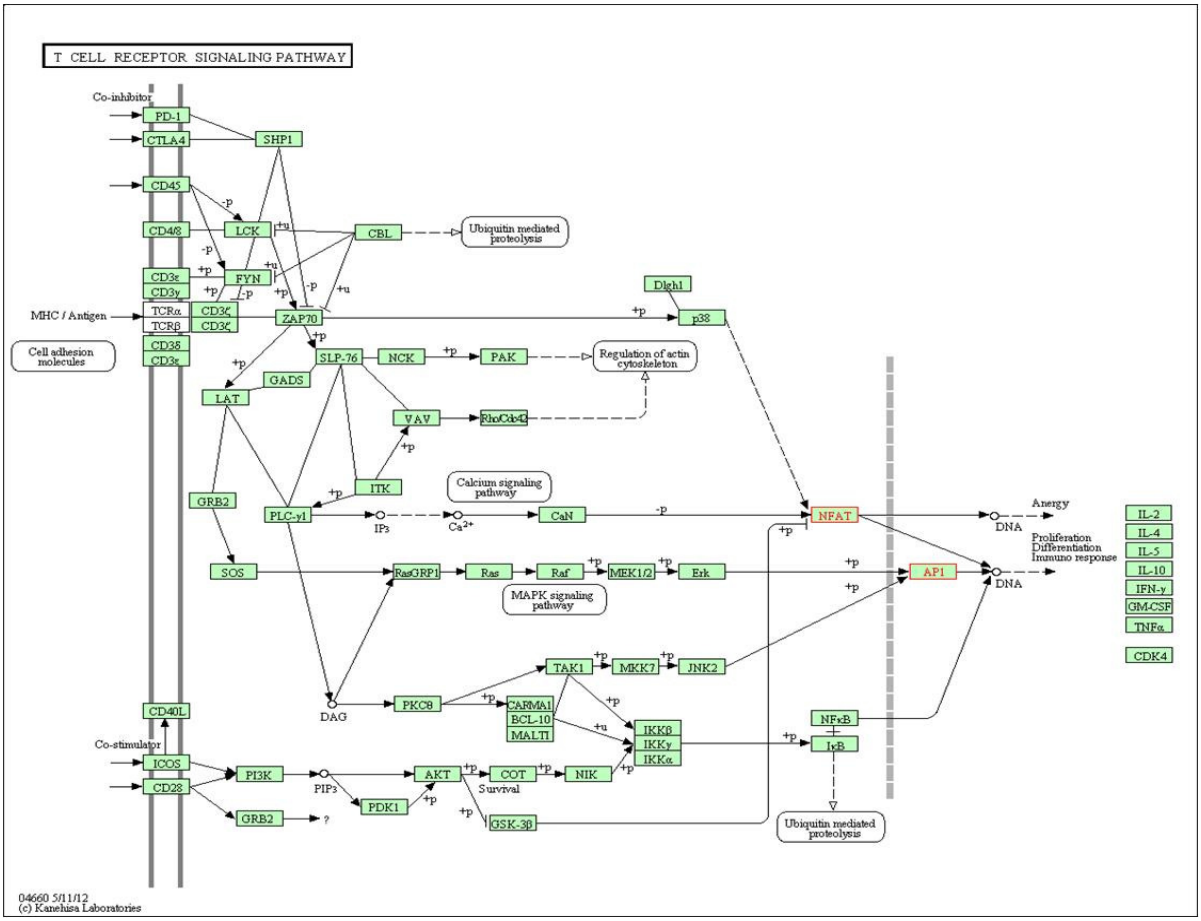
T CELL RECEPTOR SIGNALING PATHWAY
Co-inhibitor
PD-1
CTLA4
SHP1
CD45
CD4/8
LCK
CBL
Ubiquitin mediated proteolysis
CD3ε
CD3γ
FYN
Dlgh1
MHC / Antigen
TCRα
TCRβ
CD3ζ
CD3ζ
ZAP70
p38
Cell adhesion molecules
CD3δ
CD3ε
SLP-76
NCK
PAK
Regulation of actin cytoskeleton
GADS
LAT
VAV
RhoGdi-G
ITK
Calcium signaling pathway
GRB2
PLC-γ1
IP3
Ca2+
CaN
NFAT
Anergy
DNA
Proliferation
Differentiation
Immuno response
IL-2
IL-4
IL-5
IL-10
IFN-γ
GM-CSF
TNFα
CDK4
SOS
RasGRP1
Ras
Raf
MEK1/2
Erk
AP1
DNA
MAPK signaling pathway
TAK1
MKK7
JNK2
CD40L
DAG
PKCθ
CARMA1
BCL-10
MALT1
IKKβ
IKKγ
IKKα
NFκB
IκB
Co-stimulator
ICOS
CD28
PI3K
PIP3
AKT
COT
NIK
Survival
PDK1
GSK-3β
GRB2
Ubiquitin mediated proteolysis
04660 5/11/12
(c) Kanehisa Laboratories

Generation of a Stable NFATc1 Knockdown and Overexpression Model in Human Pancreatic Cancer Cell Lines

Once I had determined that NFATc1 gene levels were increased in response to P-S, I wanted to assess the effect that both genetic silencing and overexpression of NFATc1 would have on P-S efficacy in pancreatic cancer cells. Utilizing both a wild type and mutant K-Ras cell line, I would be able to delineate whether or not the oncogene status of K-Ras had an effect on the potency of P-S in both BxPC-3 and MIA PaCa-2 cells. As mentioned, K-Ras mutation status reduces the efficacy of many chemotherapeutic agents in pancreatic cancer. Accordingly, an NFATc1 knock-down (Kd) model was generated in BxPC-3 (wild type K-Ras) cells, and in MIA PaCa-2 (mutant K-Ras) cells. In addition, an NFATc1 overexpression (Ov.) model in MIA-PaCa-2 cells.

I generated stable NFATc1 knock-down models in BxPC-3 and MIA PaCa-2 cells utilizing a shRNA lentivirus (Figure 3-1). We generated two NFATc1 knockdown clones from BxPC-3 cells, along with a non-targeting shRNA control (Figure 3-1A), though in subsequent experiments I used the second clone, shNFATc1 #2, which not only shows decreased NFATc1 protein levels (Figure 3-2A, B), but also decreased in NFATc1 at the transcriptional level (Fig 3-1A). A 70.9% ($p=0.003$) reduction of NFATc1 was observed in shNFATc1 #2, referred to as BxPC-3 Kd (Figure 3-1A).

In addition, I generated two NFATc1 knockdown clones from MIA PaCa-2 cells, along with a non-targeting shRNA control (Figure 3-1B). I observed a marked decrease in NFATc1 gene expression in the second clone, shNFATc1 #2, referred to as MIA PaCa-2 Kd. Particularly, there was a 67.7% ($p=0.001$) decrease in NFATc1 at the transcriptional level (Figure 3-1B). I

then overexpressed NFATc1 in MIA PaCa-2 cells (Figure 3-1B), where I observed a 2.5-fold increase in gene expression (p=0.015).

P-S Efficacy is Increased with Genetic Abrogation of NFATc1

An MTT cell viability assay was used to determine the IC_{50} of P-S in the transfected cell lines (Table 3-2). Transfected BxPC-3 and MIA PaCa-2 cells were incubated with P-S for 24 hr. A significant enhancement of potency of P-S was observed in both NFATc1 BxPC-3 and MIA PaCa-2 Kd cells (3- and 2.4 fold, respectively). These results suggest that P-S is able to elicit its anticancer effects independent of K-Ras mutation status. P-S was 1.2-fold less potent in MIA PaCa-2 cells where NFATc1 was overexpressed. Taken together, these results emphasize that NFATc1 protein levels determines, at least to some extent, how responsive pancreatic cancer cells are to treatment with P-S.

Effect of COX-2 Independent Agents on IC_{50} in BxPC-3 Cells

I then determined whether NFATc1 determined the effect of non-NSAID compounds. Specifically, I studied the effect of 5-FU (a pyrimidine analogue that inhibits DNA synthesis), valproic acid (an anticonvulsant drug and histone deacetylase inhibitor), and irinotecan (a semisynthetic analogue of the natural alkaloid camptothecin that inhibits topoisomerase 1) on cell viability in BxPC-3 WT and Kd cells (Table 3-3). Among all three drugs, an enhanced potency was observed in Kd cells in comparison to WT: 2.2-fold potency enhancement with 5-FU; 1.6-fold with valproic acid, and 2.2-fold with irinotecan. The fold enhancement of these compounds was similar to the 3-fold potency enhancement of P-S in BxPC-3 Kd cells (Table 3-3). These findings indicate that NFATc1 protein expression in pancreatic cancer cells decreases the potency of both COX-2 dependent as well as COX-2 independent agents. Further, they

indicate that by decreasing NFATc1 expression, all agents reduced cell viability with enhanced potency.

Genetic Silencing of NFATc1 Decreases Cytoplasmic NFATc1, COX-2 and c-Myc Protein Expression in BxPC-3 and MIA PaCa-2 Kd Cells

BxPC-3 NFATc1 WT and Kd cells were treated with vehicle (DMSO), P-S 0.5x and 1.0xIC_{50}, or sulindac 1.0xIC_{50} for 24 hr. Cells were lysed and proteins extracted and analyzed by western blot (Figure 3-2). A 71.4% ($p<0.05$) decrease in NFATc1 protein expression was observed in Kd cells in comparison to WT in untreated cells (Figure 3-1B). As the concentration of P-S increased, however, an induction was observed in NFATc1 protein expression: 12-fold increase at P-S 0.5xIC_{50}, and an 18-fold increase at P-S 1.0xIC_{50}. Sulindac also increased NFATc1 expression 20-fold more vs. control. While NFATc1 expression increased in Kd cells in response to treatment with P-S, it was consistently statistically less than WT cells: 60% ($p<0.05$) less at P-S 0.5x$IC_{50,}$ and 46.2% less at P-S 1.0xIC_{50}. Sulindac treated Kd cells showed a 31.0% less NFATc1 protein expression in comparison to WT (Figure 3-2A, B).

While no difference in COX-2 protein expression (Figure 3-2C) was also observed in untreated Kd vs WT cells, COX-2 expression was induced more dramatically in WT cells than in Kd cells. COX-2 protein expression was 80.2% less ($p<0.05$) in Kd vs. WT at P-S 0.5xIC_{50}, and 52.1% less ($p<0.05$) at P-S 1.0xIC_{50}. Sulindac also induced COX-2 expression in both Kd and WT cells, though Kd cells expressed 7.35% less COX-2 protein.

I also evaluated the effect of NFATc1 abrogation on c-Myc protein expression in BxPC-3 Kd and WT cell lines (Figure 3-2D). In untreated cells, the Kd cell line exhibited 54.5% less ($p<0.05$) c-Myc protein expression compared to WT. In contrast to COX-2, however, c-Myc

expression decreased in response to P-S in a concentration-dependent manner: 72.7% less ($p<0.05$) in Kd cells vs. WT at P-S 0.5xIC_{50}, and 61.5% less at 1.0xIC_{50} ($p<0.05$) (Figure 3-2D). In cells treated with sulindac Kd cells had 73.3% less ($p<0.05$) c-Myc expression than WT cells (Figure 3-2D).

MIA PaCa-2 NFATc1 WT, Kd and Ov. cells were treated with vehicle, P-S 0.5x and 1.0xIC_{50}, or sulindac 1.0xIC_{50} for 24 hr. Cells were lysed and proteins extracted and analyzed by western blot (Figure 3-4). In untreated cells, a 90.0% ($p<0.05$) decrease in NFATc1 protein expression was observed in Kd cells, with a modest 10% increase in Ov. cells. As observed in BxPC-3 cells, NFATc1 protein expression increased in response to increasing concentrations of P-S in both Kd and WT cells, though protein expression was consistently less in Kd cells vs. WT: 33.3% less at P-S 0.5xIC_{50}, and 23.7% less at 1.0xIC_{50}. In Mia PaCa-2 Ov. cells, NFATc1 protein was increased over WT, although this increase was not statistically significant (Figure 3-4).

Induction of Nuclear NFATc1 Protein Expression is Decreased in Response to Treatment with P-S in Kd Cell Lines

I treated BxPC-3 WT and Kd cells with P-S and evaluated the effect on the nuclear expression of NFATc1 (Figure 3-3). As previously mentioned, nuclear localization is indicative of the active form of the NFATc1. In BxPC-3 untreated cells, there was a 71.4% reduction in nuclear NFATc1 expression in Kd cells in comparison to WT (Figure 3-3A). However, with increasing concentrations of P-S, NFATc1 expression was increased, both in Kd and WT cells, though Kd cells had consistently lower expression of the protein than WT.

Particularly, in Kd cells, going from control to P-S 0.5xIC_{50}, a 75% ($p<0.05$) increase in NFATc1 protein expression was observed. At P-S 1.0xIC_{50}, 85.7% ($p<0.05$) increase in NFATc1 expression was observed in comparison to control in Kd cells. However, comparing Kd to WT at P-S 1.0xIC_{50}, there was a 75.4% reduction in NFATc1 expression (Figure 3-3A). In sum, in both Kd and WT cells, NFATc1 nuclear expression is induced with increasing concentrations of P-S, though nuclear expression is statistically lower in Kd cells when compared to WT cells.

To address the induction of nuclear NFATc1 expression that I saw in both Kd and WT cells, the ratio of cytoplasmic to nuclear NFATc1 expression was analyzed in BxPC-3 cells (Figure 3-3B). In Kd cells, the ratio of NFATc1 expression was statistically higher than WT, indicating that Kd cells had considerably lower nuclear NFATc1 expression than WT cells. Specifically, the ratio of cytoplasmic to nuclear NFATc1 expression in Kd vs. WT cells was: control (2:1) vs. (1:1), P-S 0.5xIC_{50} (3:1) vs. (2:1), P-S 1.0xIC_{50} (2:1) vs. (1:1), and sulindac 1.0x IC_{50} (2:1) vs. (1:1). These results show that inhibition of NFATc1 expression via shRNA techniques reduces the induction of the protein in response to treatment with P-S.

I also treated MIA PaCa-2 WT, Kd and Ov. cells with P-S and evaluated its effect on the nuclear expression of NFATc1 (Figure 3-5). In untreated cells, there was a 72.3% ($p<0.05$) decrease in NFATc1 protein expression in Kd vs. WT cells, and a 2-fold ($p<0.05$) increase in NFATc1 protein expression in Ov. vs. WT cells. NFATc1 protein expression increased in all cell lines with increasing concentration of P-S. Kd cells expressed significantly less NFATc1 in comparison to WT. Ov. cells had increased NFATc1 protein expression than WT: at P-S 0.5xIC_{50} there was a 1.8-fold ($p<0.05$) increase in NFATc1 protein expression, and at P-S 1.0xIC_{50} a 3.8-fold ($p<0.05$) fold increase over WT. Similar results were observed with treatment with sulindac.

The ratio of cytoplasmic to nuclear NFATc1 expression in MIA PaCa-2 Kd vs. WT cells was similar to the results obtained in BxPC-3 cells, that Kd cells expressed less nuclear NFATc1 protein. Specifically, the cytoplasmic to nuclear ratio in Kd vs. WT was: control (3:1) vs (2:1), P-S 0.5xIC_{50} (4:1) vs. (3:1), P-S 1.0xIC_{50} (8:1) vs. (3:1), and sulindac (12:1) vs. (10:1). When comparing Ov. to WT, the cytoplasmic to nuclear ratio was decreased, indicative of increased nuclear NFATc1 protein expression, particularly with increased concentrations of P-S. Comparing Ov. to WT, the ratios were: control (2:1) vs. (2:1), P-S 0.5xIC_{50} (2:1) vs. (2:1), P-S 1.0xIC_{50} (2:1) vs. (3:1), and sulindac (1:1) vs. (10:1).

Effect of P-S on NFATc1 Cytoplasmic and Nuclear Protein Expression in BxPC-3 WT and Kd Cell Lines

BxPC-3 cells were treated with vehicle or P-S 1.0xIC_{50} for 24 hr (Figure 3-6). Cells were fixed and incubated with NFATc1 primary, followed secondary antibody as described in Methods. NFATc1 fluorescence intensity was greater in WT cells than Kd, with some NFATc1 localizing to the nucleus. With increasing concentration of P-S, NFATc1 expression was induced in both WT and Kd cells, though there was a greater in induction in WT cells.

Effect of P-S on Ras MAPK and PI3K pathways in BxPC-3 cells

BxPC-3 NFATc1 WT and Kd cells were treated with vehicle, P-S 0.5x and 1.0xIC_{50}, or sulindac 1.0xIC_{50} for 24 hr (Figure 3-7). Cells were lysed and proteins extracted and analyzed by western blot. Membranes were probed with primary antibodies to pAKT, and -ERK, followed by secondary as described in Methods. A slight decrease in pERK was observed in Kd cells in comparison to WT (Figure 3-7). There was no difference in pAKT expression.

P-S Inhibits Tumor Growth in a Xenograft Model for Pancreatic Cancer

We then determined in vivo the effect of P-S in a pancreatic cancer model in which we used cells with stably altered expression of NFATc1 (subcutaneous xenografts).

Six-week-old female BALB/c nude mice were subcutaneously injected with MIA PaCa-2 as described in Methods. Following a prevention protocol, animals were first treated by gavage with P-S (100 mg/kg/d), or vehicle (corn oil) for one week prior to subcutaneous injection. Animals were treated for 4 weeks. Upon completion of the study, animals were euthanized and tumors collected and measured. Figure 3-8 shows tumor volume was significantly reduced by 50.4% in WT treated in comparison to WT vehicle ($p= 0.013$), and 62.8% in Kd treated compared to Kd vehicle ($p=0.0005$). While tumor volume was also reduced by 25.9% in Ov. treated in comparison to Ov. vehicle, it was not significant (Figure 3-8).

P-S Reduces Nuclear NFATc1 Localization in MIA PaCa-2 Xenograft.

Finally, we examined whether P-S alters the cellular localization of NFATc1. To this end, OCT-embedded MIA PaCa-2 xenograft tissue were stained with NFATc1 and analyzed by confocal laser microscopy. NFATc1 protein expression was reduced by 78.3% in WT treated tissue in comparison to WT control (Figure 3-9A). While Kd treat (Figure3-9B) and Ov. Treated tissue (Figure 3-9C) showed a slight reduction in NFATc1 protein expression in comparison to their respective controls, and this was not significant. Kd xenografts expressed 5.3-fold less NFATc1 protein than WT, while Ov. xenografts showed 5.9-fold more NFATc1 protein in comparison to WT.

DISCUSSION

In order to elucidate the mechanism of P-S, an affymetrix gene expression microarray was performed on MIA PaCa-2 cells. Reports showed that NFAT gene expression was upregulated in response to treatment with P-S. Many studies have reported that NFATc1 gene/protein upregulation in pancreatic cancer propagates a pro-proliferative effect, further attenuating tumor progression (Schumacker 2006). In addition to aiding in pancreatic cancer progression, NFATc1 increases the transcriptional activation of both c-Myc (Guzy, et al. 2006) and COX-2 (Nussmeier, et al. 2005), two proteins involved in the continued growth of pancreatic cancer.

We first set out to analyze the role of NFATc1 and the ways in which it mediates pancreatic cancer cell response to P-S. An NFATc1 genetic knock-down and overexpression cell line was generated. NFATc1 gene and protein levels were analyzed by qRT-PCR and western blot to confirm transfection efficiency. While a complete knock-down of NFATc1 expression was not achieved, I was able to generate ~70% knock-down of its expression in both BxPC-3 and MIA PaCa-2 cell lines. In both cell lines, there was approximately a 2-fold potency enhancement of P-S in Kd cells. In MIA PaCa-2 Ov. cells, however, P-S had a 1-2-fold reduction in potency. These results highlight: (1) K-Ras mutation status did not have an effect on the efficacy of P-S, and (2) NFATc1 protein expression in pancreatic cancer cells mediates their responsiveness to treatment with P-S.

I also analyzed the effect of P-S on COX-2 and c-Myc protein expression. Upon treatment with P-S, a significant decrease in COX-2 and c-Myc protein expression was observed in NFATc1 Kd BxPC-3 and MIA PaCa-2 cell lines in comparison to their respective WT cell lines. This corroborates the findings of other groups that genetic knock-down of NFATc1 has a

profound effect on c-Myc and COX-2 protein expression (Iniguez, et al. 2000, Guzy, et al. 2006, Muller, et al. 2010). That COX-2 expression increased with increasing concentrations of P-S suggests that NFATc1 may play a protective role in tumor progression. When the cell is exposed to chemotherapeutic agents like P-S, as a last resort, NFATc1 upregulates the expression of pro-proliferative proteins. Conceivably, this upregulation of COX-2 may play a role in the activation of proliferative pathways like PI3K and Ras MAPK. Accordingly, the effect of P-S on Ras MAPK and PI3K pathways as analyzed in BxPC-3 cells. There were no significant changes in p-AKT expression (downstream of PI3K). A slight decrease in pERK (member of the Ras MAPK pathway) was observed in Kd cells in comparison to WT. While further analysis into the activity of the two aforementioned pathways in response to treatment with P-S should be pursued, my findings suggest that knock-down of NFATc1 expression upregulates their activity.

In addition to analyzing NFATc1 protein expression by western blot, its expression was also observed by immunocytochemistry. In WT untreated cells, some nuclear localization of NFATc1was observed, indicative of active NFATc1, while Kd cells showed little to no nuclear localization of NFATc1. In both WT and Kd cells, treatment with P-S increases cytoplasmic and nuclear localization of NFATc1, though the ratio of cytoplasmic to nuclear localization in Kd cells is significantly higher. These findings demonstrate that P-S induces NFATc1 expression in both Kd and WT cells, however, because Kd cells express lower levels of the gene and protein, NFATc1 induction does not affect the efficacy of the compound to the extent we observed in WT cell lines.

To determine whether or not the enhanced potency was limited to P-S, I assessed the effect of 5-FU, valproic acid, and irinotecan on cell viability in BxPC-3 WT and Kd cells. An enhanced potency was observed in Kd cells in comparison to WT amongst all three drugs. These

results show that NFATc1 protein expression mediates the effect of COX-2 dependent and COX-2 independent agents in pancreatic cancer cells.

Next, I extended the study of NFATc1 into a pancreatic cancer xenograft model. Here, I showed that tumor growth was significantly reduced by genetic silencing of NFATc1. There was a 57% reduction in tumor growth in Kd vehicle in comparison to WT vehicle, highlighting that even without treatment with P-S, tumor growth is notably reduced in the absence of NFATc1. A 62.8% reduction in tumor growth was observed in Kd xenografts ($p=0.0005$). Tumor growth was also reduced in WT xenografts by 50.4% ($p= 0.013$), though it was not as significant as in Kd xenografts, again, highlighting that the abundance of NFATc1 decreases the potency of P-S. Ov. xenografts, where NFATc1 protein expression is upregulated, showed less of a response to treatment with P-S, demonstrating only a 25.9% reduction in tumor volume, emphasizing that NFATc1 overexpression reduces P-S's efficacy.

NFATc1 protein expression correlates with P-S efficiency. Kd xenografts expressed 5.3-fold less NFATc1 protein than WT, while Ov. xenografts showed 5.9-fold more NFATc1 protein in comparison to WT. Again, underscoring that P-S reduced NFATc1 protein expression by 78.3% in WT treated xenografts. On the other hand, Kd and Ov. xenografts showed no significant reduction in NFATc1 protein expression in response to drug.

In summation, I have shown that NFATc1 protein expression regulates tumor growth. In the absence of NFATc1 alone, tumor progression was significantly inhibited; the addition of P-S treatment further reduced tumor growth. When NFATc1 was overexpressed, there was no obvious effect on tumor growth. These findings indicate that overexpression of NFATc1 in

pancreatic cancer causes some resistance to treatment with P-S, and when expression was reduced P-S was able to significantly inhibit cancer growth.

FIGURES

Table 3-2. P-S Reduces cell viability more efficiently in the absence of NFATc1 protein expression. NFATc1 Kd or Ov. BxPC-3 and MIA PaCa-2cells were incubated with P-S for 24 hr. Utilizing an MTT cell viability assay to determine the effect of treatment on IC_{50}, a significant enhancement of potency of P-S was observed in both NFATc1 (A) BxPC-3 (3-fold) and (B) MIA PaCa-2 (2.4-fold) Kd cells. P-S demonstrated decreased potency in NFATc1 Ov. cells (-1.2-fold).

A.

BxPC-3

	P-S (μM)	Potency Enhancement
WT	106± 4.0	-
Kd Control	104 ± 2.0	-
Kd	35± 2.0	3

B.

MIA PaCa-2

	P-S (μM)	Potency Enhancement
WT	85± 1.0	-
Kd Control	93 ± 1.0	-
Kd	38± 2.0	2.4
Ov.	111± 2.0	-1.2

Table 3-3. Effect of COX-2 independent agents on IC_{50} in BxPC-3 WT and Kd cells. 5-FU, valproic acid and irinotecan were incubated in BxPC-3 WT and Kd cells for 24 hr. Cell viability by a MTT assay. All 3 compounds had enhanced potency in NFATc1 Kd cells in comparison to WT.

	WT	Kd	Potency Enhancement
5-FU (μM)	586 ± 2.0	263 ± 2.0	2.2
Valproic acid (μM)	543 ± 1.0	338 ± 3.0	1.6
Irinotecan (μM)	58.5 ± 4.0	26.8 ± 2.0	2.2

Figure 3-1. Generation of a stable NFATc1 knockdown and overexpression model in human pancreatic cancer cell lines. BxPC-3 and MIA PaCa-2 cells were transfected with NFATc1 shRNA or cDNA, clones selected and relative mRNA levels analyzed. (A) In BxPC-3 cells, there was a reduction in NFATc1 mRNA of 70.9% (p=0.003). A reduction of 67.7% (p=0.001) in NFATc1 MIA PaCa-2 cells was observed. Further, a 2.5-fold increase in gene expression (p=0.015) was detected in MiaPaCa-2 NFATc1 overexpression cells.

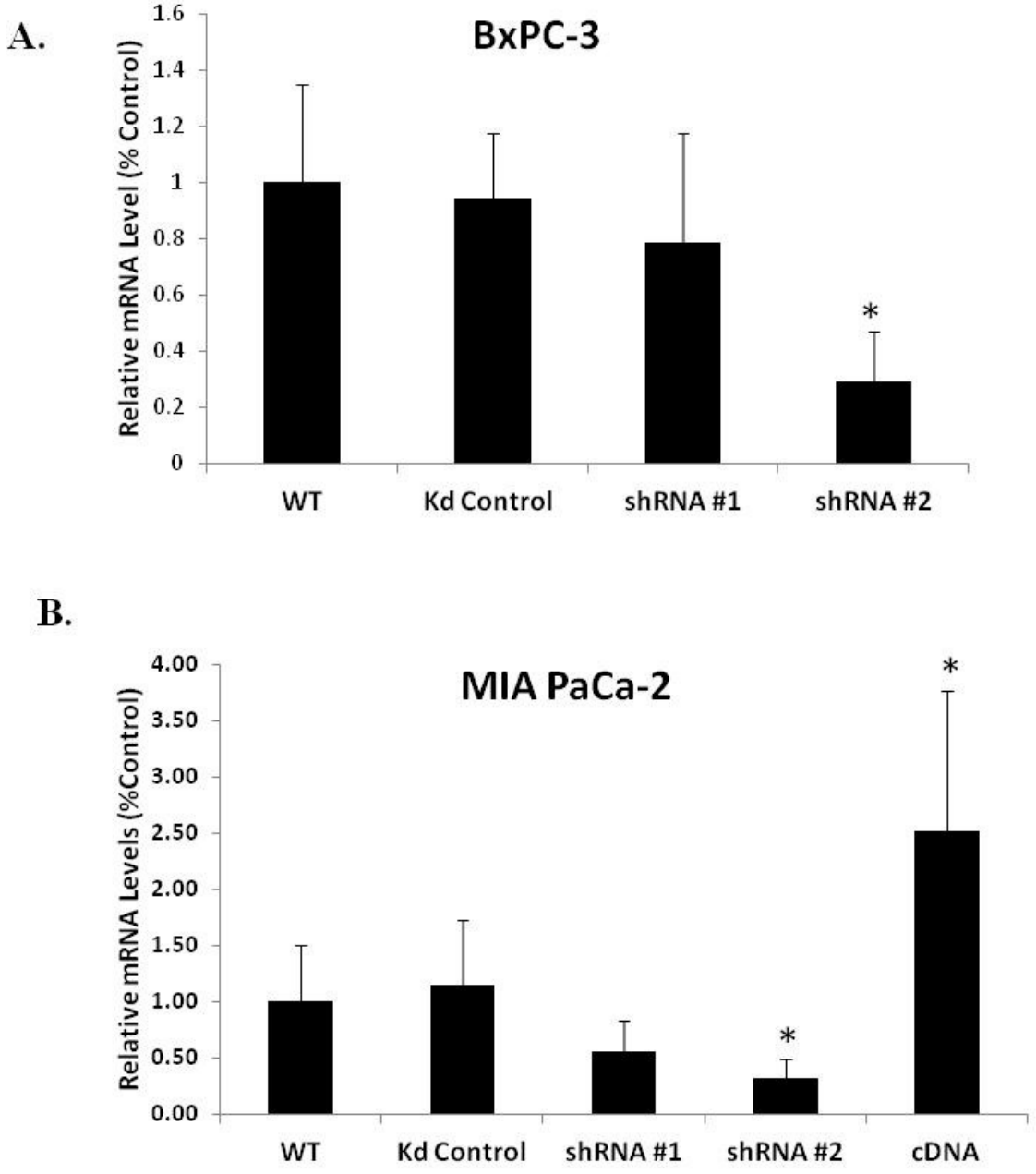

Figure 3-2. Genetic abrogation of NFATc1 decreases NFATc1, COX-2 and c-Myc protein expression in BxPC-3 Kd cells. (A) BxPC-3 NFATc1 WT and Kd cells were treated with vehicle, P-S 0.5 and 1.0xIC_{50}, or sulindac 1.0xIC_{50} for 24 hr. Cells were lysed and proteins extracted and analyzed by western blot. (B) While NFATc1 protein expression increased in both WT and Kd cells in response to treatment with P-S, Kd cells demonstrated significantly less NFATc1 and (C) COX-2 protein expression. (D) c-Myc protein expression was significantly less in Kd cells in comparison to WT, increasing concentrations of P-S elicited decreased protein expression of c-Myc. (* = $p<0.05$)

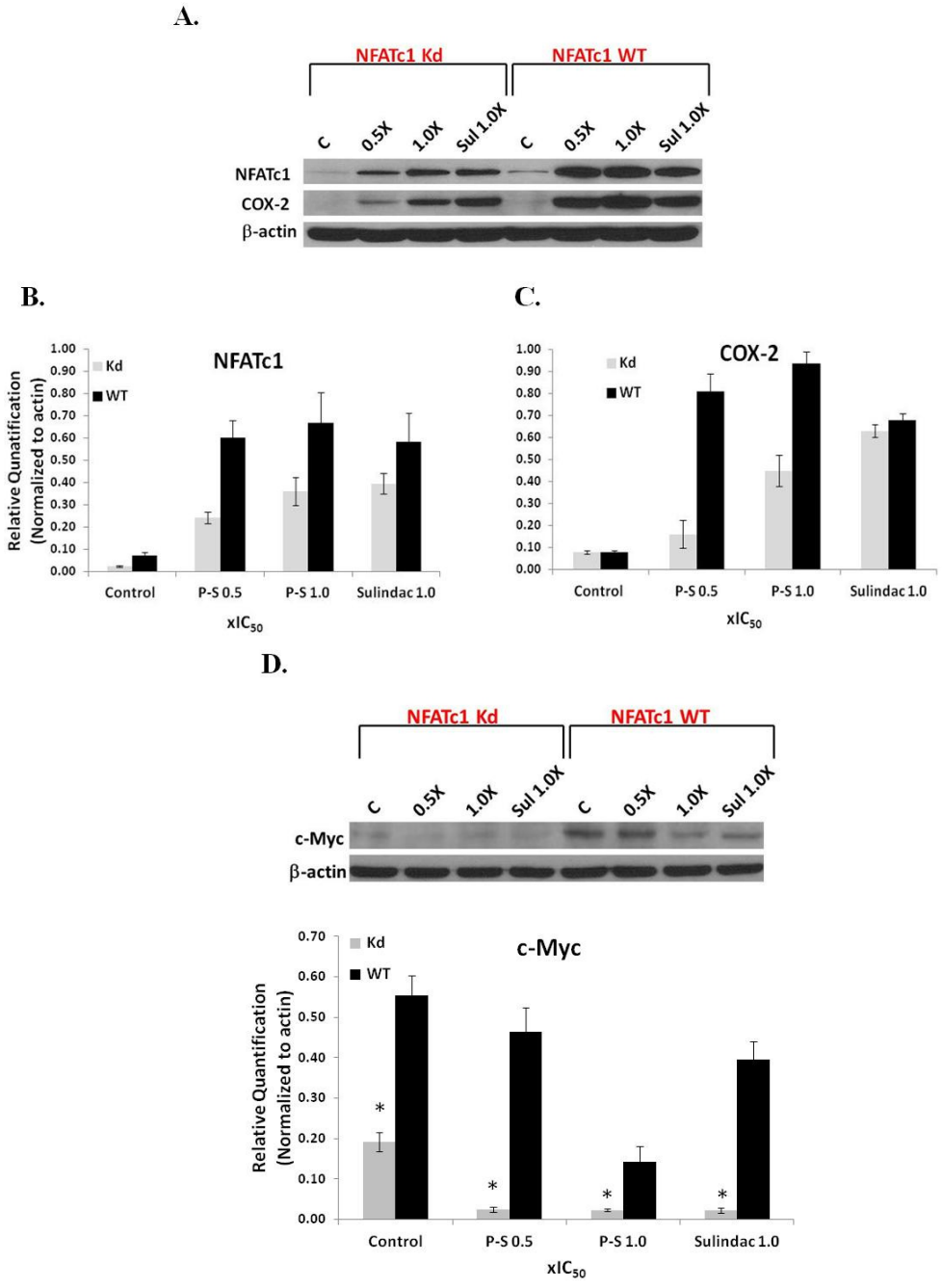

Figure 3-3. Induction of Nuclear NFATc1 Protein Expression is Decreased in Response to Treatment with P-S in BxPC-3 Kd Cell Lines. Cells were treated with increasing concentrations of P-S, lysed and nuclear proteins extracted. (A) NFATc1 nuclear protein expression was significantly lower in Kd cells in comparison to WT. With increasing concentration of P-S, both Kd and WT cells showed an increase in nuclear NFATc1 protein expression, though Kd cells demonstrated significantly less protein levels. (B) Ratio of cytoplasmic to nuclear NFATc1 protein levels were analyzed, showing significantly less NFATc1 protein expression in nuclear vs. cytoplasmic extracts. (* = $p<0.05$)

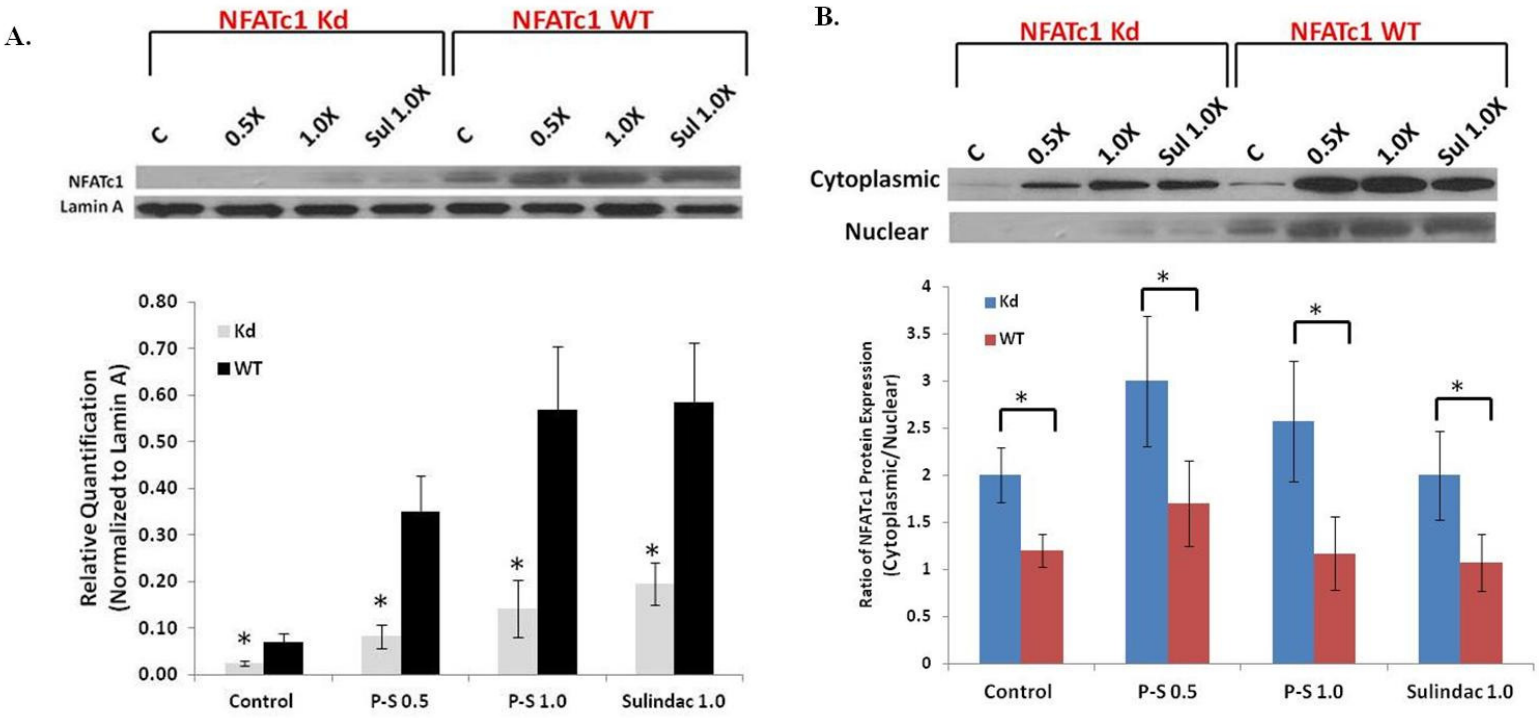

Figure 3-4. Cytoplasmic NFATc1 expression increases in response to P-S in MIA PaCa-2 cells. Mia PaCa-2 NFATc1 WT, Kd and Ov. cells were treated with vehicle, P-S 0.5 and 1.0xIC_{50}, or sulindac 1.0xIC_{50} for 24 hr. Cells were lysed and proteins extracted and analyzed by western blot. A significant decrease in NFATc1 protein expression was observed in Kd cells, with a slight increase in Ov. cells. A similar increase in NFATc1 protein expression in response to treatment with P-S or sulindac was observed in WT, Kd and Ov. cells. (* = $p<0.05$)

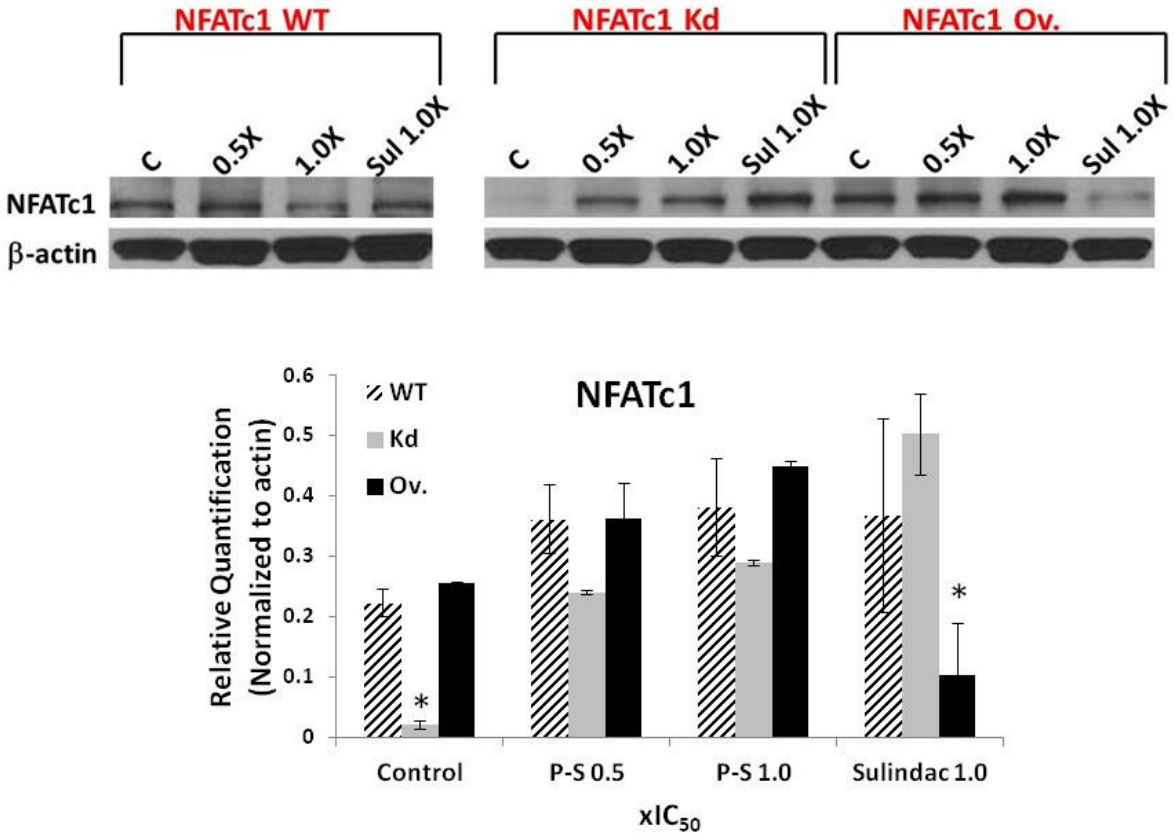

Figure 3-5. Induction of Nuclear NFATc1 Protein Expression is Decreased in Response to Treatment with P-S in MIA PaCa-2 Kd Cell Lines. Cells were treated with increasing concentrations of P-S, lysed and nuclear proteins extracted. (A) NFATc1 nuclear protein expression was significantly lower in Kd cells in comparison to WT. Ov. cells showed a statistically significant increase in nuclear NFATc1 expression in comparison to WT. (B) Ratio of cytoplasmic to nuclear NFATc1 protein levels were analyzed, showing significantly less NFATc1 protein expression in Kd and WT nuclear vs. cytoplasmic extracts. In Ov. cells the ratio was slightly lower than WT (not significant), indicating that these cells had higher levels of nuclear NFATc1 expression than WT. (* = $p<0.05$)

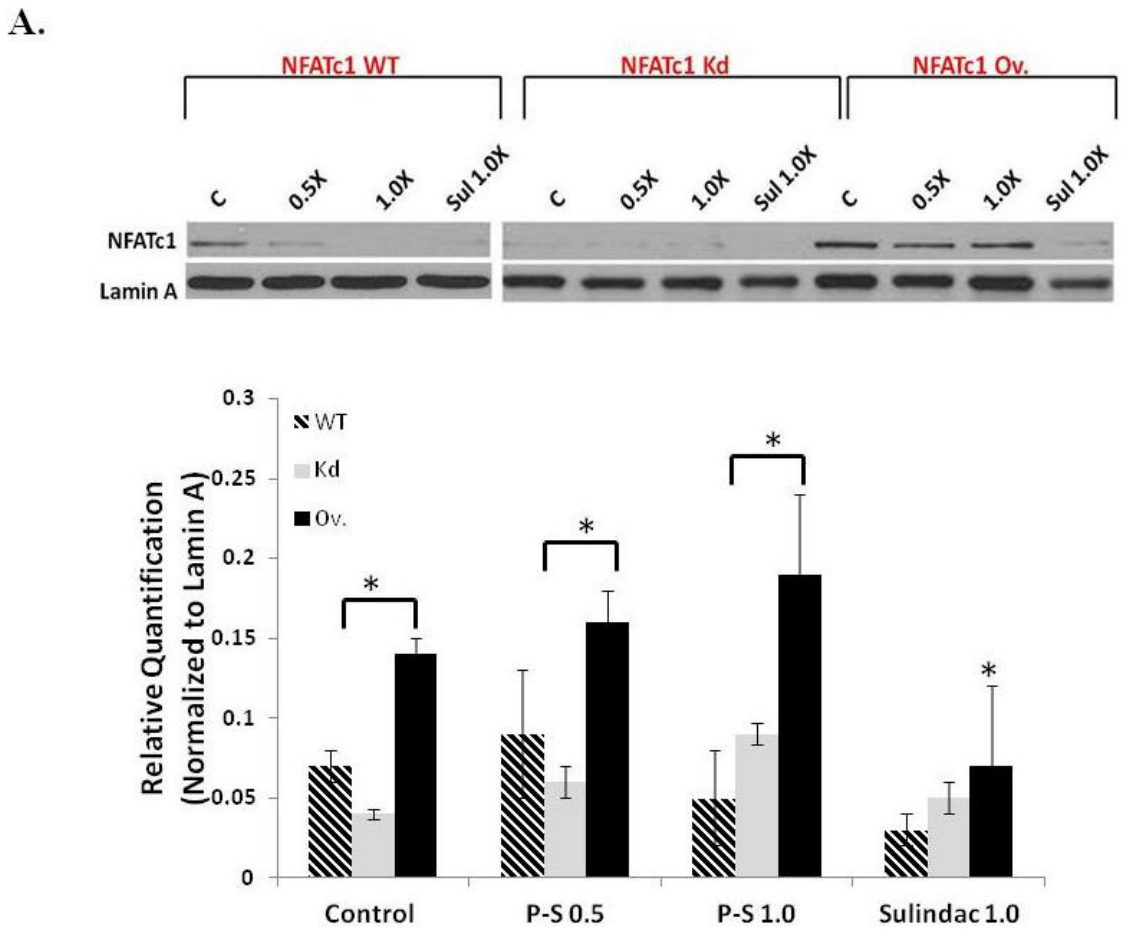

B.

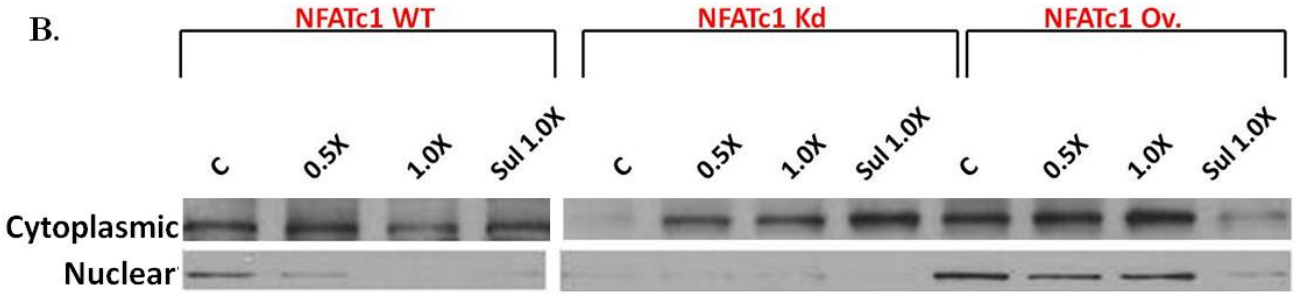
NFATc1 WT
NFATc1 Kd
NFATc1 Ov.
C
0.5X
1.0X
Sul 1.0X
C
0.5X
1.0X
Sul 1.0X
C
0.5X
1.0X
Sul 1.0X
Cytoplasmic
Nuclear

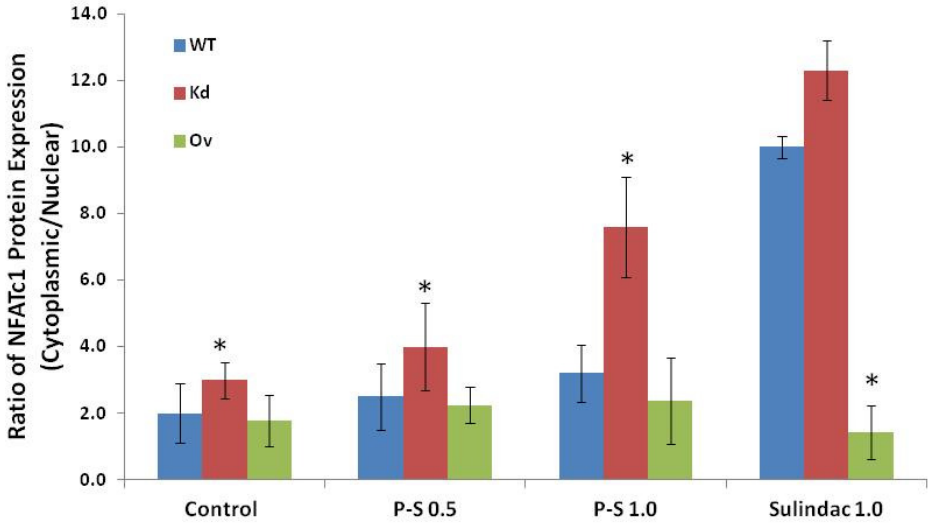
Ratio of NFATc1 Protein Expression (Cytoplasmic/Nuclear)
14.0
12.0
10.0
8.0
6.0
4.0
2.0
0.0
WT
Kd
Ov
*
*
*
*
Control
P-S 0.5
P-S 1.0
Sulindac 1.0

Figure 3-6. NFATc1 protein expression and nuclear localization decreases with genetic abrogation of NFATc1. BxPC-3 cells were treated with vehicle or P-S 1.0xIC_{50} for 24 hr. Cells were fixed and incubated with NFATc1 primary, then secondary antibody. Cells were imaged by fluorescence microscopy. Kd cells showed less cytoplasmic and nuclear expression of NFATc1. In both WT and Kd cells, treatment with P-S increases cytoplasmic levels of NFATc1 protein.

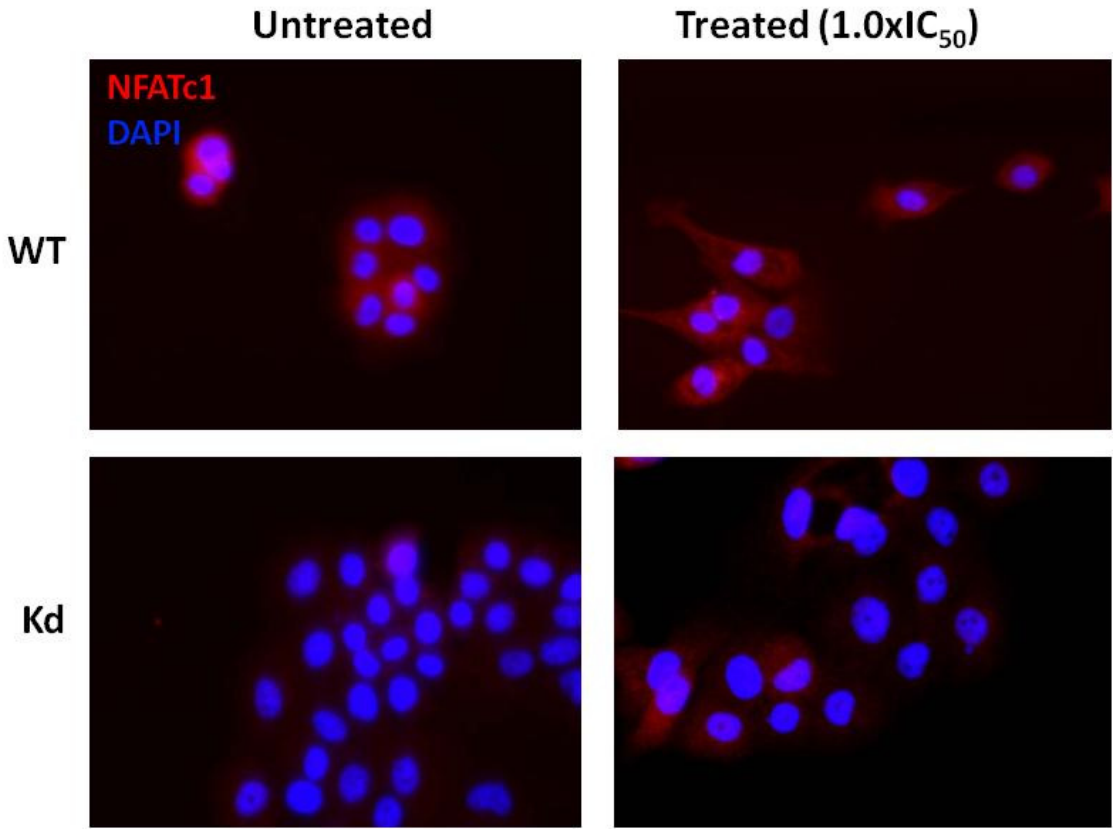

Figure 3-7. Effect of P-S on Ras MAPK and PI3K Pathways in BxPC-3 Cells. BxPC-3 NFATc1 WT and Kd cells were treated with vehicle, P-S 0.5 and 1.0xIC_{50}, or sulindac 1.0xIC_{50} for 24 hr. Cells were lysed and proteins extracted and analyzed by western blot. A slight decrease in pERK was observed in Kd cells in comparison to WT. No observable changes were seen in pAKT expression.

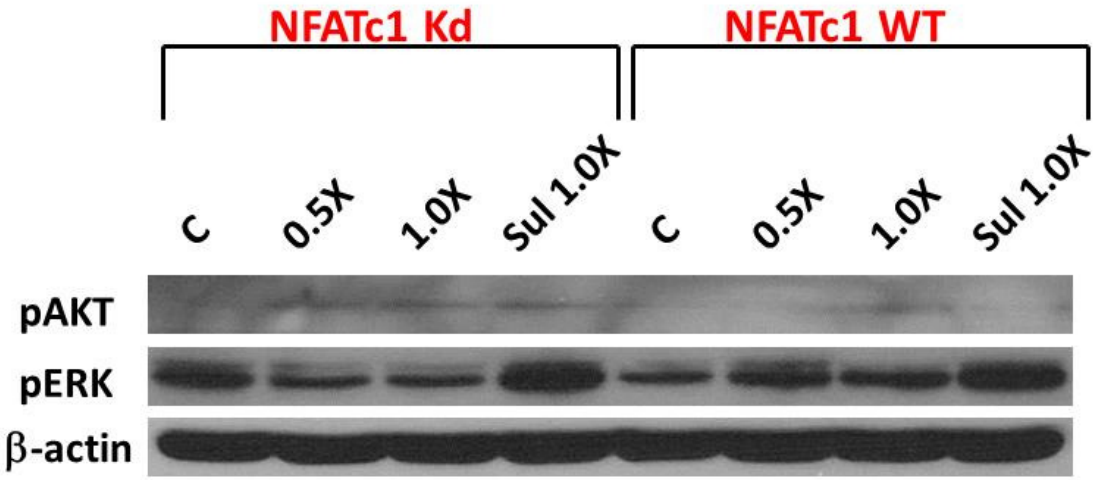

Figure 3-8. P-S Inhibits Tumor Growth In Xenograft Model For Pancreatic Cancer. Six-week-old female BALB/c nude mice were subcutaneously injected with $3.0x10^6$ ($1.5x10^6$ in right and left flank, respectively) MIA PaCa-2 cells (WT. Kd, and Ov.). Following a prevention protocol, animals were first treated by gavage with P-S (100 mg/kg/d), or vehicle (corn oil) for one week prior to subcutaneous injection. Animals were treated for 4 weeks. Upon completion of the study, animals were euthanized and tumors collected and measured. Tumor volume was significantly reduced in (A) WT treated (* p= 0.013), and (B) Kd treated (*p=0.0005) in comparison to their respective vehicle. Tumor volume was also reduced in (C) Ov. treated animals in comparison to vehicle, though it was not significant.

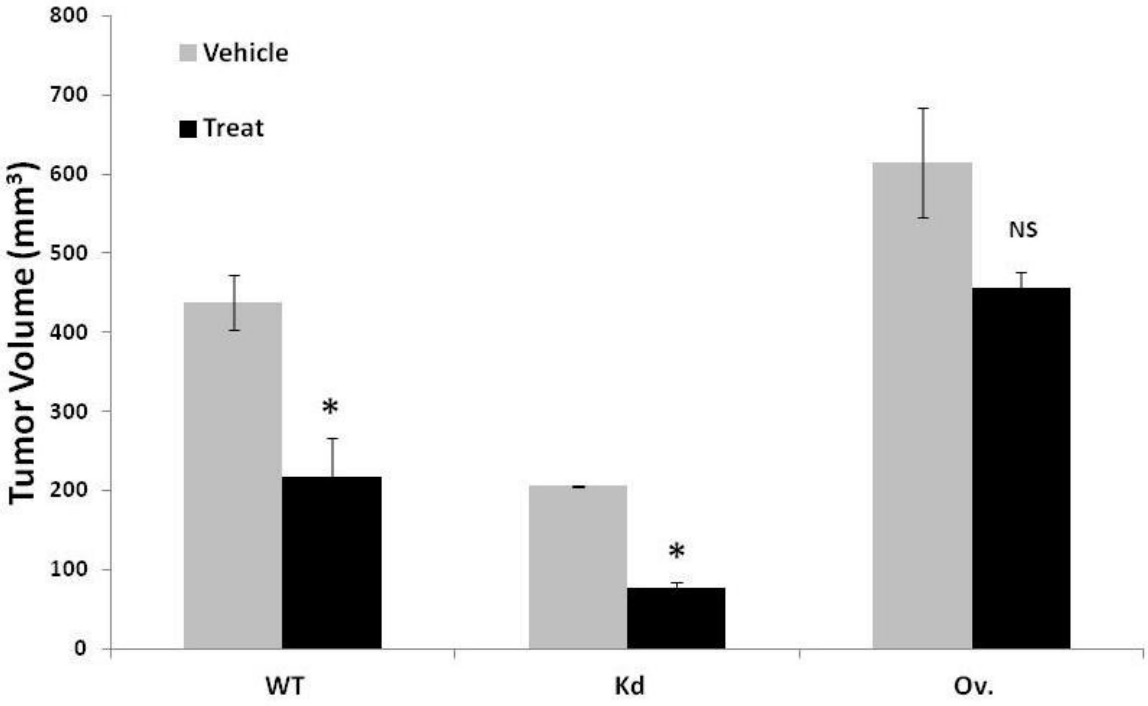

Figure 3-9. P-S Reduces nuclear NFATc1 Localization in MIA PaCa-2 Xenograft. OCT-embedded tissue from MIA PaCa-2 xenograft were stained with primary antibody to NFATc1 and analyzed by confocal laser microscopy. (A) NFATc1 protein expression was reduced by (A) 78.3% in WT tissue. While (B) Kd and (C) Ov. tissue showed a slight reduction in NFATc1 protein expression, it was not significant. Kd xenografts showed 5.3-fold less NFATc1 protein expression in comparison to WT, while Ov. showed 5.9-fold more NFATc1 protein expression in comparison to WT. (* = $p<0.05$)

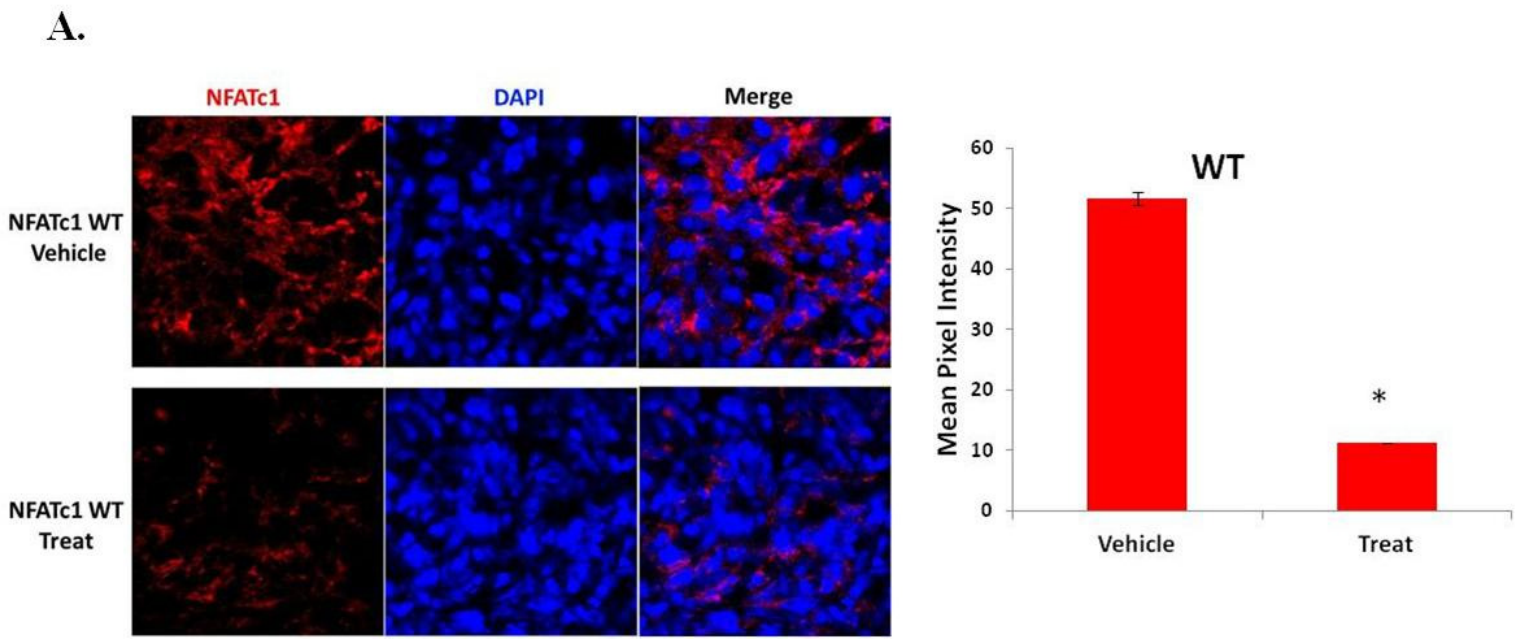

B.

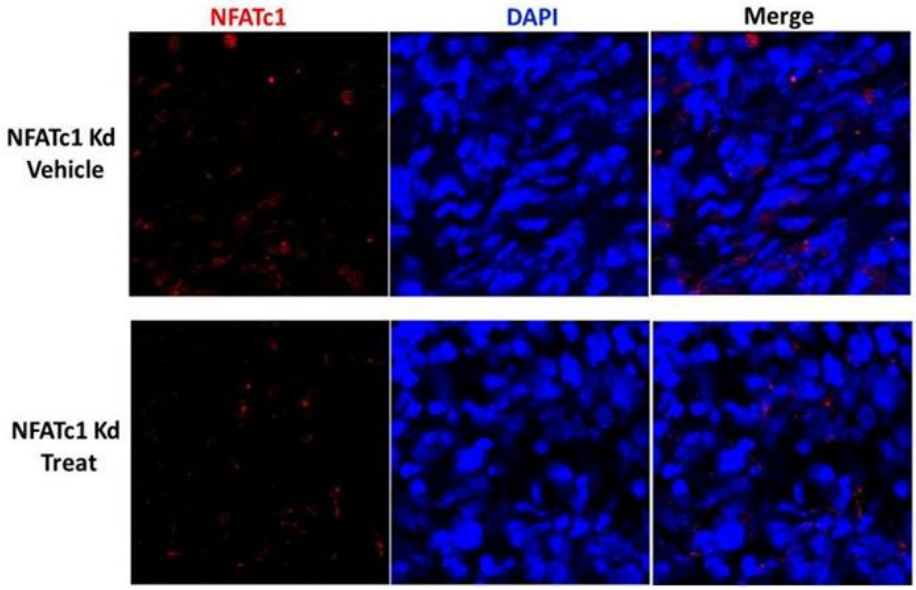
NFATc1
DAPI
Merge
NFATc1 Kd Vehicle
NFATc1 Kd Treat

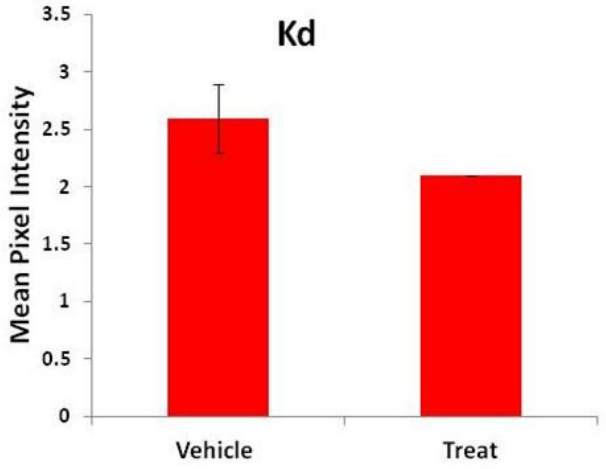
Kd
Mean Pixel Intensity
3.5
3
2.5
2
1.5
1
0.5
0
Vehicle
Treat

C.

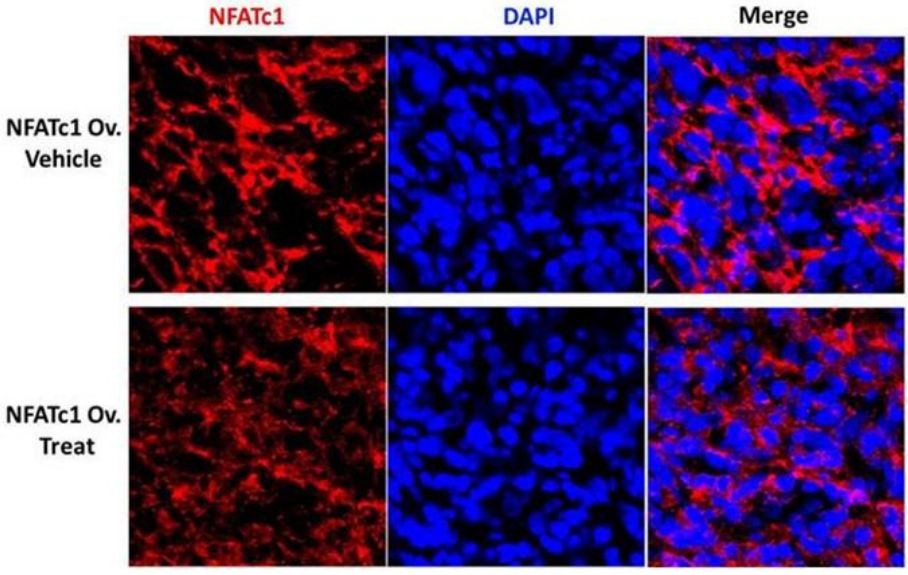
NFATc1
DAPI
Merge
NFATc1 Ov. Vehicle
NFATc1 Ov. Treat

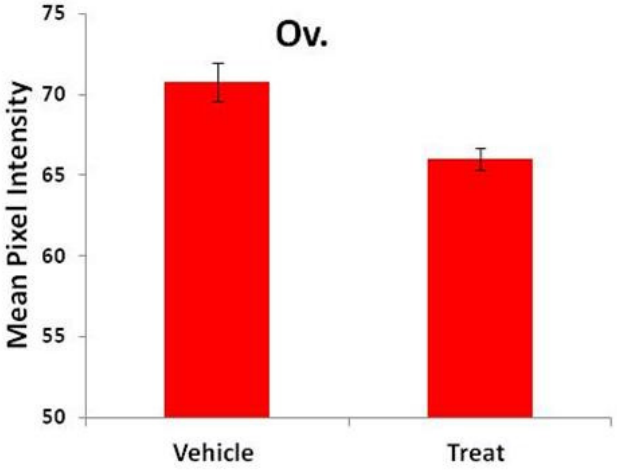
Ov.
Mean Pixel Intensity
75
70
65
60
55
50
Vehicle
Treat

CHAPTER IV

P-S and CsA COMBINATION

INTRODUCTION

In the cytoplasm, NFAT is activated by cell surface receptors that are coupled to Ca^{2+} mobilization. Briefly, activation of phospholipase Cγ (PLCγ) by ligand binding to immunoreceptors, receptor tyrosine kinases and G-protein-coupled receptors leads to the production of inositol-1,4,5-trisphosphate ($InsP_3$), resulting in the release of Ca^{2+} from endoplasmic reticulum Ca^{2+} stores. This triggers a process known as store-operated Ca^{2+} entry (SOCE) (Feske 2007, Hogan, Lewis and Rao 2010), which leads to the activation of calmodulin and calcineurin (Hogan, et al. 2003). This phosphatase, calcineurin, then dephosphorylates the regulatory domain of NFAT, leading to NFAT nuclear translocation. Once inside the nucleus NFAT can cooperate with multiple transcriptional partners, including AP1, forkhead box P-family proteins (such as FOXP2 and FOXP3) and proteins of the GATA family, to initiate and maintain specific transcriptional programs that vary with cell type and the pattern of stimulation (Hogan, et al. 2003, Macian 2005, Crabtree, et al. 2009).

The bulk of the evidence implicating the Ca^{2+}–NFAT signaling pathway in the pathogenesis of solid tumors comes from studies of breast cancer and pancreatic ductal carcinoma (Buchholz, et al. 2006, Yoeli-Lerner, Chin, Hansen and Toker 2009). Studies have reported constitutive overexpression and aberrant nuclear translocation of NFATc1 in biopsies

from patients with pancreatic cancers. Furthermore, it was shown that NFATc1 can directly induce transcriptional activation of the MYC oncogene by binding to the proximal MYC promoter (Buchholz, et al. 2006, Guzy, et al. 2006). Other studies have shown that NFAT transcription factors are involved in cancer cell proliferation in prostate tumors (Lehen'kyi, Flourakis, Skryma and Prevarskaya 2007) and can also be important in malignant melanoma and endometrial carcinoma (Flockhart, et al. 2009, Sales, et al. 2010). Therefore, in addition to their well-defined role in the immune system, NFAT transcription factors have been shown in recent years to be of crucial importance for tumor cell proliferation, migration and angiogenesis (Muller, et al. 2010).

CsA Inhibits Ca^{2+}–NFAT Signaling

The immunosuppressive drug cyclosporin A (CsA) inhibits calcineurin activity (Liu, et al. 1991). CsA is a highly specific probe of the NFAT signaling pathway. Calcineurin removes several phosphate residues from the N terminus of the NFATc1 proteins, the Ca^{2+}-calcineurin-sensitive subunits of NFAT transcription complexes. Removal of the phosphates exposes nuclear localization sequences in NFATc1 leading to its rapid entry into the nucleus (Beals, Clipstone, Ho and Crabtree 1997). CsA inhibition of calcineurin phosphatase activity allows NFATc1 to remain phosphorylated, thus localized to the cytoplasm where it is unable to aid in the transcription of relevant genes.

Interplay between ROS and Ca^{2+} Signaling in Cancer Progression

Previous studies from our lab have shown that P-S induces reactive oxygen species (ROS) in colon cancer cells (Sun, et al. 2008, Mackenzie, et al. 2010), and that the induction of

ROS leads to apoptosis, necrosis, and finally cancer cell death, while leaving noncancerous cells intact.

ROS are broadly defined as oxygen-containing, highly reactive chemical species. There are two types of ROS, those that are free radicals, which contain one or more unpaired electrons in their outer molecular orbitals, and non-radical ROS, which do not have unpaired electrons but are chemically reactive and can be converted to radical ROS. Examples of radical ROS that are commonly seen in biological systems are superoxide, nitric oxide and hydroxyl radicals (Trachootham, et al. 2009).

Compared with normal cells, malignant cells seem to function with higher levels of endogenous oxidative stress (Szatrowski, et al. 1991, Kawanishi, et al. 2006). Although the precise pathways leading to ROS stress in cancer cells remain unclear, several intrinsic and extrinsic mechanisms are thought to cause oxidative stress during cancer development and disease progression. Activation of oncogenes, aberrant metabolism, mitochondrial dysfunction and loss of functional p53 are intrinsic factors known to cause increased ROS production in cancer cells (Irani, et al. 1997, Horn, et al. 2007, Rodrigues, et al. 2008). The expression of genes that are associated with tumor transformation, such as Ras, Bcr-Abl and c-Myc, were found to induce ROS production (Behrend, et al. 2003, Kissil, et al. 2007).

Therapeutic selectivity is essential in cancer treatment. As cancer cells have elevated ROS generation and are under increased intrinsic oxidative stress, it is conceivable that these malignant cells would be more dependent on antioxidants for cell survival and, therefore, more vulnerable to further oxidative insults induced by ROS-generating agents or by compounds that abrogate the key antioxidant systems in cells (Trachootham, et al. 2009).

P-S has shown minimal toxicity in preclinical animal models. In addition, research into possible mechanisms of P-S's anticancer properties lean towards the induction ROS (Sun, et al. 2011). However, ROS and Ca^{2+} signaling systems have been shown to be intimately integrated, with either having the ability to regulate the other. In concert, the two can regulate the balance of cell proliferation, cell cycle arrest and cell death in favor of cancer growth (Lee, et al. 2002). Because a steady induction of ROS may in part play a role in Ca^{2+}–NFATc1 activation, inhibition of the pathway using CsA may further increase the chemotherapeutic efficacy of P-S.

In this chapter, I show that P-S significantly increases ROS in pancreatic cancer cells. This increase in ROS by P-S may play a role in an increase in Ca^{2+}–NFAT signaling. To circumvent an increase in NFATc1 expression that we saw in chapter III, a combination with P-S and CsA may demonstrate greater anticancer effects on pancreatic cancer growth.

MATERIALS AND METHODS

Reagents

Phospho-Sulindac (P-S) was synthesized as reported. All general solvents and reagents were of HPLC grade or the highest grade commercially available.

Cell Lines

Human pancreatic cancer cell line BxPC-3 was obtained from ATTC (Manassas, VA). Cells were grown at 37°C in 5% CO_2 in the specific medium suggested by ATCC and supplemented with 10% fetal calf serum (Mediatech, Herndon, VA), penicillin (50 U/ml) and streptomycin (50 µg/ml; Life Technologies, Grand Island, NY).

BxPC-3 PaCa-2 NFATc1 knockdown cell line was generated using MISSION Lentiviral Packaging Mix (Sigma Aldrich). Cells were infected with the lentivirus and then subjected to 3 ug/ml of puromycin to generate stable cell lines. Decreased levels of NFATc1 were confirmed by western blot.

Cell Viability Assay

Cell viability was measured by the 3-(4,5-dimethylthiazol-2-yl)-2,5-diphenyltetrazolium bromide assay following the protocol of the manufacturer (Roche Diagnostics). Briefly, cells were pre-treated with 1µM CsA for 1h, followed either 0.5x or 1.0xIC_{50} of P-S. Cells were treated for 24 hr, and cell viability measured.

Immunocytochemistry

Cells were seeded in an 8-well glass chamber slide (Lab-Tek, Rochester, NY). The following day, cells were treated with of P-S 1.0xIC_{50}, CsA (1µM), or ionomycin (1µM) for 24

hr. Cells were fixed in 4% paraformaldehyde (15 min). Block and NFATc1 antibody (Abcam, Cambridge, MA) incubations were in PBS, 2% BSA and 0.3% Triton. Cells were mounted with Vectashield mounting media with diamidinophenylindole (DAPI) (Vector Laboratories Inc., Burlingame, CA). Cells were imaged using Zeiss Axioplan inverted fluorescence microscope (Thornwood, NY, USA)

ROS Determination

Cells (1.0×10^5 cells per well) were treated with or without P-S for 1 hr. After treatment, cells were trypsinized and stained with 10 μM DCFDA for 30 min at 37 °C and the fluorescence intensity was analyzed by FACScaliber (BD Bioscience, San Jose, CA).

Determination of ROS by Fluorescence Microscopy

Cells were seeded in 4-well chamber glass slides (Lab-Tek, Rochester, NY). The following day, cells were treated with 10μm DCFDA and either vehicle or P-S for 1 hr. Cells were imaged using Zeiss (Thornwood, NY, USA) Axioplan inverted fluorescence microscope. Images were acquired using a Zeiss Axiocam MRM digital camera and Zeiss Axiovision imaging software.

Western Blot

After treatment, cells were lysed on ice with 1% Triton lysis buffer with 2.5 mmol/L 4-nitrophenylphosphate, 1% SDS, and 0.25% sodium deoxycholate for 30 min. The cell lysate (25 μg) was loaded onto SDS-electrophoresis gel and transferred onto a PVDF membrane. The membrane was then immunoblotted with NFATc1 (Abcam), p-NFATc1 (Santa Cruz

Biotechnology) antibodies. Secondary antibodies conjugated with horseradish peroxidase (HRP) (Santa Cruz Biotechnology) were applied to membrane, followed by development on X-ray film.

Statistical Analysis

Results from at least 3 independent experiments and expressed as mean $\pm$ SD were analyzed by the student's t-test. *$p<0.05$ was considered significant.

RESULTS

The Combination of P-S with CsA Enhances the Potency of P-S in BxPC-3 Cells

BxPC-3 NFATc1 WT and Kd cells were pre-treated with 1μM CsA for 1 hr, followed by either 0.5x or 1.0xIC_{50} of P-S. Cells were treated for 24 hr. Utilizing an MTT cell viability assay to determine the effect of treatment on IC_{50}, a 1.2-fold enhancement of potency of P-S was observed in combination with CsA in WT cells (Table 4-1), while no effect was observed in Kd cells.

P-S Combined with CsA Inhibits NFATc1 Expression in BxPC-3 Cells

BxPC-3 NFATc1 WT and Kd cells were treated with vehicle, P-S 0.5xIC_{50} + CsA and 1.0xIC_{50} + CsA, or CsA alone for 24 hr (Figure 4-1). Cells were lysed and proteins extracted and analyzed by western blot. A significant decrease in cytoplasmic NFATc1 protein expression was observed in both Kd and WT cells. I also analyzed nuclear NFATc1 expression (data not shown), NFATc1 protein was not detected, even with increasing concentrations of P-S.

P-S Combined with CsA Reduces NFATc1 Protein Expression in BxPC-3 Cells

BxPC-3 cells were treated with vehicle or P-S 1.0xIC_{50} , CsA (1μM), ionomycin (1μM) (intracellular calcium stimulant), or P-S + CsA for 24 hr. Cells were fixed and incubated with NFATc1 primary, then secondary antibody. Cells were imaged by fluorescence microscopy. NFATc1 showed some nuclear localization in untreated cells (Figure 4-2). P-S increased cytoplasmic localization of NFATc1, while CsA reduced it. Ionomycin increases both nuclear and cytoplasmic NFATc1 protein expression. The combination of P-S and CsA reduced cytoplasmic and nuclear NFATc1 protein expression (Figure 4-2).

P-S Induces ROS in BxPC-3 Cells

BxPC-3 cells (1.0×10^5 cells per well) were treated with vehicle or P-S 1.0xIC_{50} for 1 hr andf ROS levels were determined using the DCFDA general ROS probe (Figure 4-3A). There was a 3-fold increase in ROS in cells treated with P-S ($p = 0.05$). Live cell imaging for ROS levels was also performed in BxPC-3 cells treated either with vehicle or P-S for 1h (Figure 4-3B), again using the DCFDA general ROS probe. Cells were imaged by fluorescence microscopy. There was a notable increase in ROS in cells treated with P-S in comparison to vehicle.

DISCUSSION

It has been previously demonstrated that P-S induces ROS in cancer cells (Cao and Li 2002, Sun, et al. 2008, Mackenzie, et al. 2010, Sun, et al. 2011). As cancer cells have elevated ROS generation and are under increased intrinsic oxidative stress, these cells are more vulnerable to further oxidative insults induced by ROS-generating agents, such as P-S. Flow cytometry and fluorescence microscopy data showed a significant increase in ROS in response to treatment with P-S. This induction of ROS may contribute to the anticancer effects of P-S in pancreatic cancer cells.

In chapter III, I showed that P-S increased cytoplasmic and nuclear NFATc1 protein expression in a concentration-dependent manner in both Kd and WT cells. This increase in NFATc1 expression could have deleterious effects, especially if calcium flux is triggered by any intracellular mechanism. Because NFATc1 activation is initiated by fluctuations in intracellular calcium levels, inhibiting calcium-calcineurin activity with CsA may further increase the chemotherapeutic efficacy of P-S. It is speculated that a steady induction of ROS may in part play a role in Ca^{2+}–NFATc1 activation, as ROS and Ca^{2+} signaling systems have been shown to be intimately integrated, with either having the ability to regulate the other (Lee, et al. 2002). Thus the combination of P-S and CsA would circumvent any off-target effects of ROS induction.

In fact, treatment of BxPC-3 NFATc1 WT and Kd cells with P-S and CsA elicited a 1.2-fold enhancement of potency of P-S in WT cells, while no effect was observed in Kd cells (as NFATc1 protein expression was reduced by RNAi). In addition to analyzing what effect the combination would have on the efficacy of P-S, I determined the effect on NFATc1 protein

expression. To note, western blot and fluorescent microscopy data revealed that the combination of P-S and CsA inhibited nuclear and cytoplasmic NFATc1 protein expression in BxPC-3 cells.

In summary, I have shown that P-S significantly increases ROS in pancreatic cancer cells. This increase in ROS by P-S may play a role in the increased NFATc1 protein expression that we observed in chapter III. Combination treatment with CsA both enhanced the efficacy of P-S, as well as inhibited NFATc1 nuclear and cytoplasmic protein expression in pancreatic cancer cells.

FIGURES

Table 4-1. Combination of P-S and CsA Enhances Potency of P-S in BxPC-3 Cells. BxPC-3 NFATc1 WT and Kd cells were treated with P-S CsA, or both for 24 hr. Utilizing an MTT cell viability assay to determine the effect of treatment on IC_{50}, a significant enhancement of potency of P-S was observed in combination with CsA, specifically in WT cells.

	P-S (μM)	P-S+ CsA (μM)	Potency Enhancement
WT	85± 1.0	67	1.2
Kd	38± 2.0	37	-

Figure 4-1. Combination of P-S & CsA Inhibits NFATc1 Expression in BxPC-3 Cells. BxPC-3 NFATc1 WT and Kd cells were treated with vehicle, P-S 0.5 xIC_{50} + CsA and 1.0xIC_{50} + CsA, or CsA alone for 24 hr. Cells were lysed and proteins extracted and analyzed by western blot. A significant decrease in NFATc1 protein expression was observed in both Kd and WT cells.

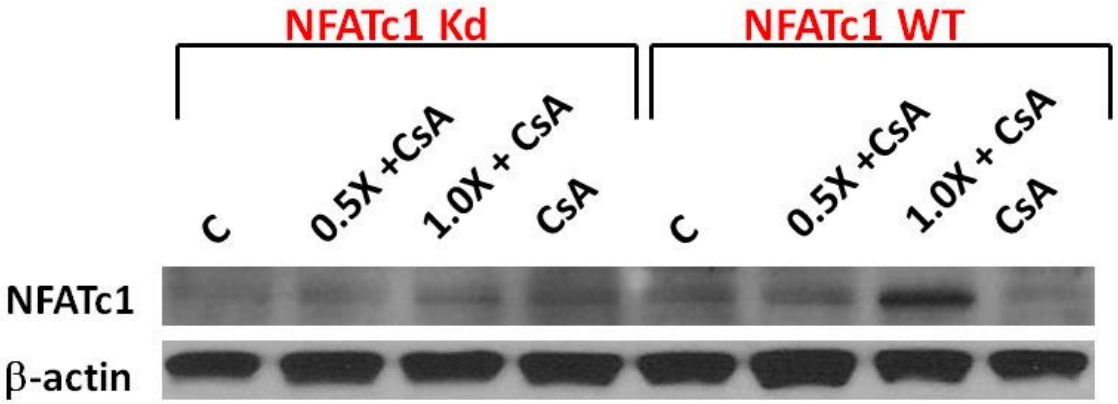

Figure 4-2. Combination of P-S and CsA Reduces NFATc1 Protein Expression in BxPC-3 Cells. BxPC-3 cells were treated with vehicle or P-S 1.0xIC_{50} , CsA (1μM), ionomycin (1μM), or P-S + CsA for 24 hr. Cells were fixed and incubated with NFATc1 primary, then secondary antibody. Cells were imaged by fluorescence microscopy. NFATc1 showed some nuclear localization in untreated cells. Treatment with P-S increased cytoplasmic and nuclear localization of NFATc1, while CsA reduced both. Ionomycin increases both nuclear and cytoplasmic NFATc1 protein expression. Combination with P-S and CsA reduces total NFATc1 protein expression.

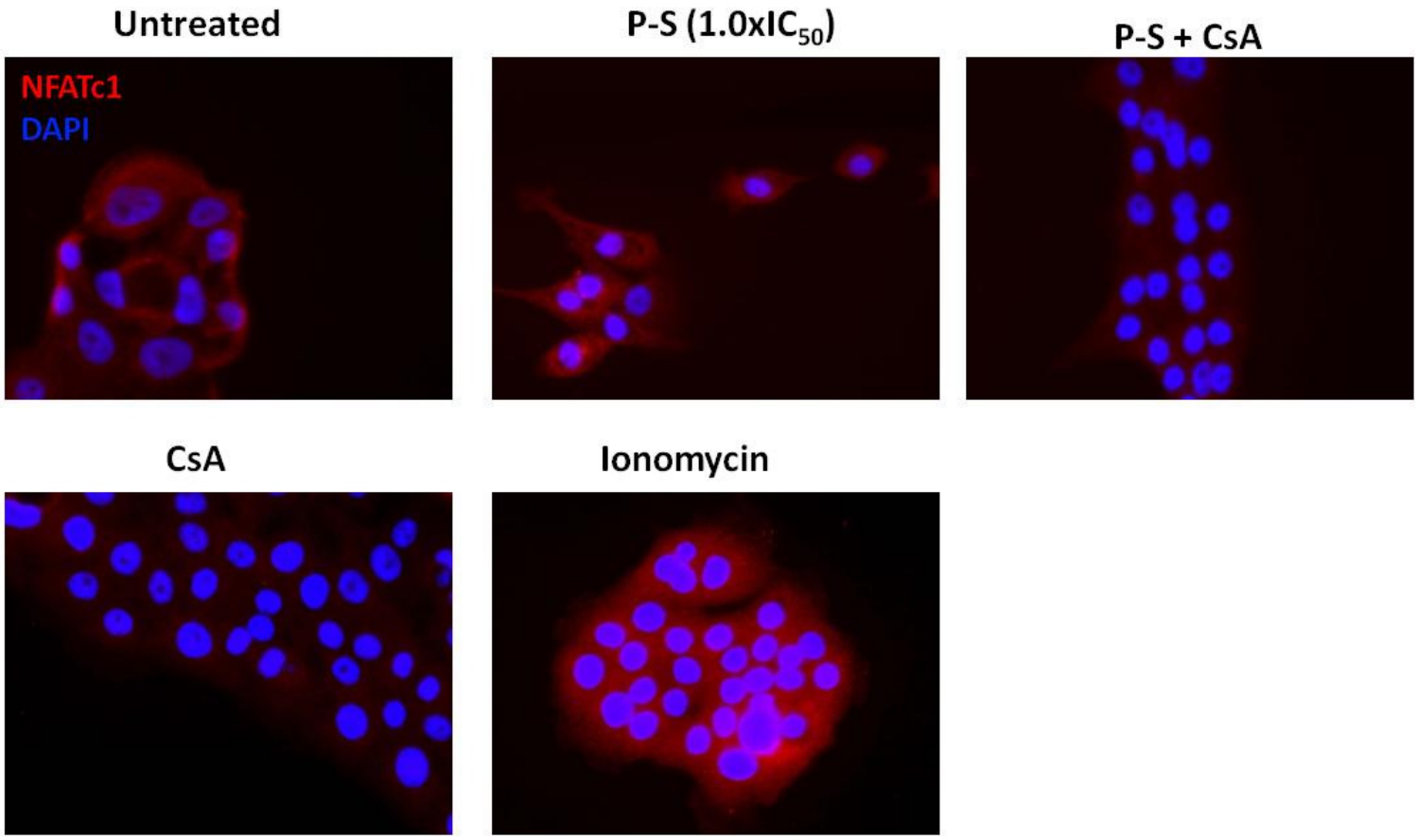

Figure 4-3. P-S Induces ROS in BxPC-3 Cells. (A) BxPC-3 cells were treated with vehicle or P-S 1.0xIC_{50} for 1 hr. After treatment, cells were trypsinized and stained with 10 µM DCFDA for 30 min at 37 °C and the fluorescence intensity analyzed by FACScaliber. There was a significant increase in ROS in treated cells (* = $p<0.05$). Live cell imaging for ROS levels was also performed in BxPC-3 cells (B). Cells were seeded in 4-well chamber glass slides. The following day, cells were treated with 10µm DCFDA and either vehicle or P-S for 1 hr. Cells were imaged by fluorescence microscopy. There was a notable increase in ROS in cells treated with P-S.

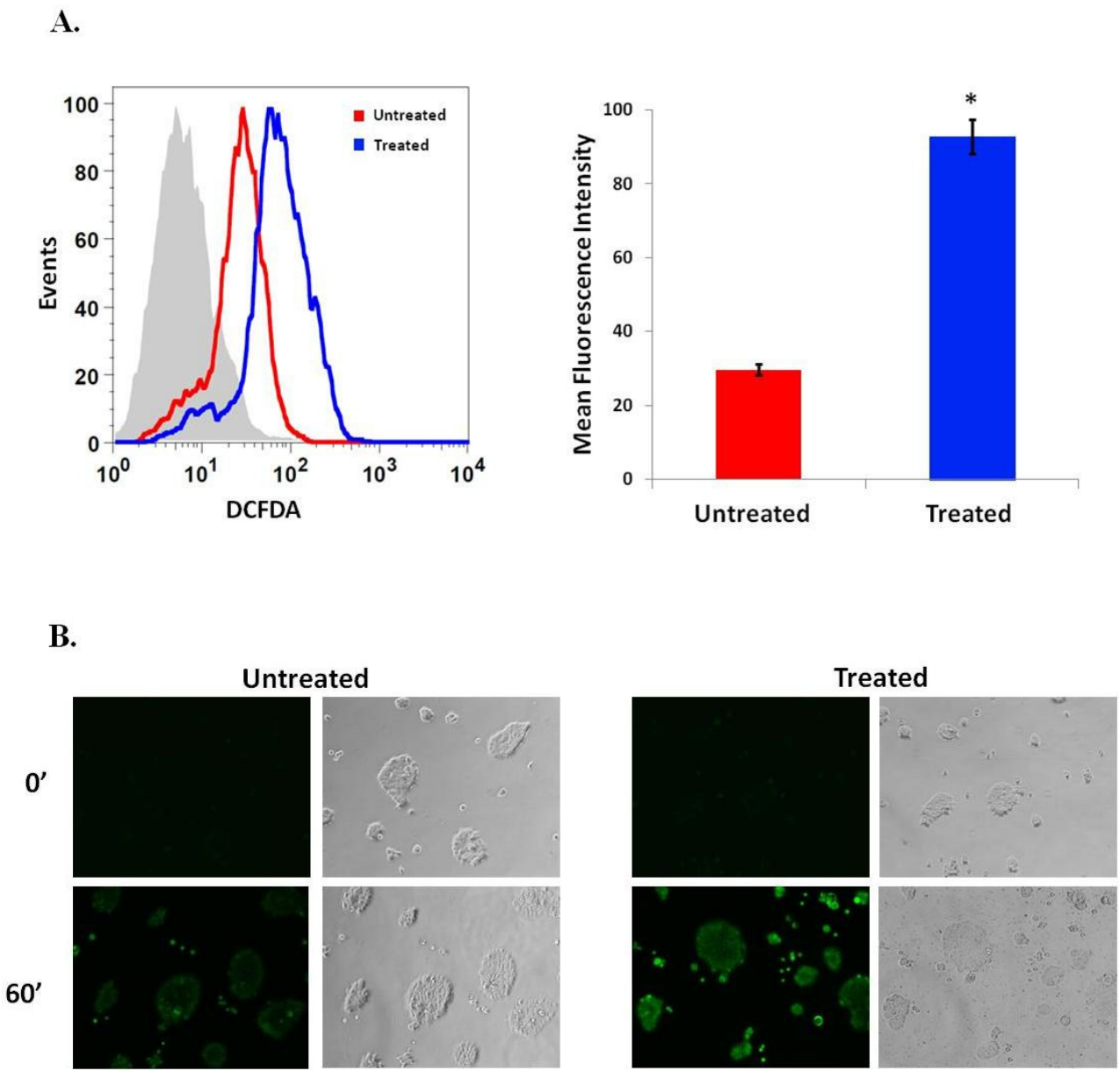

CONCLUSIONS AND FUTURE DIRECTIONS

PROPOSED MODEL

The work presented in the previous chapters has illustrated several aspects of both the effect and mechanism of action of P-S. Based on these data, we can propose a mechanistic model for the effect of P-S on pancreatic cancer. This model is summarized in the diagram below.

There are two major proximal events, the induction of ROS followed by alterations in intracellular activity downstream of Ca^{2+}. The next pivotal event is the dephosphorylation of NFATc1 which in turn leads to its translocation into the nucleus. Once in the nucleus NFATc1 binds to its DNA recognition sequences affecting the transcription of multiple genes that are critical to the fate of the target cell, such as c-Myc and COX-2. P-S increases cytoplasmic and nuclear NFATc1 protein expression. Combination with CsA, reduces the induction of nuclear and cytoplasmic NFATc1 protein expression CsA can be conceptualized in this diagram as affecting calcium homeostasis which in turn modulates the activity of NFATc1. The possibility of a feedback loop where nuclear NFATc1 is shuttled back to the cytoplasm may exist in response to treatment with P-S in Kd cells.

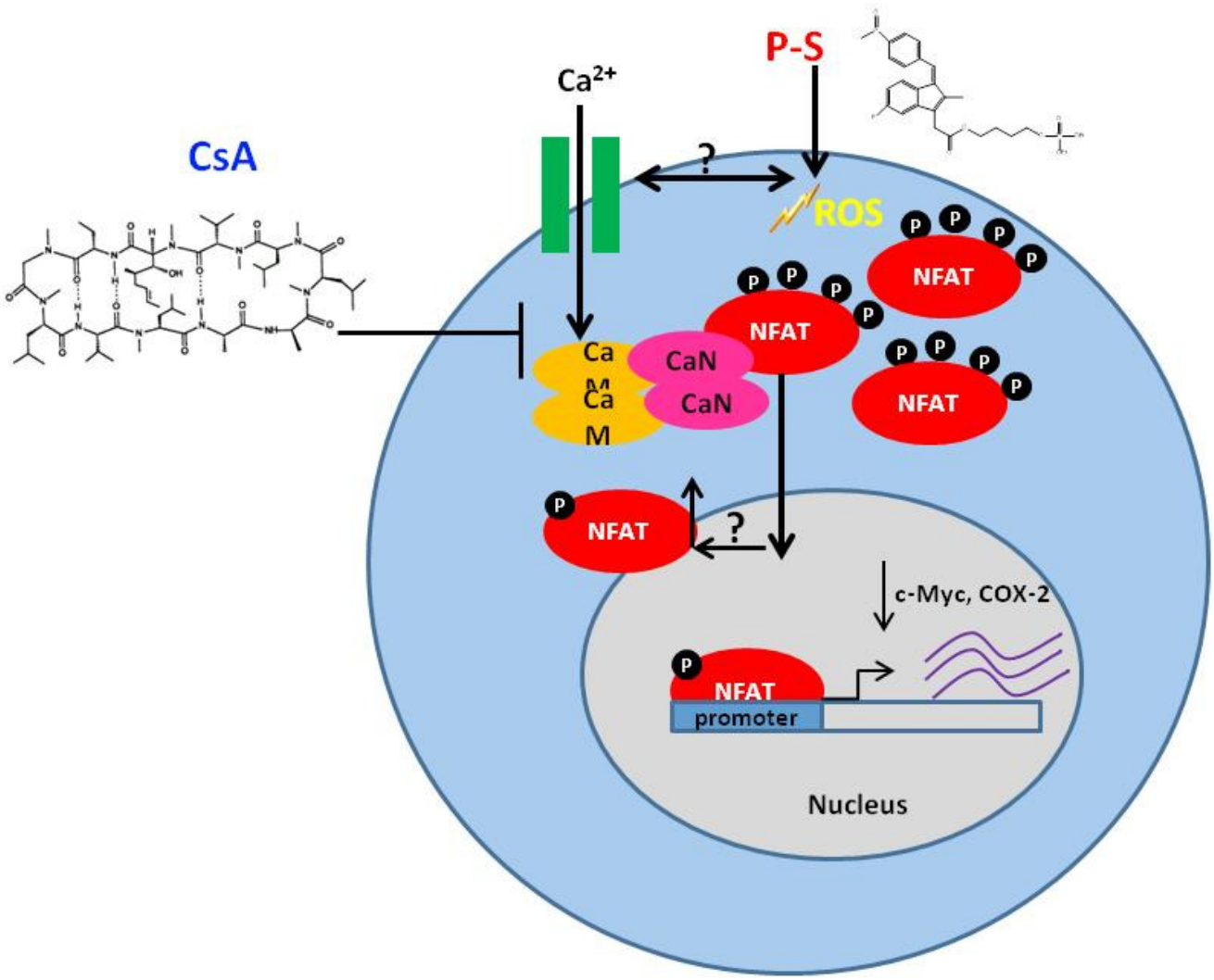
P-S
Ca2+
CsA
?
ROS
NFAT
NFAT
NFAT
Ca
M
CaN
CaN
NFAT
?
c-Myc, COX-2
NFAT
promoter
Nucleus

CONCLUSIONS

In Chapter I, the pharmacokinetics of P-S were analyzed, revealing that P-S undergoes extensive transformations in vivo and in vitro yielding at least eight metabolites. In particular, P-S undergoes reduction and oxidation yielding P-S sulfide and P-S sulfone. It is further hydrolyzed releasing sulindac, which generates sulindac sulfide and sulindac sulfone, all of which are glucuronidated. In mice, P-S is rapidly absorbed, metabolized and distributed to the blood and other tissues. These metabolites, together with the intact P-S, may play important roles in cancer control. The pharmacokinetics and biodistribution features of P-S provide a likely explanation of its superior safety, especially regarding its ability to spare the gastroduodenal mucosa.

In Chapter II, I showed that P-S is highly efficacious. Effective chemotherapy candidates are often those that both block cellular proliferation and increase apoptosis. Here I have shown that P-S is able to fulfill both requirements, with greater efficiency than sulindac. I have also shown that P-S inhibits cancer growth more efficaciously than sulindac both *in vitro* and *in vivo*. It is clear that, even though incompletely delineated, the mechanism of action of P-S in controlling pancreatic cancer is unique. As outlined in Future Directions, presented later on, additional work will clarify more details of this model.

In Chapter III, I showed that P-S operated with enhanced potency in the absence of NFATc1 in both wildtype and mutant K-Ras cell lines. I also demonstrated the enhanced potency of three COX-2 indedependent agents in the absence of NFATc1. I also showed that P-S increases total NFATc1 protein expression in pancreatic cancer cells, though this induction is

significantly less in Kd cells. Quite possibly, a feedback loop may exist that shuttles nuclear NFATc1 into the cytoplasm. Decreased nuclear NFATc1 localization in Kd cells decreases transcription of COX-2 and c-Myc genes, in effect decreasing their protein expression. I also demonstrated that NFATc1 protein expression regulates tumor growth. In the absence of NFATc1 alone, tumor progression was significantly inhibited; the addition of P-S treatment further reduced tumor growth. When NFATc1 was overexpressed, there was no significant effect on tumor growth. This highlights that overexpression of NFATc1 in pancreatic cancer causes some resistance to treatment with P-S, and by reducing NFATc1 expression, P-S was able to significantly inhibit cancer growth.

In Chapter IV, I showed that when combined with P-S, CsA enhanced the efficacy of P-S and that this combination inhibited NFATc1 protein expression in pancreatic cancer cells. I also showed that P-S significantly increases ROS in pancreatic cancer cells. This increase in ROS by P-S may play a role in the increased total NFATc1 protein expression that we observed in Chapter III. Combination P-S and CsA was able to inhibit both total NFATc1 protein expression.

In sum, NFATc1 overexpression in pancreatic cancer affects their response to treatment. Furthermore, P-S alone or in combination with CsA, or any similarly acting Ca^{2+}/NFATc1 inhibitor, is a viable therapeutic approach for pancreatic cancer treatment.

FUTURE DIRECTIONS

Although a significant amount of work regarding the efficacy and mechanism of action of P-S in pancreatic cancer has been accomplished, this work is still preclinical and by necessity somewhat limited. For P-S to achieve its expected full potential as a chemotherapeutic agent against one of the most dreadful human cancers, several aspects of its pharmacology need to be further explored and solidified. Ultimately, only human clinical trials will render the final verdict as to the clinical utility of this promising agent.

The work presented here has addressed several fundamental questions, but as often is the case in science, has also generated some exciting new questions that will drive the future direction of this work. Below, I have highlighted the key issues that remain to be explored:

- Studies to date of phospho-sulindac and structurally similar compounds indicate that the *mode of delivery* impacts their efficacy. Work involving formulation of these compounds into liposomes enhances their efficacy. Although an enhanced permeability and retention (EPR) effect does not occur in pancreatic cancer, other modes of delivery such as nanoscience-based drug delivery offer an exciting possibility.
- *Drug Combinations:* Given the complexity of pancreatic cancer and the encouraging results that are observed with CsA, further exploration of P-S with CsA and P-S combined with other compounds is justified and may deem highly productive. Additional compounds of interest include conventional agents such as gemcitabine or other chemotherapeutics. Or potential partnering compounds may be selected based on their known mechanistic approaches such as peptide inhibition of NFATc1.

- *Mechanistic Questions*: A more thorough analysis of calcium signaling in response to P-S will provide helpful insights to the drugs mechanism. Firstly, a live-imaging method to analyze intracellular calcium flux is essential. Secondly, because in the nucleus NFATc1 is inactivated by the coordinated action of NFAT kinases, GSK3 and DYRK (Arron, et al. 2006), resulting in NFAT rephosphorylation and relocation to the cytoplasm by kinases, their protein expression and activity profiles in response to treatment to P-S will provide much understanding as to why NFATc1 protein expression is increased solely in the cytoplasm.
- *Broader Anticancer Effect*: Evidence accumulated to date indicates that P-S possesses an intrinsic anticancer activity that extends beyond pancreatic cancer (i.e. colon and other types of cancer). As multiple cancers share fundamental mechanisms of carcinogenesis, it is possible that the same insights into P-S's cellular mechanisms in pancreatic cancer shown here can be applied to other cancer types. Future studies will undoubtedly explore this possibility, opening the way for a broader anticancer application for this very important molecule.

REFERENCES

Akunda, J. K., et al. (2007), "Cyclooxygenase-2 Deficiency Increases Epidermal Apoptosis and Impairs Recovery Following Acute Uvb Exposure," *Mol Carcinog*, 46, 354-362.

Almhanna, K., and Kim, R. (2008), "Second-Line Therapy for Gemcitabine-Refractory Pancreatic Cancer: Is There a Standard?," *Oncology (Williston Park)*, 22, 1176-1183; discussion 1190, 1192, 1196.

Arner, E. S., and Holmgren, A. (2006), "The Thioredoxin System in Cancer," *Semin Cancer Biol*, 16, 420-426.

Arron, J. R., et al. (2006), "Nfat Dysregulation by Increased Dosage of Dscr1 and Dyrk1a on Chromosome 21," *Nature*, 441, 595-600.

Bachrach, U. (2004), "Polyamines and Cancer: Minireview Article," *Amino Acids*, 26, 307-309.

Bajrami, B., Zhao, L., Schenkman, J. B., and Rusling, J. F. (2009), "Rapid Lc-Ms Drug Metabolite Profiling Using Microsomal Enzyme Bioreactors in a Parallel Processing Format," *Anal Chem*, 81, 9921-9929.

Bardeesy, N., and DePinho, R. A. (2002), "Pancreatic Cancer Biology and Genetics," *Nat Rev Cancer*, 2, 897-909.

Batist, G., Harris, L., Azarnia, N., Lee, L. W., and Daza-Ramirez, P. (2006), "Improved Anti-Tumor Response Rate with Decreased Cardiotoxicity of Non-Pegylated Liposomal Doxorubicin Compared with Conventional Doxorubicin in First-Line Treatment of Metastatic Breast Cancer in Patients Who Had Received Prior Adjuvant Doxorubicin: Results of a Retrospective Analysis," *Anticancer Drugs*, 17, 587-595.

Beals, C. R., Clipstone, N. A., Ho, S. N., and Crabtree, G. R. (1997), "Nuclear Localization of Nf-Atc by a Calcineurin-Dependent, Cyclosporin-Sensitive Intramolecular Interaction," *Genes Dev*, 11, 824-834.

Behrend, L., Henderson, G., and Zwacka, R. M. (2003), "Reactive Oxygen Species in Oncogenic Transformation," *Biochem Soc Trans*, 31, 1441-1444.

Berndt, C., Lillig, C. H., and Holmgren, A. (2007), "Thiol-Based Mechanisms of the Thioredoxin and Glutaredoxin Systems: Implications for Diseases in the Cardiovascular System," *Am J Physiol Heart Circ Physiol*, 292, H1227-1236.

Boolbol, S. K., et al. (1996), "Cyclooxygenase-2 Overexpression and Tumor Formation Are Blocked by Sulindac in a Murine Model of Familial Adenomatous Polyposis," *Cancer Res*, 56, 2556-2560.

Breslin, T. M., et al. (2001), "Neoadjuvant Chemoradiotherapy for Adenocarcinoma of the Pancreas: Treatment Variables and Survival Duration," *Ann Surg Oncol*, 8, 123-132.

Brown, J. R., and DuBois, R. N. (2005), "Cox-2: A Molecular Target for Colorectal Cancer Prevention," *J Clin Oncol*, 23, 2840-2855.

Buchholz, M., et al. (2006), "Overexpression of C-Myc in Pancreatic Cancer Caused by Ectopic Activation of Nfatc1 and the Ca2+/Calcineurin Signaling Pathway," *EMBO J*, 25, 3714-3724.

Buck, E., et al. (2006a), "Rapamycin Synergizes with the Epidermal Growth Factor Receptor Inhibitor Erlotinib in Non-Small-Cell Lung, Pancreatic, Colon, and Breast Tumors," *Mol Cancer Ther*, 5, 2676-2684.

Buck, E., et al. (2006b), "Inactivation of Akt by the Epidermal Growth Factor Receptor Inhibitor Erlotinib Is Mediated by Her-3 in Pancreatic and Colorectal Tumor Cell Lines and Contributes to Erlotinib Sensitivity," *Mol Cancer Ther*, 5, 2051-2059.

Cai, Y., et al. (2008), "A New Prostate Cancer Therapeutic Approach: Combination of Androgen Ablation with Cox-2 Inhibitor," *Int J Cancer*, 123, 195-201.

Cao, Y., and Prescott, S. M. (2002), "Many Actions of Cyclooxygenase-2 in Cellular Dynamics and in Cancer," *J Cell Physiol*, 190, 279-286.

Cao, Z., and Li, Y. (2002), "Chemical Induction of Cellular Antioxidants Affords Marked Protection against Oxidative Injury in Vascular Smooth Muscle Cells," *Biochem Biophys Res Commun*, 292, 50-57.

Chulada, P. C., et al. (2000), "Genetic Disruption of Ptgs-1, as Well as Ptgs-2, Reduces Intestinal Tumorigenesis in Min Mice," *Cancer Res*, 60, 4705-4708.

Crabtree, G. R., and Schreiber, S. L. (2009), "Snapshot: Ca2+-Calcineurin-Nfat Signaling," *Cell*, 138, 210, 210 e211.

Evans, D. B., et al. (1992), "Preoperative Chemoradiation and Pancreaticoduodenectomy for Adenocarcinoma of the Pancreas," *Arch Surg*, 127, 1335-1339.

Feske, S. (2007), "Calcium Signalling in Lymphocyte Activation and Disease," *Nat Rev Immunol*, 7, 690-702.

Flockhart, R. J., Armstrong, J. L., Reynolds, N. J., and Lovat, P. E. (2009), "Nfat Signalling Is a Novel Target of Oncogenic Braf in Metastatic Melanoma," *Br J Cancer*, 101, 1448-1455.

Gavrieli, Y., Sherman, Y., and Ben-Sasson, S. A. (1992), "Identification of Programmed Cell Death in Situ Via Specific Labeling of Nuclear DNA Fragmentation," *J Cell Biol*, 119, 493-501.

Grosch, S., Tegeder, I., Niederberger, E., Brautigam, L., and Geisslinger, G. (2001), "Cox-2 Independent Induction of Cell Cycle Arrest and Apoptosis in Colon Cancer Cells by the Selective Cox-2 Inhibitor Celecoxib," *FASEB J*, 15, 2742-2744.

Guldenschuh, I., et al. (2001), "Relationship between Apc Genotype, Polyp Distribution, and Oral Sulindac Treatment in the Colon and Rectum of Patients with Familial Adenomatous Polyposis," *Dis Colon Rectum*, 44, 1090-1097; discussion 1097-1099.

Gupta, R. A., and Dubois, R. N. (2001), "Colorectal Cancer Prevention and Treatment by Inhibition of Cyclooxygenase-2," *Nat Rev Cancer*, 1, 11-21.

Guzy, R. D., and Schumacker, P. T. (2006), "Oxygen Sensing by Mitochondria at Complex Iii: The Paradox of Increased Reactive Oxygen Species During Hypoxia," *Exp Physiol*, 91, 807-819.

Haanen, C. (2001), "Sulindac and Its Derivatives: A Novel Class of Anticancer Agents," *Curr Opin Investig Drugs*, 2, 677-683.

Hayashi, T., et al. (2009), "Suppressive Effect of Sulindac on Branch Duct-Intraductal Papillary Mucinous Neoplasms," *J Gastroenterol*, 44, 964-975.

Hezel, A. F., Kimmelman, A. C., Stanger, B. Z., Bardeesy, N., and Depinho, R. A. (2006), "Genetics and Biology of Pancreatic Ductal Adenocarcinoma," *Genes Dev*, 20, 1218-1249.

Hingorani, S. R., et al. (2003), "Preinvasive and Invasive Ductal Pancreatic Cancer and Its Early Detection in the Mouse," *Cancer Cell*, 4, 437-450.

Hogan, P. G., Chen, L., Nardone, J., and Rao, A. (2003), "Transcriptional Regulation by Calcium, Calcineurin, and Nfat," *Genes Dev*, 17, 2205-2232.

Hogan, P. G., Lewis, R. S., and Rao, A. (2010), "Molecular Basis of Calcium Signaling in Lymphocytes: Stim and Orai," *Annu Rev Immunol*, 28, 491-533.

Horn, H. F., and Vousden, K. H. (2007), "Coping with Stress: Multiple Ways to Activate P53," *Oncogene*, 26, 1306-1316.

Hruban, R. H., et al. (2006), "Pathology of Genetically Engineered Mouse Models of Pancreatic Exocrine Cancer: Consensus Report and Recommendations," *Cancer Res*, 66, 95-106.

Hruban, R. H., et al. (2001), "Pancreatic Intraepithelial Neoplasia: A New Nomenclature and Classification System for Pancreatic Duct Lesions," *Am J Surg Pathol*, 25, 579-586.

Huang, L., et al. (2011), "Chemotherapeutic Properties of Phospho-Nonsteroidal Anti-Inflammatory Drugs, a New Class of Anticancer Compounds," *Cancer Res*, 71, 7617-7627.

Huang, L., et al. (2010), "Phospho-Sulindac (Oxt-922) Inhibits the Growth of Human Colon Cancer Cell Lines: A Redox/Polyamine-Dependent Effect," *Carcinogenesis*, 31, 1982-1990.

Iniguez, M. A., Martinez-Martinez, S., Punzon, C., Redondo, J. M., and Fresno, M. (2000), "An Essential Role of the Nuclear Factor of Activated T Cells in the Regulation of the Expression of the Cyclooxygenase-2 Gene in Human T Lymphocytes," *J Biol Chem*, 275, 23627-23635.

Irani, K., et al. (1997), "Mitogenic Signaling Mediated by Oxidants in Ras-Transformed Fibroblasts," *Science*, 275, 1649-1652.

Javle, M. M., et al. (2007), "Epithelial-Mesenchymal Transition (Emt) and Activated Extracellular Signal-Regulated Kinase (P-Erk) in Surgically Resected Pancreatic Cancer," *Ann Surg Oncol*, 14, 3527-3533.

Kaimul, A. M., Nakamura, H., Masutani, H., and Yodoi, J. (2007), "Thioredoxin and Thioredoxin-Binding Protein-2 in Cancer and Metabolic Syndrome," *Free Radic Biol Med*, 43, 861-868.

Kalser, M. H., Barkin, J., and MacIntyre, J. M. (1985), "Pancreatic Cancer. Assessment of Prognosis by Clinical Presentation," *Cancer*, 56, 397-402.

Kawanishi, S., Hiraku, Y., Pinlaor, S., and Ma, N. (2006), "Oxidative and Nitrative DNA Damage in Animals and Patients with Inflammatory Diseases in Relation to Inflammation-Related Carcinogenesis," *Biol Chem*, 387, 365-372.

Kindler, H. L., et al. (2010), "Gemcitabine Plus Bevacizumab Compared with Gemcitabine Plus Placebo in Patients with Advanced Pancreatic Cancer: Phase Iii Trial of the Cancer and Leukemia Group B (Calgb 80303)," *J Clin Oncol*, 28, 3617-3622.

Kissil, J. L., et al. (2007), "Requirement for Rac1 in a K-Ras Induced Lung Cancer in the Mouse," *Cancer Res*, 67, 8089-8094.

Klinkenbijl, J. H., et al. (1999), "Adjuvant Radiotherapy and 5-Fluorouracil after Curative Resection of Cancer of the Pancreas and Periampullary Region: Phase Iii Trial of the Eortc Gastrointestinal Tract Cancer Cooperative Group," *Ann Surg*, 230, 776-782; discussion 782-774.

Langenbach, R., Loftin, C., Lee, C., and Tiano, H. (1999), "Cyclooxygenase Knockout Mice: Models for Elucidating Isoform-Specific Functions," *Biochem Pharmacol*, 58, 1237-1246.

Lee, G., et al. (2002), "T0070907, a Selective Ligand for Peroxisome Proliferator-Activated Receptor Gamma, Functions as an Antagonist of Biochemical and Cellular Activities," *J Biol Chem*, 277, 19649-19657.

Lehen'kyi, V., Flourakis, M., Skryma, R., and Prevarskaya, N. (2007), "Trpv6 Channel Controls Prostate Cancer Cell Proliferation Via Ca(2+)/Nfat-Dependent Pathways," *Oncogene*, 26, 7380-7385.

Liu, J., et al. (1991), "Calcineurin Is a Common Target of Cyclophilin-Cyclosporin a and Fkbp-Fk506 Complexes," *Cell*, 66, 807-815.

Macian, F. (2005), "Nfat Proteins: Key Regulators of T-Cell Development and Function," *Nat Rev Immunol*, 5, 472-484.

Mackenzie, G. G., et al. (2010), "Phospho-Sulindac (Oxt-328), a Novel Sulindac Derivative, Is Safe and Effective in Colon Cancer Prevention in Mice," *Gastroenterology*, 139, 1320-1332.

Mantovani, A., Marchesi, F., Porta, C., Sica, A., and Allavena, P. (2007), "Inflammation and Cancer: Breast Cancer as a Prototype," *Breast*, 16 Suppl 2, S27-33.

Martin, S. J., et al. (1995), "Early Redistribution of Plasma Membrane Phosphatidylserine Is a General Feature of Apoptosis Regardless of the Initiating Stimulus: Inhibition by Overexpression of Bcl-2 and Abl," *J Exp Med*, 182, 1545-1556.

Maruyama, K. (2011), "Intracellular Targeting Delivery of Liposomal Drugs to Solid Tumors Based on Epr Effects," *Adv Drug Deliv Rev*, 63, 161-169.

Maulik, N., and Das, D. K. (2008), "Emerging Potential of Thioredoxin and Thioredoxin Interacting Proteins in Various Disease Conditions," *Biochim Biophys Acta*, 1780, 1368-1382.

Molina, M. A., Sitja-Arnau, M., Lemoine, M. G., Frazier, M. L., and Sinicrope, F. A. (1999), "Increased Cyclooxygenase-2 Expression in Human Pancreatic Carcinomas and Cell Lines: Growth Inhibition by Nonsteroidal Anti-Inflammatory Drugs," *Cancer Res*, 59, 4356-4362.

Muller, M. R., and Rao, A. (2010), "Nfat, Immunity and Cancer: A Transcription Factor Comes of Age," *Nat Rev Immunol*, 10, 645-656.

Nakajima, S., et al. (2004), "N-Cadherin Expression and Epithelial-Mesenchymal Transition in Pancreatic Carcinoma," *Clin Cancer Res*, 10, 4125-4133.

Neoptolemos, J. P., et al. (2001), "Adjuvant Chemoradiotherapy and Chemotherapy in Resectable Pancreatic Cancer: A Randomised Controlled Trial," *Lancet*, 358, 1576-1585.

Nussmeier, N. A., et al. (2005), "Complications of the Cox-2 Inhibitors Parecoxib and Valdecoxib after Cardiac Surgery," *N Engl J Med*, 352, 1081-1091.

Ogino, S., et al. (2008), "Cyclooxygenase-2 Expression Is an Independent Predictor of Poor Prognosis in Colon Cancer," *Clin Cancer Res*, 14, 8221-8227.

Oshima, M., et al. (1996), "Suppression of Intestinal Polyposis in Apc Delta716 Knockout Mice by Inhibition of Cyclooxygenase 2 (Cox-2)," *Cell*, 87, 803-809.

Ouyang, N., et al. (2006), "Nitric Oxide-Donating Aspirin Prevents Pancreatic Cancer in a Hamster Tumor Model," *Cancer Res*, 66, 4503-4511.

Pao, W., et al. (2004), "Egf Receptor Gene Mutations Are Common in Lung Cancers from "Never Smokers" and Are Associated with Sensitivity of Tumors to Gefitinib and Erlotinib," *Proc Natl Acad Sci U S A*, 101, 13306-13311.

Pao, W., et al. (2005), "Kras Mutations and Primary Resistance of Lung Adenocarcinomas to Gefitinib or Erlotinib," *PLoS Med*, 2, e17.

Papahadjopoulos, D., et al. (1991), "Sterically Stabilized Liposomes: Improvements in Pharmacokinetics and Antitumor Therapeutic Efficacy," *Proc Natl Acad Sci U S A*, 88, 11460-11464.

Pelicano, H., Carney, D., and Huang, P. (2004), "Ros Stress in Cancer Cells and Therapeutic Implications," *Drug Resist Updat*, 7, 97-110.

Piazza, G. A., et al. (2009), "A Novel Sulindac Derivative That Does Not Inhibit Cyclooxygenases but Potently Inhibits Colon Tumor Cell Growth and Induces Apoptosis with Antitumor Activity," *Cancer Prev Res (Phila)*, 2, 572-580.

Pollard, M., Luckert, P. H., and Schmidt, M. A. (1983), "The Suppressive Effect of Piroxicam on Autochthonous Intestinal Tumors in the Rat," *Cancer Lett*, 21, 57-61.

Rao, K. V., et al. (1996), "Differential Activity of Aspirin, Ketoprofen and Sulindac as Cancer Chemopreventive Agents in the Mouse Urinary Bladder," *Carcinogenesis*, 17, 1435-1438.

Ratnayake, J. H., Hanna, P. E., Anders, M. W., and Duggan, D. E. (1981), "Sulfoxide Reduction. In Vitro Reduction of Sulindac by Rat Hepatic Cytosolic Enzymes," *Drug Metab Dispos*, 9, 85-87.

Raut, C. P., Evans, D. B., Crane, C. H., Pisters, P. W., and Wolff, R. A. (2004), "Neoadjuvant Therapy for Resectable Pancreatic Cancer," *Surg Oncol Clin N Am*, 13, 639-661, ix.

Riely, G. J., and Ladanyi, M. (2008), "Kras Mutations: An Old Oncogene Becomes a New Predictive Biomarker," *J Mol Diagn*, 10, 493-495.

Rigas, B., and Sun, Y. (2008), "Induction of Oxidative Stress as a Mechanism of Action of Chemopreventive Agents against Cancer," *Br J Cancer*, 98, 1157-1160.

Rigas, B., and Williams, J. L. (2008), "No-Donating Nsaids and Cancer: An Overview with a Note on Whether No Is Required for Their Action," *Nitric Oxide*, 19, 199-204.

Rodrigues, M. S., Reddy, M. M., and Sattler, M. (2008), "Cell Cycle Regulation by Oncogenic Tyrosine Kinases in Myeloid Neoplasias: From Molecular Redox Mechanisms to Health Implications," *Antioxid Redox Signal*, 10, 1813-1848.

Rothenberg, M. L., et al. (1996), "A Phase Ii Trial of Gemcitabine in Patients with 5-Fu-Refractory Pancreas Cancer," *Ann Oncol*, 7, 347-353.

Saitoh, M., et al. (1998), "Mammalian Thioredoxin Is a Direct Inhibitor of Apoptosis Signal-Regulating Kinase (Ask) 1," *EMBO J*, 17, 2596-2606.

Sales, K. J., et al. (2010), "Interleukin-11 in Endometrial Adenocarcinoma Is Regulated by Prostaglandin F2alpha-F-Prostanoid Receptor Interaction Via the Calcium-Calcineurin-Nuclear Factor of Activated T Cells Pathway and Negatively Regulated by the Regulator of Calcineurin-1," *Am J Pathol*, 176, 435-445.

Sarkar, F. H., Adsule, S., Li, Y., and Padhye, S. (2007), "Back to the Future: Cox-2 Inhibitors for Chemoprevention and Cancer Therapy," *Mini Rev Med Chem*, 7, 599-608.

Schumacker, P. T. (2006), "Reactive Oxygen Species in Cancer Cells: Live by the Sword, Die by the Sword," *Cancer Cell*, 10, 175-176.

Shiff, S. J., and Rigas, B. (1999), "The Role of Cyclooxygenase Inhibition in the Antineoplastic Effects of Nonsteroidal Antiinflammatory Drugs (Nsaids)," *J Exp Med*, 190, 445-450.

Sobolewski, C., Cerella, C., Dicato, M., Ghibelli, L., and Diederich, M. (2010), "The Role of Cyclooxygenase-2 in Cell Proliferation and Cell Death in Human Malignancies," *Int J Cell Biol*, 2010, 215158.

Sonpavde, G., et al. (2007), "Phase Ii Study of Azacitidine to Restore Responsiveness of Prostate Cancer to Hormonal Therapy," *Clin Genitourin Cancer*, 5, 457-459.

Sucic, M., et al. (2003), "Expression of Cyclooxygenase-2 in Fine-Needle Aspirates from Breast Carcinoma and Benign Breast Diseases," *Breast*, 12, 51-57.

Sun, Y., Huang, L., Mackenzie, G. G., and Rigas, B. (2011), "Oxidative Stress Mediates through Apoptosis the Anticancer Effect of Phospho-Nonsteroidal Anti-Inflammatory Drugs: Implications for the Role of Oxidative Stress in the Action of Anticancer Agents," *J Pharmacol Exp Ther*, 338, 775-783.

Sun, Y., and Rigas, B. (2008), "The Thioredoxin System Mediates Redox-Induced Cell Death in Human Colon Cancer Cells: Implications for the Mechanism of Action of Anticancer Agents," *Cancer Res*, 68, 8269-8277.

Surh, Y. J., and Kundu, J. K. (2005), "Signal Transduction Network Leading to Cox-2 Induction: A Road Map in Search of Cancer Chemopreventives," *Arch Pharm Res*, 28, 1-15.

Szatrowski, T. P., and Nathan, C. F. (1991), "Production of Large Amounts of Hydrogen Peroxide by Human Tumor Cells," *Cancer Res*, 51, 794-798.

Taketo, M. M. (1998), "Cyclooxygenase-2 Inhibitors in Tumorigenesis (Part Ii)," *J Natl Cancer Inst*, 90, 1609-1620.

Tegeder, I., Pfeilschifter, J., and Geisslinger, G. (2001), "Cyclooxygenase-Independent Actions of Cyclooxygenase Inhibitors," *FASEB J*, 15, 2057-2072.

Thun, M. J., Namboodiri, M. M., and Heath, C. W., Jr. (1991), "Aspirin Use and Reduced Risk of Fatal Colon Cancer," *N Engl J Med*, 325, 1593-1596.

Tiano, H. F., et al. (2002), "Deficiency of Either Cyclooxygenase (Cox)-1 or Cox-2 Alters Epidermal Differentiation and Reduces Mouse Skin Tumorigenesis," *Cancer Res*, 62, 3395-3401.

Tinsley, H. N., et al. (2009), "Sulindac Sulfide Selectively Inhibits Growth and Induces Apoptosis of Human Breast Tumor Cells by Phosphodiesterase 5 Inhibition, Elevation of Cyclic Gmp, and Activation of Protein Kinase G," *Mol Cancer Ther*, 8, 3331-3340.

Trachootham, D., Alexandre, J., and Huang, P. (2009), "Targeting Cancer Cells by Ros-Mediated Mechanisms: A Radical Therapeutic Approach?," *Nat Rev Drug Discov*, 8, 579-591.

Ulrich, C. M., Bigler, J., and Potter, J. D. (2006), "Non-Steroidal Anti-Inflammatory Drugs for Cancer Prevention: Promise, Perils and Pharmacogenetics," *Nat Rev Cancer*, 6, 130-140.

Waddell, W. R., Ganser, G. F., Cerise, E. J., and Loughry, R. W. (1989), "Sulindac for Polyposis of the Colon," *Am J Surg*, 157, 175-179.

Waddell, W. R., and Loughry, R. W. (1983), "Sulindac for Polyposis of the Colon," *J Surg Oncol*, 24, 83-87.

Waypa, G. B., et al. (2006a), "Increases in Mitochondrial Reactive Oxygen Species Trigger Hypoxia-Induced Calcium Responses in Pulmonary Artery Smooth Muscle Cells," *Circ Res*, 99, 970-978.

Waypa, G. B., and Schumacker, P. T. (2006b), "Role for Mitochondrial Reactive Oxygen Species in Hypoxic Pulmonary Vasoconstriction," *Novartis Found Symp*, 272, 176-192; discussion 192-175, 214-177.

Wolfe, M. M., Lichtenstein, D. R., and Singh, G. (1999), "Gastrointestinal Toxicity of Nonsteroidal Antiinflammatory Drugs," *N Engl J Med*, 340, 1888-1899.

Xie, G., et al. (2011a), "The Metabolism and Pharmacokinetics of Phospho-Sulindac (Oxt-328) and the Effect of Difluoromethylornithine," *Br J Pharmacol*.

Xie, G., et al. (2012), "The Metabolism and Pharmacokinetics of Phospho-Sulindac (Oxt-328) and the Effect of Difluoromethylornithine," *Br J Pharmacol*, 165, 2152-2166.

Xie, G., et al. (2011b), "Phospho-Ibuprofen (Mdc-917) Is a Novel Agent against Colon Cancer: Efficacy, Metabolism, and Pharmacokinetics in Mouse Models," *J Pharmacol Exp Ther*, 337, 876-886.

Xu, D. K., et al. (2008), "[Association between Single Nucleotide Polymorphisms in the Promoter of Cyclooxygenase Cox-2 Gene and Hereditary Susceptibility to Pancreatic Cancer]," *Zhonghua Yi Xue Za Zhi*, 88, 1961-1965.

Yang, W., et al. (2012), "Pharmacokinetics and Tissue Distribution Profile of Icariin Propylene Glycol-Liposome Intraperitoneal Injection in Mice," *J Pharm Pharmacol*, 64, 190-198.

Yip-Schneider, M. T., et al. (2007), "Suppression of Pancreatic Tumor Growth by Combination Chemotherapy with Sulindac and Lc-1 Is Associated with Cyclin D1 Inhibition in Vivo," *Mol Cancer Ther*, 6, 1736-1744.

Yiu, G. K., and Toker, A. (2006), "Nfat Induces Breast Cancer Cell Invasion by Promoting the Induction of Cyclooxygenase-2," *J Biol Chem*, 281, 12210-12217.

Yoeli-Lerner, M., Chin, Y. R., Hansen, C. K., and Toker, A. (2009), "Akt/Protein Kinase B and Glycogen Synthase Kinase-3beta Signaling Pathway Regulates Cell Migration through the Nfat1 Transcription Factor," *Mol Cancer Res*, 7, 425-432.

Zhao, X., et al. (2008), "Cyclooxygenase-2 Expression During Immortalization and Breast Cancer Progression," *Cancer Res*, 68, 467-475.